UNIVERSITÁ DEGLI STUDI DI MILANO
Facoltà di Medicina Veterinaria
Dipartimento di Scienze veterinarie e Sanità pubblica

PhD COURSE OF
VETERINARY HYGIENE AND ANIMAL PATHOLOGY
XXVIII cycle

"Aquatic pollution and biological monitoring of the marine environment: toxicology, histopathology and ecological risk of selected fish species"

PhD student:
Dr. Santagostino Sara Francesca
Matr. R10039

PhD Supervisor: Prof. Paola Roccabianca
PhD Coordinator: Prof. Giuseppe Sironi

Academic Year 2014-2015

TABLE OF CONTENTS

List of Tables and Figures

List of Abbreviations

Ag	Silver
Al	Aluminium
As	Arsenic
Ba	Barium
Ca	Calcium
Cd	Cadmium
Co	Cobalt
Cr	Chromium
Cu	Copper
DDT	1,1,1- trichloro-2,2-bis(4-chlorophenyl) ethane
Fe	Iron
HCH	β-1,2,3,4,5,6-hexachlorocyclohexane
GC/MS	Gas Chromatography/Mass spectrometry
Hg	Mercury
ICP/MS	Inductively Coupled Plasma Mass Spectrometry
IOCs	Persistent Inorganic Contaminants
K	Potassium
Mg	Magnesium
Mn	Manganese
Mo	Molybdenum
Na	Sodium
Ni	Nickel
OCs	Organochlorine compounds
OCPs	Organochlorine pollutans
Pb	Lead
PCB	Polychlorinated biphenyls
POPs	Persistent Organic Pollutans
SPE	Solid Phase Extraction
Sb	Antimony
Se	Selenium
Sn	Tin
Sr	Strontium
Tl	Thallium
Th	Thorium
Zn	Zinc
U	Uranium
V	Vanadium

Acknowledgements

I would firstly like to thank Prof. Paola Roccabianca for being such wonderful supervisor. Your expertise, patience and friendship were so much appreciated - I feel privileged to have worked with you.

I am deeply indebted to Dr. Sara Panseri for her never ending support in the lab, patiently working through calculations and samples with me.

Many thanks also to Dr. Gabriele Ghisleni for his advice and efforts before, during and after the experiments, and on support of keeping the experiment running smoothly.

I also wish to express my gratitude to all those Colleagues from the following institutions whom contributed to this research project:

- Drs. Patrizia Boracchi and Giuseppe Marano, from the University of Milan, School of Medicine, University of Milan, Italy
- Prof. Luca M. Chiesa, from the DIVET-LSA Laboratory for Animal Health and Food Security, Department of Veterinary Sciences and Public Health, School of Veterinary Medicine, University of Milan, Italy
- Dr. Giorgio Fedrizzi, from the IZS Lombardia ed Emilia Romagna, Bologna, Italy
- Dr. Massimo Tranquillo, from the IZS Lombardia ed Emilia Romagna, Bergamo, Italy
- Dr. Renato Malandra, ASL National Health Service, Veterinary Service, Milan, Italy
- Drs. Valerio Ranghieri and Nicola Zaffra, Veterinary Food Safety Consultants, Fish Market, Milan, Italy
- David E. Hinton, from Duke University, Durham, NC, USA
- Lisa A. Murphy, from the Department of Pathobiology, University of Pennsylvania School of Veterinary Medicine

Last but not least, many thanks to my Italian and American families and friends, Paolo, Drs. Debbie Gillette and Michael Goldschimdt, for all your help and guidance.

Abstract

The impact of multiple anthropogenic stressors on the marine environment has increased to large extents within the past few decades. Piscivorous fish can bioaccumulate pollutans to significantly higher concentrations than those found in the water or sediments, due to the lipid solubility and resistance of these compounds to numerous degenerative processes. The use of fish from different hydrological settings as bio-indicators represents a useful complementary choice to evaluate the levels and responses of marine organisms to pollutans, and to assess the global marine status. The purpose of this project is to evaluate the role of selected pelagic (*Thunnus thynnus*), and benthopelagic fish species (*Dentex dentex* and *Pagellus bogaraveo*) as biomonitors of Mediterranean sea pollution through the chemical identification and quantification of persistent organic and inorganic compounds in target tissues, the investigation of toxicopathic-related pathological changes, and the putative correlation between abnormal levels of pollutants and tissue lesions. Fish were selected based on length and weight. The mean concentration of metallic elements, polychlorinated biphenyls (PCBs) and organochlorine pesticides (OCs) was calculated and compared to their acceptable levels when available. Blackspot seabreams had the highest PCB concentration, whereas OCs were highest in tunas. A different spread in distinct species was documented for the following elements: Al, K, Co, Mo, Ag, Cd, Sn, and Th. For the elements without maximum dietary limits, Fe was highest in tunas, while Th was significantly predominant in dentices. Several metals were found in quantities above the acceptable levels. Specifically, the median concentrations of Hg and Cd in the pooled species were significantly higher than their relative PTWI. Significant differences among species were reported for Se, inorganic As, Ni and Zn. Other elements (Al, Cr, Cu, Sn, Pb, and Mn) were found to be at or below the corresponding acceptable levels. Histopathology evidenced acute and chronic lesions in numerous organs, comprising muscular

degeneration and necrosis, hepatic lipidosis, hepatocellular necrosis and dysplastic foci in all fish groups. Specifically, chronic lesions in liver, gills, immune and reproductive systems were common in all fish species encountered. Testicular atrophy, necrotizing branchitis, and proliferation of melanomacrophagic centers represented common findings. Although these findings revealed some differences in the patterns of histopathologic traits between pelagic and benthopelagic fishes, the overall level of histopathological injury was moderate and severe traits like neoplasms or pre-neoplastic foci were not observed. The concentrations of the other metallic elements did not influence the muscular H-indices in all species, with the exception of Na, where the interaction between concentration of Na and fish species was statistically significant. No significant differences were found between the H-indices of different species.

Given the simultaneous presence of pollutans in dangerous concentrations and the putative relationship with subacute to chronic microscopic lesions, research on fish contamination and human exposure could not be framed in terms of a single contaminant. Our findings aim to encourage cross-disciplinary discussion and to establish research and monitoring priorities in order to protect the human health. Since the risks associated with high simultaneous levels of multiple compounds have not been quantified but represent a severe health hazard, monitoring data should be collected to characterize the spatial and vertical distribution of metals in seawaters across a range of marine ecosystems. Our work confirms that histopathological evaluation of target organs should be included as a tool to determine the potential consequences of chronic toxicant exposure in wild fish.

Keywords: Fish; Semi-quantitative histopathology; Metals; Polychlorinated biphenyls (PCBs); Organochlorine pesticides (OCs); Environmental monitoring; Water pollution; Chronic toxicity.

CHAPTER 1

Introduction

1.1 The marine ecosystem

The waters of estuaries, coastal areas and "closed" seas such as the Mediterranean Sea are often characterized by high concentrations of variably toxic persistent organochlorine pollutant compounds (OPCs) and persistent inorganic contaminants (IOCs) with a high tendency to bottom sediment accumulation. Accumulation of these toxicants in aquatic organisms occurs through different mechanisms including bioconcentration by direct uptake from water, bottom sediment particle ingestion, or biomagnification throughout consumption of contaminated plankton or smaller fish (Miranda et al., 2008; Ribeiro CA et al., 2005). The high persistence of inorganic substances within organisms is correlated to their lipid solubility and resistance to numerous degradation processes. Therefore, IOCs represent a potential source of poisoning for fish, and for wild animals and humans.

Biomonitoring is defined as the global assessment of the environmental status through the use of adequate bio-indicators represented by organisms capable of perceiving environmental alterations. Given their feeding habits, predator fish can bioaccumulate IOCs and OPCs to significantly higher concentrations than those found in the water or sediment. As a matter of fact, the concentration of pollutants in the organism interferes with cellular events, inducing perturbations in energy metabolism that can be associated with tissue alterations in fish (Voegborlo et al., 2007).

According to their different hydrological setting, different species of fish may represent different biomonitoring sources. Specifically, benthopelagic fish of the Fam. Sparidae (i.e. *Dentex dentex* and *Pagellus bogaraveo*), which inhabit waters close to sea bottom, and pelagic fish belonging to Fam. Scombridae (i.e. *Thunnus thynnus*), which live and feed in open water column, may represent useful complementary biomonitors of sea pollution.

Histopathologic analysis has been previously used as an efficient and sensitive tool for detecting diseases of any source, and has been considered as one of the most important approaches to assess pollution-driven adverse effects to organisms in biomonitoring studies (Costa et al., 2009; Stentiford et al., 2003). However, the lack of information regarding lesions specifically associated to a single contaminant or a class of contaminants in fish has hampered the demonstration of a cause-effect relationship between contamination patterns and tissue damage (Costa et al., 2009). Histopathological semi-quantitative indices that integrate different microscopical alterations of a target organ into a single value have already been developed in different fish species (Bernet et al., 1999; Costa et al., 2011; Van Dyk et al., 2007). However, to our knowledge, there are no detailed histopathologic indices that integrate and unify all the lesions recorded in pelagic and benthopelagic fish.

1.2 Purpose of the study

The purpose of this project was to evaluate the role of selected wild pelagic (*Thunnus thynnus*), and benthopelagic fish species (*Dentex dentex* and *Pagellus bogaraveo*) of the Mediterranean Sea as biomonitors of aquatic pollution through the chemical quantification of OPCs and IOCs in target tissues, the investigation of possible toxicopathic-related changes, and the correlation of abnormal levels of pollutants with the observed lesions.

Particular attention was paid to the seven ‘‘target’’ non-dioxin like PCBs (congeners 28, 52, 101, 118, 138, 153 and 180) recommended for PCB monitoring by international organizations (e.g. European Union, International Council for the Exploration of the Sea (ICES), and World Health Organization) and to metals with fixed provisional tolerable weekly intake (PTWI) useful in the assessment of an ecotoxicological impact.

1.3 Hypothesis

Fish species belonging to different ecological niches and characterized by different behavioral and alimentary habits differ in bioaccumulation of toxic compounds and in severity of histopathologic lesions. Therefore, the global assessment of the marine status through the use of fish from different hydrological settings as bio-indicators represent a complementary choice to evaluate the presence and the responses of marine organisms to pollutans.

1.4 Objectives

Specifically, the main objectives of this current project could be summarized as follows:

- to assess the presence and level of metals, mineral, OCs and PCBs in selected target organs (i.e. skeletal muscle) in target fish species from different marine ecosystems;
- to test the potential of those sentinel fish for biomonitoring approaches along the Western Mediterranean Sea;
- to identify histologic lesions and structural alterations in muscle, gills, liver spleen, kidney, gonads of wild fish environmentally exposed to variable amount of toxic compounds;
- to estimate individual and group weighted indices through a semi-quantitative histopathological approach;

- to compare indices from different fish groups as an indicator of environmental pollution;
- to investigate the relationship between muscular levels of toxic compounds with defined provisional tolerable intake levels, lesion frequencies and histologic indices;
- to test the putative potential of those sentinel fish for biomonitoring approaches.

CHAPTER 2

The pollution of the aquatic environment

2.1 The Mediterranean Sea

The Mediterranean basin is one of the richest and at the same time one of the most vulnerable in the world as its marine and coastal environments are exposed to a combination of pressures as a consequence of its particular hydrographical characteristics and high anthropogenic activities (Storelli et al., 2010).

The Barcelona Convention for the Protection of the Mediterranean Sea, including the Mediterranean Action Plan (MAP) and the Mediterranean Marine Pollution Monitoring and Research Program (MEDPOL), has encouraged the implementation of monitoring programs for evaluating the health status of this water body (Storelli et al., 2010).

The impact of anthropogenic contaminants on deep-sea ecosystems is relevant within the northwestern (NW) Mediterranean basin (Koenig et al., 2013). The NW Mediterranean Sea constitutes a highly industrialized area receiving multiple land-based sources of pollution through river inputs, waste water discharges and continental runoff, as well as atmospheric deposition (Koenig et al., 2013). Recently, it has been shown that the distribution of persistent organic pollutans along the NW Mediterranean continental shelf and slope is closely related to the dispersion dynamics of organic material and fine-grained particles (Salvadó et al., 2013).

This issue is particularly relevant considering the increasing interest in deep-sea fisheries due to depleted fish stocks of the world's oceans (Koenig et al., 2013). In an attempt to set water

protection policies, the European Union (EU) has adopted the Marine Strategy Framework Directive, MSFD (EU Directive 2008/56/EC), introducing a series of criteria ("descriptors") that must be addressed in order to achievewater protection, quality standards, and "Good Environmental Status" (GES) of marine habitats (Cuevas et al., 2015). However, the choice for adequate biological endpoints and sentinel organisms is challenging and relies on solid knowledge of the etiology of stressor-induced adverse effects and the specific life-history traits that modulate those (Van der Oost et al., 2003).

2.2 Fish as indicator organism of short and long term toxicant exposures

Biomonitoring is defined as the global assessment of the environmental status through the use of adequate bio-indicators represented by organisms capable of perceiving environmental alterations. For several reasons, fish species have attracted considerable interest in studies assessing biological and biochemical responses to environmental contaminants (Van der Oost et al., 2003). Fish can be found virtually everywhere in the aquatic environment and they play a major ecological role because of their function as a carrier of energy from lower to higher trophic levels (Van der Oost et al., 2003).

Information on water pollution are determined through research in fish biomonitors of trace amounts of chemical compounds accumulated in different tissues, or with the evaluation of tissue morphological alterations induced by these substances. Additional analyses can identify changes in metabolic and biochemical processes, population dynamics and in the behavior of organisms themselves.

Given their feeding habits, predator fish can bioaccumulate OPCs and IOCs to significantly higher concentrations than those found in the water or sediment. As a matter of fact, the concentration of pollutants in the organism interferes with cellular events, inducing

perturbations in energy metabolism that can be associated with tissue alterations in fishes (Voegborlo et al., 2007).

According to their different hydrological setting, different species of fishes may represent different biomonitoring sources. Since sediments act as a sink for several metallic elements introduced to the marine environment, benthic organisms are considered as the most significant biomonitors in aquatic ecosystems for the estimation of sediment-associated metals (Abdolahpur Monikh et al., 2012). Previous studies have underlined that some demersal fish species accumulate mercury (Hg), arsenic (As), copper (Cu), cadmium (Cd), cobalt (Co), Ni (nickel), and lead (Pb) in relatively higher concentrations compared to the sediments (Rahmanpour et al., 2014; Abdolahpur Monikh et al., 2012).

Specifically, benthopelagic (demersal) fish of the Fam. Sparidae (i.e. *Dentex dentex* and *Pagellus bogaraveo*), which inhabit waters close to sea bottom, and pelagic fishes belonging to Fam. Scombridae (i.e. *Thunnus thynnus*), which dive deep sea waters and live and feed in open water column, may represent useful complementary biomonitors of sea pollution.

The black spot seabream, a very valuable, relatively long-lived demersal benthopelagic species of the Northeast Atlantic and Mediterranean Seas, has become nearly commercially extinct over fishing population collapse (Lorance, 2011). *Pagellus bogaraveo* lives and feeds on the continental shelf break and slope, on various types of bottoms (especially muddy), on seamounts (Afonso et al. 2012) and around islands at depths of up to 800 m (Menezes et al. 2006). The young are found closer to the shore, whereas the adults move to deeper waters on the continental slope and represent a major constituent of the meso-benthopelagic fish assemblage (Menezes *et al.* 2006). Fish belonging to this species are classified as protandrus hermaphrodites (i.e. they develop as functional male first, and then they can express female reproductive organs). A fraction of the population never changes

sex and is referred to as gonochoric (Lorance, 2011). Seabreams are omnivorous, with a predominantly carnivorous diet (crustaceans, molluscs, worms, small fish), and are located at trophic level 4.2. (Morato et al., 2001).

A vertical migratory behaviour was documented in seamount-associated adult blackspot seabreams, and was assumed to be an evolutionary mechanism not only for developing specific morphological and physiological adaptations for vision, but also for survivorship (Afonso et al., 2014). The blackspot seabream is now classified as "Near Threatened (NT)" in the Red List of Threatened Species in the Mediterranean Sea (Abdul Malak et al., 2011).

The common dentex is a demersal sparid coastal fish that inhabits the Mediterranean Sea. It is a gonochoristic fish (i.e. species with sexes separate, the male and female reproductive organs being in different individuals) that grows to a maximum length of 100 cm and a weight of 13 kg, with a relatively long life span (more than 20 years). As a high trophic level predator (trophic level 4.5, as reported from Marengo et al., 2014), it holds a key position in the coastal marine food webs. Despite its economic and ecological importance, scientific data on this species in its natural environment are still scant (Marengo et al., 2014).

Dentex dentex is classified by the International Union for the Conservation of Nature (IUCN) as "Vulnerable (V)" in the Red List of Threatened Species in the Mediterranean Sea (Abdul Malak et al., 2011).

Thunnus thynnus is a pelagic, oceanodromous, gonochronistic species that seasonally can be found close to shore and can tolerate a wide range of temperatures. It is a visual predator (trophic level 4.5) and preys on small schooling fishes (anchovies, sauries, hakes) or on squids and red crabs. Tunas display homing behaviour with individuals migrating back to specific spawning sites in the Mediterranean Sea (Rooker et al., 2008). Although tuna migrations between the Mediterranean Sea and the Atlantic Ocean have been well reported, part of the

bluefin tuna population remains in the Mediterranean basin for much of the year. *Thunnus thynnus* is classified by the International Union for the Conservation of Nature (IUCN) as "Endangered (ED)" in the Red List of Threatened Species in the Mediterranean Sea (Abdul Malak et al., 2011)

2.3 Histology as indicator of environmental pollution

The identification of histopathological lesions and alterations in wild organisms has been considered one of the most important approaches to assess pollution-driven adverse effects to organisms in biomonitoring studies (Cuevas et al., 2015). Histopathological analysis has been previously used as an efficient and sensitive tool for detecting diseases of any source, and it is recommended for a concurrent monitoring of fish health and aquatic pollution (Au, 2004; Costa et al., 2009; Feist et al., 2004; Stentiford et al., 2003). Given the more realistic analysis of fish health and the better extrapolation to community-based and ecosystem-based effects of toxicity, there is a growing trend for histopathologic biomarkers compared to biochemical biomarkers (Au, 2004). These biomarkers allow an easier examination of specific organs responsible for vital functions such as respiration, accumulation and biotransformation of xenobiotics in fish, for which alterations may serve as warning signs of adverse effects of animal health (Stentiford et al., 2003).

Classically, qualitative histopathological approaches have provided vital information in field-collected or tested aquatic organisms. However, the absence of numerical data makes it difficult to establish cause–effect relationships between pathology and contamination patterns, and to assess the significance of the differences between surveyed groups (Costa et al., 2009).

In an attempt to determine the degree of histopathological alterations in fish and to better understand histological findings after contaminant exposure, several authors developed the so

called "histopathologic semi-quantitative indices" (Bernet et al., 1999; Costa et al., 2011). Histopathological indices integrate different microscopical alterations of a target organ into a single value and bear an important statistical power which is critical in biomonitoring (Costa et al., 2013; Gonçalves et al., 2013; Van Dyk et al., 2007).

The wide range of sublethal changes detected across multiple organs and tissue types in several fishes indicates that multiple contaminants or agents capable of causing tissue alterations are likely to be present as pollutants in the marine environment (Schlacher et al., 2007). In particular, inflammatory and degenerative lesions of the skeletal muscles represent common findings in many fish species as a host response to pathogens or natural cell turnover, and are indistinguishable from alterations caused by environmental contaminants (Feist et al., 2015; Feist and Longshaw, 2008).

Because of its major role for the overall homeostasis in terms of nutrition, defense against toxicants and reproductive development, the liver is a susceptible target organ for a variety of toxicants (Hinton, 2001). A higher tolerance to hepatotoxins in fish has been attributed to different factors including a lower perfusion rate, toxic exposure limited to the basal hepatocellular membrane, and a homogenous distribution of biotransforming enzymes compared to most mammals (Wolf and Wolfe, 2005).

Gills interact directly with the aquatic environment and therefore represent a useful indicator of toxic damage (Evans et al., 2005). Exposure to metallic and organic contaminants has been linked to acute lesions in gills such as aneurisms, lamellar fusion, and hypertrophy/hyperplasia of the lamellar epithelium as a defense mechanism to prevent toxicants from reaching the blood stream (Da Cuña et al., 2011; Ribeiro CA et al., 2005).

Kidneys play an important role in maintaining osmotic homeostasis. Renal tissues receive large volumes of blood flow and serve as a major route of excretion for metabolites of various

xenobiotics. In fish, non-specific kidney histopathological lesions (e.g. tubular epithelial cell degeneration, necrosis and desquamation, tubular dilation, intraluminal proteinaceous or cellular casts, and necrosis of interstitial hematopoietic tissues) have been observed following exposure to organochlorine pesticides, petroleum compounds, organophosphate, herbicides and heavy metals (Au, 2004).

The dangerous level of pollutans could reflect into potential damage to the genital systems, thereby impairing reproductive success and reducing the sustainability of fish population/community (Au, 2004). Oocyte atresia, characterized by degeneration and necrosis of developing ova, occurs in the ovaries of all fish species but can become pathologic following exposure to xenobiotic compounds (Hinton et al., 1992).

CHAPTER 3

Persistent inorganic contaminants in fish

3.1 Relevant toxic compounds: persistent inorganic contaminants (IOCs)

Fish meat is considered nutritious, and highly essential in a balanced diet, being an important source of proteins and lipids of high biological value, as they accumulate minerals from the diet and deposit them in their skeletal tissues and other organs (Carvalho et al., 2005).

Although nutrient composition data for fish is widely available, knowledge of the elements present in fish is confined to selected minerals, and metallic trace element levels are known for a few seafood species only (Carvalho et al., 2005).

The oceanic burden of both essential and non-essential trace elements discharged to coastal ecosystems has been of serious environmental and health concerns (Cohen et al., 2001; Raimundo et al., 2011). The concept of environmental status takes into account the structure and functioning of the marine ecosystems together with natural physiographic, geographic and climatic factors, as well as physical and chemical conditions including those resulting from human activities in the area (Borja et al., 2010).

In recent years, the Water Framework Directive (WFD) and the Marine Strategy Framework Directive (MSFD) (EU Directive 2008/56/EC) have been implemented to improve the quality status of transitional and coastal waters (Borja et al., 2011; Raimundo et al., 2011).

Several field studies and laboratory experiments have evidenced that accumulation of metals in tissues is mainly dependent upon water concentrations of metallic elements and the length of

the exposure period, although some other environmental factors such as salinity, pH, hardness and temperature play significant roles in metal accumulation (Álvarez et al., 2009; Ansari et al., 2004; Canli and Atli, 2003). Furthermore, anatomical and physiological aspects such as the sizes of marine animals have been shown to play an important role in metal contents of tissues (Canli and Atli, 2003).

In order to ensure the protection of human health, the maximum authorized concentrations of "heavy metals" in waters and fishery products have been set by the European legislation EU Directives 2006/1181/EC and 2008/629/EC.

Metals can be categorized as biologically essential and non-essential. The non-essential metals (i.e. Al, Cd, Hg, Sn, and Pb) do not bear any recognized biological function, and their toxicity rises with increasing concentration. On the other hand, essential metals (i.e. Cu, Zn, Cr, Ni, Co, Mo, Fe, Se, V, and Mn) have a known biological role, and toxicity occurs either at metabolic deficiencies or at high concentrations (Kennedy, 2011). The most bioavailable form of metals resulting in toxicity is believed to be the dissolved ionic form. Multiple physiologic systems are affected by metals (commonly the gills) and toxicity depends on metal form and speciation, bioavailability, toxicokinetics, and toxicodynamics (Kennedy, 2011).

The biological role and functions of selected essential and not essential metallic elements considered in the study herein are reported in Table 1.

Table 1. Biological role and functions of selected essential and not-essential metallic elements in humans and fish.

Element	Essential functions	TOXIC EFFECTS ON THE ORGANISM	
		Fish	**Human**
Al	• not considered an essential element • unlikely to be a human carcinogen	• sensitive, especially in acidic water • toxicity: anorexia, weight loss, increased mortality	• retained Al accumulates in bone and brain • link with encephalopathies or Alzheimer's disease • reproductive alterations only if excessive exposure (Krewski et al., 2007)
As	• not considered an essential element	• less tolerant to dietary inorganic As • organic As (i.e. arsenobetaine) accounts for > 80 % of total As in fish National Research Council, 2005a) • fish are the major source of As for humans	• it is a chromosomal mutagen • acute toxicity: vomiting, abdominal pain, bloody diarrhea, cutaneous hyperpigmentation with depigmentation and palmoplantar hyperkeratosis • chronic toxicity: gastroenteritis, cirrhosis, portal hypertension, fatty liver, decreased hematopoiesis (Fowler et al., 2007)
Cd	• human carcinogen (Group 1) (IARC, 2012); however, little evidence of associations between oral exposure and increased cancer rates	• Cd^{2+} is the mainly absorbed species • antagonism with Ca^{2+} • toxicity: hypocalcemia, growth reduction, impairments in reproduction, development and behavior (McGeer etal.,2011); decreased protein synthesis (Muthukumaravel et al., 2007) • decreased innate immunity (Ghiasi et al., 2010)	• kidney and liver are the primary targets • chronic toxicity: glomerular dysfunction (proteinuria, glycosuria, polyuria, excretion), cortical interstitial fibrosis (EFSA, 2009; Nordberg et al., 2007) • it also causes osteomalacia and osteoporosis
Cr	• essential element • human carcinogen (Group 1) (IARC, 1990) • most common: trivalent Cr(III) • most toxic: hexavalent Cr(VI)	• assimilate Cr by ingestion or by gill uptake • acute toxicity: hematological alterations, inhibition/reduction of growth, production of reactive oxygen species (ROS) and impaired immune function (Reid, 2011; Vera-Candioti et al., 2011).	• positive *in vitro* genotoxicity results for hexavalent Cr (more toxic) and negative results for trivalent
Co	• essential element • essential component of vitamin B12 • mutagenic potential in mammalian cells	• limited information on aquatic toxicity	• the respiratory system is the target organ upon exposure through inhalation
Cu	• essential trace element; cofactor • maturation and stability of collagen and elastin; antioxidant role	• toxicosis: reproductive impairments, reduced growth and behavioral changes (Grosell, 2011); deleterious on gills, gut, sensory systems (Johnson et al., 2007) • extended exposure can evoke acclimation to Cu	• acute toxicity: salivation, epigastric pain, nausea, vomiting and diarrhea

Fe	• essential trace element; cofactor • high tolerance towards excess dietary iron in all species due to powerful mucosal block	• Fe is the 4th most abundant element on the earth, therefore, its concentration in water is pretty high • chronic toxicity: reproductive impairment	• acute toxicity: gastrointestinal erosion, toxic shock and acute hepatic necrosis
Pb	• not considered an essential nutrient • inorganic Pb is probably carcinogenic to humans (Group 2A) (IARC, 2006) and it is considered a priority hazardous substance • Pb level in bone represent a biomarker of cumulative exposure	• Pb^{2+} is the most toxic form in the aquatic environment (Mager, 2011) • acute toxicity: disruption of Na^{+}, Cl^{-} and $Ca2^{+}$ regulation and development of black tails, branchial lamellar shrinkage, blunting and fusion; increased secretion of branchial and cutaneous mucus (Olojo et al., 2004) • chronic toxicity: hematological and neurological toxic effects (Mager, 2011)	• acute toxicity: impairs cognitive function (mainly in children), hematological and cardiovascular anomalies • genotoxic
Mn	• essential trace element • considered to be one of the least toxic	• not considered to be a severe acute threat for fish • benthic invertebrates play a major role in transferring Mn to fish	• depressed iron status and haematological changes are the most common signs of Mn toxicosis
Hg	• not considered an essential element • methylmercury is possibly carcinogenic to humans (Group 2B) (IARC, 1993)	• fish are the major source of methylmercury • methylmercury affects the CNS development	• methylmercury distributes in all tissues and cross the blood-brain and placental barriers • chronic exposure: developmental CNS anomalies
Zn	• second most abundant essential element after Fe	• toxic at increased waterborne level • gills are the main target, with Ca^{2+} uptake imbalance, hypocalcemia, death (Niyogi and Wood, 2006) • it can cause growth and reproduction impairment (Hogstrand, 2011), altered gill and hearth physiology (Kori-Siakpere et al., 2008) • chronic toxicosis: acclimatation responses response for fish (Hogstrand, 2011; Niyogi and Wood, 2006)	• only exposure to high doses has toxic effects • acute toxicity (rare): abdominal pain, nausea, and vomiting, lethargy, anemia, and dizziness • chronic, high-dose toxicity: interference with the uptake of copper. Hence, many of its toxic effects are due to copper deficiency (Plum et al., 2010) • Zn is suspected to be neurotoxic at high doses • higher Zn decreases immuno-regulatory function of lymphocytes (Plum et al., 2010)Zn is lower in cases of prostatic adenocarcinomas
Ca	• do not exist in their free state, but calcium-containing minerals are common in nature	• sea fish drink enough seawater to cover the Ca need • dietary Ca can interfere with trace mineral absorption and retention. For example, high water Ca concentration reduces gill uptake of zinc from water (National Research Council, 2005b)	• renal insufficiency, and secondary renal hyperparathyroidism • vascular calcification • nephrolithiasis • several studies indicate a connection between high levels of Ca and vitamin D and pancreatic cancer

Mg	• major intracellular cation • cofactor of many enzymes	• Mg deficiency can increase the susceptibility to toxicoses from various other metals such as Al (National Research Council, 2005c)	• Mg deficiency in somehow more worrisome than Mg toxicity, and causes hyperexcitability (through a reduction in nerve resting membrane potential), reduced appetite and increases in oxidative stress • acute and chronic toxicoses: diarrhea and/ or inappetence (National Research Council, 2005c)
K	• 3rd most abundant element in most animals • it interacts with Na and Cl within the body to maintain acid-base balance and electrical and chemical concentration gradients	• K toxicosis in healthy animals is rare, since the body can readily excrete potassium as well as regulate absorption (National Research Council, 2005d)	• K is relatively nontoxic • it is required in relatively large amounts to sustain life (National Research Council, 2005d) • hyperkalemia and hypokalemia are both associated with potentially fatal arrhythmias
Na	• essential element • important for acid-base and osmotic balance	• NaCl represents about 77% of the total dissolved solids in seawater • ocean-dwelling fish constantly deal with excessively high salt environments • gills have high numbers of Na-K ATP-ase pumps to excrete the salts in seawater and retain the water to osmoregulate (National Research Council, 2005e)	• Na toxicity is now a well known cause of hypertension (Gomez-Sanchez, 2015), especially if low levels of K are present • no relationship between increased salt intake and risk of osteoporosis (Cohen and Roe, 2000)
Se	• essential trace element	• toxicity: loss of coordination, muscular spasms, loss of equilibrium, swollen abdomen, anemia, increased myeloid cells; reduced growth and feed efficiency	• acute toxicity: hypotension and tachycardia • neurotoxicity of acute Se exposure and also following low-level chronic Se overexposure (Vinceti et al., 2014)
Sr	• it is the most abundant trace element in the ocean water	• highest uptake of Sr • accumulated in otoliths, vertebrae and opercula • fish bioaccumulate strontium with an inverse correlation to levels of Ca in water	• seafood and beverage represent the main sources • Sr is chemically similar to Ca: this allows Sr to exchange for Ca in bone and other compartments: possible basis for neurotoxicity and neuromuscular perturbations (ATSDR, 2004)
Ba	• 2 forms of Ba (Ba sulfate and Ba carbonate), are often found in nature	• limited information on aquatic toxicity	• acute toxicity: gastroenteritis, abdominal pain, hypopotassemia, hypertension, cardiac arrhythmias, and skeletal muscle paralysis
Mo	• essential element • enter water under normal conditions	• not very toxic to fish, except for rainbow trouts (Tucker, 2012)	• generally considered to be of low human toxicity • chronic exposure at high levels: higher serum uric acid levels and a gout-like illness

Ag	• metallic Ag is inert • antimicrobial properties: chemotherapeutic antibacterial and antifungal agent	• at concentrations normally encountered in the environment, food-chain biomagnification of silver in aquatic systems is unlikely • it can cause an increased in plasma ammonia (Hogstrand and Wood, 1997)	• low toxicity in the human body • Ag metabolism is modulated by induction and binding to metallothionein, which help mitigating cellular toxicity
Ni	• essential trace element • Group I carcinogen (IARC, 1990), except metallic nickel	• toxicity: surfacing, rapid mouth and opercular movements, convulsions and loss of equilibrium., destruction of the gill lamellae, decreased glycogen in muscle and liver (Brix et al., 2004) • it can cause reduction in superoxide dismutase, and contractions of vascular smooth muscle (similar to those associated with hypertension in mammals) (Brix et al., 2004)	• *H. pylori* contains a nickel-dependent urease whose activity is correlated with the development of peptic ulcers (Denkhaus and Salnikow, 2014)
Sb	• natural element in environmental media • Sb^{3+} most common and toxic, and Sb^{5+}	• does not appear to accumulate in fish and other aquatic animals (ATSDR, 1992)	• emetic properties • oral exposure affects the gastrointestinal system
Tl	• not essential trace element	• it kills fish slowly at concentrations of 1–60 ppm	• the exact mechanism of toxicity is unknown • acute toxicity: gastroenteritis and peripheral neuropathy (Peter and Viraraghavan, 2005) • chronic toxicity: anorexia, headache, alopecia, blindness (Peter and Viraraghavan, 2005)
Sn	• non essential element • it exists as Sn^{2+} and Sn^{4+} oxidation states	• ditributyltin (organic Sn compound) causes atrophy of thymus (National Research Council, 2005f)	• increased Sn chloride causes decreased absorption of Zn and Se (National Research Council, 2005f)
V	• essential trace element	• moderate, non-cumulative toxicity in fish	• lung toxicity and gastrointestinal toxicity following acute respiratory and oral exposures; toxicosis via ingestion through food is very uncommon (National Research Council, 2005g)
Th	• extremely slow rate of decay; the total amount of natural Th in the earth remains almost the same	• the majority of thorium body burden in fish is in the gastrointestinal tract (Poston 1982) • thorium does not biomagnify in predators due to consumption of contaminated prey organisms	• gastrointestinal absorption is usually very low
U	•	• U toxicity is low relative to many other metals and is further reduced by increased pH, calcium, carbonates, phosphate, and dissolved organic matter in the water (Goulet et al., 2005)	• decreased renal function

In addition to the accumulation in the edible part of the fish, numerous metallic elements can induce pathological lesions detectable macroscopically or histologically. The histopathological lesions are often indicative of tissue damage as a result of chronic contamination, especially at the level of gills, spleen and liver. Furthermore, an increased frequency of hepatic and splenic tumors has been reported in various species of fish following the exposure to environmental carcinogens (Ribeiro CA et al., 2005). Alterations like epithelial lifting, hyperplasia and hypertrophy of the epithelial cells, besides partial fusion of some secondary lamellae, are examples of defence mechanisms. Generally, these changes aim to increase the distance between the external environment and the blood, and thus serve as a barrier to the entrance of contaminants (Evans et al., 2005). Additionally, the majority of the branchial lesions caused by sublethal exposures affect the lamellar epithelium. However, some alterations in blood vessels may also occur, when fishes suffer a more severe type of stress (Da Cuña et al., 2011; Ribeiro CA et al., 2005).

3.2 Analytical chemistry: fundamentals of ICP-MS instrument

Inductively coupled plasma–mass spectrometry (ICP-MS) has been gaining favor within laboratories around the world as the technique of choice for trace metal analysis (Thomas, 2008). ICP-MS is able to detect metallic elements that are at or below the single part per trillion (ppt) for much of the periodic table (Fig. 1). Therefore, ICP-MS is widely used for environmental analysis.

Major advancements for routine elemental analysis by ICP-MS included development of: (1) a stable plasma source capable of ionizing most elements of the periodic table, (2) an interface system to transfer ions from the corrosive high temperature (6000-10,000°K- atmospheric pressure (760 torr) environment of the Ar plasma into the mass spectrometer analyzer region at

room temperature and low pressure (10^{-5} torr), and (3) technology to remove interferences, notably collision/reaction cells (CRCs).

Samples are introduced into argon plasma as aerosol droplets. The plasma dries the aerosol, dissociates the molecules, and then removes an electron from the components, thereby forming singly-charged ions, which are directed into a mass filtering device known as the mass spectrometer.

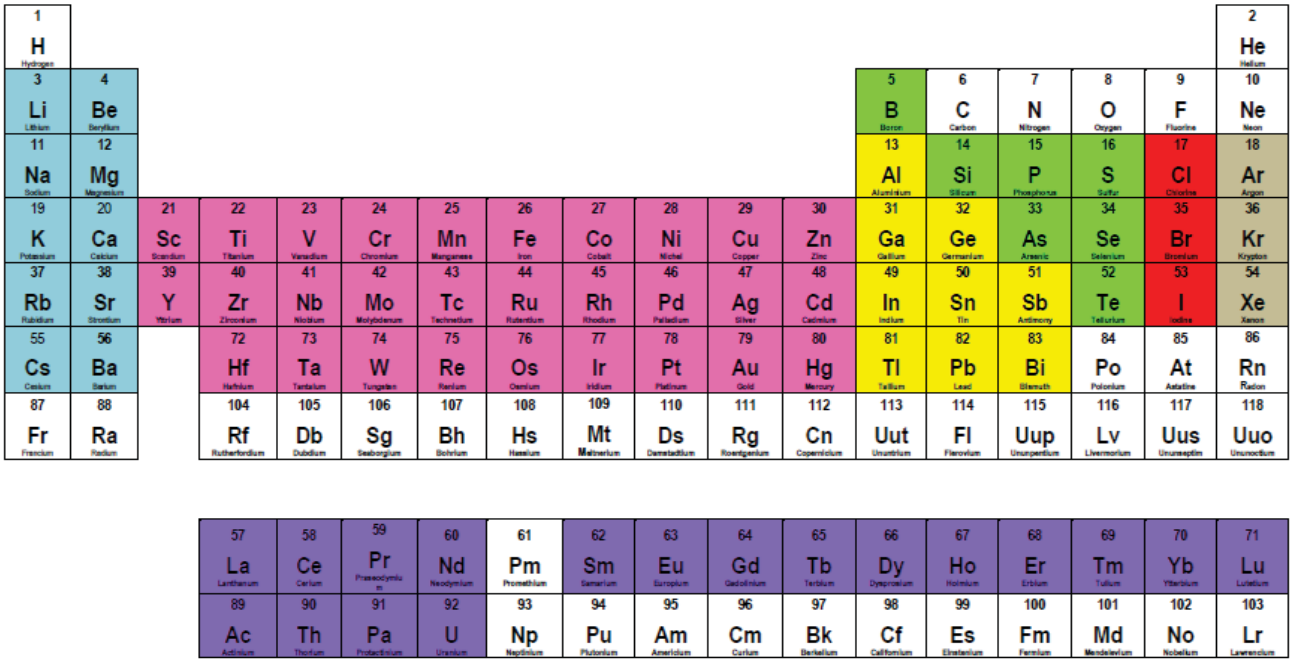

Fig.1. Metallic elements analyzed by ICP-MS (in color).

An ICP-MS consists of the following components:

1. Sample introduction system – composed of a nebulizer and spray chamber

   Most samples introduced into an ICP-MS system are liquids. It is necessary to break the liquid sample into small droplets before they can be introduced into the argon plasma.

The conventional way for liquid sample introduction in ICP-MS is based on a peristaltic pump, nebulizer, and spray chamber. The nebulizer converts the sample into a fine aerosol mist using a stream of Argon gas. The finer aerosol droplets are optimal for efficient ionization in the ICP.

2. ICP torch and RF coil – generates the argon plasma

The plasma generation in an ICP source is obtained with an oscillating magnetic field generated by a metal coil (usually copper) that encircles the distal (open) end of a series of concentric quartz tubes (the ICP torch). A high-voltage radiofrequency (RF) of 1000-1500 W is applied to the coil for plasma generation, and the flowing Argon gas ionizes to form a high temperature (~6000-10,000 K) plasma that becomes self-sustaining.

3. Interface region

The interface allows the plasma and the ion lens system to coexist and the ions generated by the plasma to pass into the ion lens region. The interface consists of two or three inverted funnel-like devices called cones, usually made of Ni or Pt, each containing a small (≤ 1mm) central orifice; the outer "sampler" cone has a larger (~2.5x) orifice compared to the inner "skimmer" cone. A pressure reduction (to 1-3 torr) in the interface region between the cones, maintained with a mechanical roughing pump, causes the incoming ion beam to dramatically expand behind the sampler cone such that the orifice of the second skimmer cone consistently passes on an ion distribution that is representative of the central analyte-rich portion of the plasma.

4. Vacuum system

Ions flow from the interface to the detector of an ICP-MS, and collisions between ions and any gas molecules should be avoided. In order to accomplish so, the vacuum system removes nearly all of the gas molecules (argon) in the space between the

interface and the detector using a combination of a turbomolecular pump and mechanical roughing pump.

5. Ion lens optics & Collision/reaction cell

The sampled ions exiting the interface region next pass through ion lens optics, which consist of one or more positively charged (typically stainless steel) lenses. This precedes the mass spectrometer and it is used to remove interferences that can degrade the detection limits achieved. The resulting positively charged ion stream then passes through the collision-reaction cell, which may be used to remove or highly attenuate polyatomic interferences.

6. Mass spectrometer - quadrupole

It filters out non-analyte, matrix, and interfering ions, allowing only the desired analyte ions of a single mass-to-charge ratio (m/z) to be transmitted to the detector, serving as a mass filter. Most laboratories are equipped with an ICP-MS with a quadrupole mass spectrometer, which consists of four parallel (conductive) rods, often made of gold-coated ceramic or molybdenum. Setting radiofrequencies (RF) and voltages applied to each set of opposing rods produce a dynamic electrostatic field within the space between the rods. Ions of a given mass-to-charge ratio remain stable within the rods and pass through to the detector.

7. Detector

The detector (usually an electron multiplier) receives and amplifies an ion signal that is proportional to concentration. Upon exiting the mass spectrometer, positive ions strike the first negative dynode of the detector, where secondary electrons are emitted from the dynode surface upon impact, and start the amplification process. The electrons released from the first negative dynode strike a positively charged second dynode,

where more electrons are released. The electron emission cascade continues until a measurable pulse is created. By counting the pulses generated, the system counts the ions that hit the first dynode.

8. Data handling and system controller

   A software controls the mass spectrometer and performs calculations on the data collected.

3.3 Material and methods

3.3.1 Case selection and collection

A total of 46 randomly selected wild caught fish were obtained from the FAO catch areas 37.1.1.in the Western Mediterranean Sea. Fish sampling occurred during the fall/winter and early spring 2012/2013.Fish were captured by drift longlining (Atlantic bluefin tuna, n=20), shore *angling* (blackspot seabreams, n=13), and trammel nets (common dentices, n=13). All fish were homogeneously selected for size (age), grossly inspected, sacrificed by cervical sectioning, and individually labeled. Fish were transported refrigerated on ice, and were weighted, measured and processed at the laboratory.

3.3.2 Histopathologic evaluation and semi-quantitative scoring system

Tissue samples were obtained from dorsal skeletal muscle, liver, spleen, gills, and reproductive tract for all groups, whereas samples from posterior kidneys were obtained only for seabreams and dentices. After dissection, all samples were fixed in 50% neutral-buffered formalin for 10 hours, routinely processed, stained with hematoxylin and eosin (HE) and mounted with DPX.

Sections were separately evaluated by two pathologists and a specific lesional scoring system was applied based on the presence and severity of all the microscopical structural and cellular

abnormalities. From each of the 3 groups, fish characterized by the lowest levels of contaminants were selected as the negative control. For all selected organs, a qualitative description of was firstly performed; secondly, both individual and group-weighted semi-quantitative indices were developed for each organ, allowing the integration of all the main recorded microscopic anomalies into a single index (H-index). Briefly, the semi-quantitative histopathologic approach consider the concepts of biological significance (weight, i.e. the impact of the lesion on the organism itself) and the degree of dissemination (score, i.e. the extension of the lesions). Specifically, histologic findings were scored as grade 0—absence of detectable abnormalities; grade 1—mild focal changes; grade 2—mild multifocal tissue alterations (tissue still recognizable); grade 3—moderate focal changes; grade 4—moderate multifocal changes; grade 5—fairly extensive lesions with disruption of the tissue architecture; grade 6—severe coalescing lesions effacing the tissue architecture.

For each organ, the histopathological alterations were divided into 4 reaction patterns: circulatory, regressive, progressive and inflammatory. The histopathologic traits in the 3 groups are summarized in Table 2. Based on their values as stated on the previous proposals (Bernet et al., 1999, Costa et al., 2009, Gonçalves et al., 2013), a weight between 1 (minimal significance), 2 (moderate impact) and 3 (highest severity) was defined for each pattern.

The H-indices were calculated through the Formula (1), as described by Gonçalves et al., 2013:

$$I_h = \frac{\sum_1^j w_j a_{jh}}{\sum_1^j M_j}$$

where I_h is the histopathological index for the individual h; w_j the weight of the j_{th} histopathological alteration; a_{jh} is the score value attributed to the j_h alteration and M_j is the attributable maximum (weight × maximum score) for the j_{th} alteration,which normalizes I_h to a value between 0 and 1.

Table 2. Observed histologic reaction patterns in fish and relative weight (w).

Organ	Reaction Pattern		Weight
Muscle	Circulatory	Hyperemia	1
		Hemorrhage	1
		Edema	1
	Regressive	Floccular degeneration	2
		Zenker's necrosis	3
	Progressive	Myofiber regeneration	2
		Reactive perimisial cells	2
		Lipidosis	2
	Inflammatory	Mixed inflammatory infiltrate	2
		Parasites	3
Gills	Circulatory	Hyperemia	1
		Hemorrhage	1
	Regressive	Necrosis	3
		Crystals	1
	Progressive	Lamellar fusion	3
		Mucous production	2
	Inflammatory	Granulomas	2
		Bacteria	2
		Parasites	3
Liver	Circulatory	Hyperemia	1
	Regressive	Degeneration	2
		Necrosis	3
		Anisokaryosis	2
	Progressive	Lipidosis	3
		Hypertrophy of MMCs	3
		Extramedullary hematopoiesis	1
		Vascular medial thickening	2
	Inflammatory	Mixed inflammatory infiltrate	2
Spleen	Circulatory	Hyperemia	1
	Regressive	Lymphoid depletion	3
		Atherosclerosis	2
	Progressive	Lipidosis	3
		Hypertrophy of MMCs	3
		Vascular medial thickening	2
	Inflammatory	Mixed inflammatory infiltrate	2
		Parasites	3
Kidneys	Circulatory	Hyperemia	1
	Regressive	Decreased hematopoietic tissue	2
		Tubular necrosis	3
		Anisokaryosis	2
		Glomerular fibrosis	2
	Progressive	Hypertrophy of MMCs	3
	Inflammatory	Mixed inflammatory infiltrate	2
		Bacteria	1
Gonads	Circulatory	Hyperemia	1
	Regressive	Germ cell atrophy/atresia	2
	Progressive	Fibrosis	2
		Hypertrophy of MMCs	3
	Inflammatory	Mixed inflammatory infiltrate	2
		Granulomas	2
		Bacteria	2

3.3.3 ICP-MS analysis

Sample preparation

The presence and level of 27 metallic elements was investigated in dorsal skeletal muscle (50-70 g) from all fish species. Based on the last electron subshell in the atom to be occupied, metallic elements were divided into four broad categories: s-block (Na, Mg, K, Ca, Sr, Ba), p-block (Al, As, Sb, Se, Sn, Tl, Pb), d-block transition (V, Cr, Mo, Mn, Zn, Co, Cd, Hg, Ag, Ni, Cu, Fe), and f-block (U, Th), as previously reported by Duffus (2002). This scheme is based on a consideration of general reactivity, and provides the basis for a rational consideration of the chemical and biological behaviour of metallic elements and their compounds.

All samples were individually placed in plastic bags, freeze-dried for 24 h, and then grounded into a fine powder using a porcelain mortar and pestle. Powdered samples were diluted concentrated HNO_3 (Suprapur HNO3 65%, Merck, Darmstadt, Germany), placed in a graphite heating block (DigiPREP digestion system, SCP Science), and digested at 75°C for 12 h. Digested samples were diluted 1:10 with double deionized water (ddH_2O) and then further diluted 1:5 with a 2 % HNO_3.

Double deionized water was used as a blank and included in each batch to determine contamination during sample preparation.

Chemicals and reagents

All solutions were prepared with analytical reagent grade chemicals and Milli-Q® Ultrapure Water Solutions Type 1 (Millipore S.A., St Quentin en Yvelines, France). Working standards were prepared in 6% (v/v) nitric acid solution without further purification.

Internal standard solutions (100 mg L^{-1}) of Bi, Ge, In, Li, Lu, Rh, Sc, Tb were purchased from Agilent Technologies (Waldbronn, Germany), and were diluted to a 1 mg L^{-1}. A multi-element

standard stock solution (10 μg mL^{-1}) composed by 26 elements was also purchased from Agilent Technologies. This stock solution was used throughout for preparation of calibration standards. Mercury (Hg) was added from its 10 μg mL^{-1} stock solution because of its incompatibility with other elements.

The measurement of individual peaks of standard materials with their retention times and peak heights were determined prior the analysis of the samples of interest. Precision and accuracy of analysis were also ensured through repeated analysis of samples against certified reference materials (CRMs) for all metals. In the method validation, the certified reference material IAEA-407 fish homogenate was purchased from the International Atomic Energy Agency, Analytical Quality Control Service (Vienna, Austria), and was used as provided without further grinding.

Instrument parameters

Muscular samples were analyzed with inductively coupled plasma mass spectrometry (ICP/MS, Agilent 7700X ICP-MS, (Agilent Technologies, Waldbronn, Germany) equipped with a CETAC ASX 500 Model 510 autosampler (CETAC, Omaha, NE), as previously reported (Arnold et al., 2014; Mok et al., 2014, Noël et al., 2005).

The Agilent 7700 ICP–MS was equipped with the following: concentric quartz nebulizer with quartz spray chamber and connecting pipe (Agilent Technologies, Waldbronn, Germany); 0.25 mm ID pump tubing for internal standards; 1.02 mm ID pump tubing for sample uptake; 1.52 mm ID pump tubing for draining; and nickel-tipped sampling and skimmer cones. The sample solutions were pumped by a peristaltic pump from tubes arranged on the autosampler, and aspirated into the argon plasma.

For better operating conditions, the instrument was operated with standard 1,550 W radio frequency (RF) power, and 14.9 L/min argon plasma gas flow. Carrier gas (helium) was optimized at 1.00 L/min. Electrostatic lens voltage was set at in the range of 190 – 195 V. Typical optimized nebulizer gas and auxiliary gas flows were 0.9 L/min helium.

Results were expressed in μg/g on a wet weight basis, as required by EU Directive 2006/1881/EC. The limit of quantification was 0.005 μg/g. Levels of Hg, Al, Cr, Mn, Ni, Cu, Zn, As, Se, Cd, Sn, Sb, Pb, U were compared to the corresponding Provisional Tolerable Weekly Intake (PTWI) or Tolerable Daily Intake (TDI) established by the Joint FAO/WHO Expert Committee on Food Additives *(*JECFA*)* and the European Food Safety Authority (EFSA).

3.3.4 Statistical analysis

In order to evaluate the spread of environmental IOCs in fish, the association between the presence of contamination and the species was assessed for each metallic element through logistic regression models. For each model, the presence/absence of metallic element was considered the response variable, with the presence defined as any concentration of metal higher than the limit of quantification (0.005 μg/g), and the absence otherwise. Fish species were included as categorical covariates in regression models, codified through dummy variables. Model results were reported as estimated proportions of contaminated fish for each species. The association was evaluated through tests of hypothesis with a two-step procedure. In the first step, the null hypothesis of no overall difference among the species was assessed using the Likelihood Ratio test. In each case, when the null hypothesis was rejected ($p<0.05$) comparisons between each couple of fish species (*Dentex* vs *Pagellus*; *Dentex* vs *Thunnus*; and *Pagellus* vs *Thunnus*) were performed. Since the proportions of contaminated fish were often equal or near to 100% (or 0% in some case), we used the Fisher exact test, which is adequate in

such cases. The no difference between species was considered the null hypothesis. The p-values were corrected for test multiplicity by Bonferroni's rule.

The distribution of the concentration of metallic elements was compared among fish species. The following criteria were adopted: 1) only those fish in which the metal was present (define above) were considered; 2) species with few contaminated fishes (less than 5) were excluded. Due to the relatively low dimension of the sample, and the non symmetric (non Gaussian) distribution of metal concentrations, robust methods of analysis were needed. Therefore, we compared median concentrations among fish species through quantile regression models (Koenker, 2005; Cade and Noon, 2003). For each metallic element, the model included metal concentration as response variable and fish species as covariate. Results were reported as median concentrations for each species, and compared using the two-step approach previously described. The variance-covariance matrix of estimates was calculated by the xy bootstrap method, and then used for performing Wald tests.

The median concentrations were further compared with the acceptable levels defined by JEFCA, where available. For each metallic element, when the test of no overall difference of median concentrations was rejected in the analysis described above, a test of hypothesis comparing the median concentration with the acceptable level of the metal was performed for each species. Otherwise, fish species were pooled, and the overall median concentration was compared with the acceptable level. In each case, the null hypothesis was that the median concentration was equal to the acceptable level.

The association between H-indices and fish species was investigated for each organ (muscle, liver, spleen, gills, kidneys and gonads). Quantile regression models were fitted, with the histopathologic indices as response variables and fish species as covariates. The procedure of analysis was equivalent to the one previously described.

Furthermore, we investigated the effect of IOC concentrations on the muscular H-indices. Only the fish in which the metal was present were considered (as described previously for the analysis of metal concentrations). For each metallic substance, a quantile regression model with muscular H index as response and fish species and metal concentration as covariates, was fitted. The relationships between the H index and concentrations of metals were assessed by the following procedure:

- a model in which the variation of the median histopathologic index determined by a variation of metal concentration is allowed to be different for distinct fish species (interaction model) was first considered; the null hypothesis of no interaction (i.e. no difference among species of the effect of metal concentration on the median H-index) was assessed. If the null hypothesis was rejected, the procedure ended; otherwise, it continued at the following step.
- a model in which metal concentration determines the same variation of the median H-index for each fish species (additive model) was fitted; the null hypothesis of no effect of metal concentration was assessed.

All the tests described above were done with bootstrapped Wald tests, as previously described. Evidence of a relationship between IOC concentration and concentration of metals derives from the rejection of the null hypothesis of the no interaction test (step 1) or the no effect test for metal concentration (step 2). Otherwise, no evident effect of metal concentration can be deduced.

3.4 Results

3.4.1 Caseload selection and groups

A total of 46 fishes from the Mediterranean Sea were collected between April 2013 and October 2013. The medium weight of the three fish categories was 37.45 kg (range 31-45 kg) for tunas, 1.23 kg (range 0.8-2.5 kg) for seabreams, and 1.89 kg (range 0.9-3.2) for dentices. The medium length of seabreams was 21.71 cm (range 18-29 cm), 43.30 cm (range 38.6-50 cm) for dentices, and 133.15 cm (range 118-141 cm) for tunas. Based on the general aspect, shape, relative dimension, position and colour of the gonads, all fishes were considered sexually mature. Specifically, dentices and seabreams were classified as stage 2C or 3 based on the revised MEDITS scale of maturity for the Mediterranean demersal species, whereas tunas were classified as stage 2 based on the ICES teleost maturity scale (Ungaro, 2008). Detailed descriptions of the aforementioned scales are reported in Table 3.

Table 3. Macroscopic evaluation and staging of gonads with application of maturation scales

ICES TELEOST MATURITY SCALE		
Stage	Maturation state	Macroscopic gonadal aspect
1	VIRGIN	Male: undeveloped, very thin translucent testes lying along an unbranched blood vessel. Female: undeveloped, small elongated white translucent ovaries.
2	MATURING	Male: testes are increasing in volume and are creamy-white; however, sperm cannot be extruded with only moderate pressure. Female: ovaries are increasing in volume, with larger eggs; however eggs cannot be extruded with only moderate pressure.
3	SPAWNING	Male: will extrude sperm under moderate pressure to advanced stage of extruding sperm freely with some sperm still in the gonad. Female: will extrude eggs under moderate pressure to advanced stage of extruding eggs freely with some eggs still in the gonad.
4	SPENT	Male: testes are shrunken, firm, not translucent, with little sperm in the gonads, but often some in the gonoducts which can be extruded. Female: ovaries are shrunken firm, not translucent, with few residual eggs and much slime; no development.

REVISED MEDITS SCALE FOR THE MEDITERRANEAN DEMERSAL BONY FISH		
Stage	Maturation state	Macroscopic gonadal aspect
0	UNDETERMINED	Sex not distinguished by naked eye. Gonads very small and translucid.
1	IMMATURE/VIRGIN	Male: small transparent, colourless or grey testes, usually shorter than 1/4 of the body cavity, situated close to vertebral column. Female: small transparent, colourless or grey ovaries, usually shorter than 1/4 of the body cavity, situated close to vertebral column. Eggs not visible to the naked eye.
2a	VIRGIN-DEVELOPING	Male: thin whitish testes shorter than 1/2 of the body cavity. Female: small pinkish/reddish ovaries shorter than 1/2 of the body cavity. Eggs not visible to naked eye.
2b	RECOVERING	Male: whitish/pinkish testes, more or less symmetrical, as long as about 1/2 of the body cavity.

		Female: pinkish-reddish/reddish-orange and translucent, ovaries as long as 1/2 of the body cavity. Blood vessels visible. Eggs not visible by naked eye.
2c	MATURING	Male: whitish to creamy testes long about 2/3 of the body cavity. Under light pressure, sperm is not expelled. Female: ovaries are granular, pink to yellow, as long as 2/3 of the body cavity. Eggs are visible to naked eye. Under light pressure, eggs are not expelled.
3	MATURE/SPAWNER	Male: whitish-creamy soft testes as long as from 2/3 to full length of the body cavity. Under light pressure, sperm could be expelled. In a more advanced maturity stage, sperm escapes freely. Female: ovaries are orange-pink, with conspicuous superficial blood vessels, as long as from 2/3 to full length of the body cavity. Large transparent, ripe eggs are clearly visible and could be expelled under light pressure. In a more advanced condition, eggs escape freely.
4a	SPENT	Male: bloodshot and flabby testes shrunk to 1/2 length of the body cavity. Female: reddish flaccid ovaries shrunk to 1/2 length of the body cavity; they may contain remnants of disintegrating eggs.
4b	RESTING	Male: whitish/pinkish testes, as long as 1/3 of the body cavity. Female: pinkish and translucent ovaries as long as 1/3 of the body cavity. Eggs not visible to naked eye.

3.4.2 Gross examination

No masses, ulcers, hemorrhages, gill anomalies, skeletal malformations, and external or visceral parasites were macroscopically detected in the 46 individuals. Twenty-four fishes were female, whereas 22 were male.

3.4.3 Persistent inorganic pollutans

The concentrations of metallic elements (μg/g) in the dorsal skeletal muscle of the 3 analyzed species are listed in Tables 4, 5 and 6 for Atlantic bluefin tunas, blackspot seabreams and common dentices respectively. The presence of metallic elements in skeletal muscles was analyzed, and the estimated proportions of contaminated fish are reported in Table 7. The proportions of Sb, Tl and U were equal to 0% for each fish species, meaning that the concentrations recorded were below the detection level of 0.005 μg/g. For several elements, the proportions were equal to 100% (Table 7); in such cases the p-values were not reported, as they were trivially equal to one. A different spread in distinct species was documented for the following elements: Al, K, Co, Mo, Ag, Cd, Sn, and Th.

Major differences were found between *Pagellus* on one side, and *Thunnus* and *Dentex* on the other side. The blackspot seabreams (*Pagellus*) were characterized by a higher frequency of Al and Sn (100.0% for both; significantly different with respect to *Thunnus* and *Dentex*), whereas tunas and dentices showed a higher frequency of Cd and Th. The frequencies of Cd and Th in the latter species were significantly different with respect to the former one, although not significantly different one another. Ag was predominant in tunas (85.0%, significantly different with respect to seabreams and dentices). Mo had a higher frequency in tunas. Other differences were found for Co and K, with a higher frequency in seabreams and tunas than in dentices. No significant differences were found for Pb.

The median concentrations of metallic elements are reported in Table 8; for this purpose, the concentrations of Sb, Tl, and U were excluded. A graphical representation of the median concentrations of metallic elements is depicted in Fig.2 (A, B, C). For the elements without maximum dietary limits, the concentration of Fe (37.634) was highest in tunas, with a significant difference compared to the other species. Na (1348.823), Sr (1.718) and Ba (0.046)

were significantly higher in seabreams. Also, higher median concentrations of Mg, Ca and V were evidenced in seabreams, although a significant difference at a level of 0.05 did not emerged when compared to the other species. In dentices, Th (0.093) was significantly predominant. Despite Mo (0.031) was also higher in dentices, no statistically significant differences were noted.

Several metals were found in quantities above the acceptable levels as defined by JECFA (Table 9). Specifically, no significant differences among fish species were found for Hg and Cd. However, the median concentrations of Hg (0.780) and Cd (0.04) in the pooled species were significantly higher than their relative PTWI. Significant differences among species were reported for Se, inorganic As, Ni and Zn. Furthermore, their median concentrations were significantly higher than the tolerable weekly intakes. Specifically, Se inorganic As and were excessively present in all species (Se: 0.682, 0.821, and 3.196 for *Dentex*, *Pagellus* and *Thunnus* respectively; inorganic As: 17.25, 4.085, 2.371 for *Dentex*, *Pagellus* and *Thunnus* respectively). An excessive amount of Ni was noted for *Pagellus* (0.058) and *Thunnus* (0.043), whereas Zn (11.464) was increased above tolerable levels only in tunas. Other elements (Al, Cr, Cu, Sn, Pb, and Mn) were found to be at or below the corresponding acceptable levels.

Table 4. part one: *Thunnus thynnus.* Fish length (cm), weight (kg) and metal concentration (µg/g) in skeletal muscles.

Fish	Weight	Lenght	Hg	Na	Mg	Al	K	Ca	V	Cr	Mn	Fe	Co	Ni	Cu
T 1	39	130	0.466	718.44	243.29	0.01	2378.85	84.92	0.045	0.036	0.116	47.07	0.010	0.045	2.346
T 2	32	125	0.994	580.06	333.88	0.005	3217.45	35.49	0.043	0.038	0.184	42.89	0.011	0.036	2.113
T 3	63	150	1.082	710.43	373.93	0.005	0.005	41.58	0.038	0.031	0.105	35.96	0.022	0.037	3.448
T 4	160	210	0.518	659.57	335.90	0.005	0.005	39.64	0.027	0.025	0.080	29.19	0.006	0.034	0.755
T 5	14	88	0.777	871.30	283.45	0.005	2456.56	88.82	0.032	0.029	0.214	21.88	0.005	0.035	0.534
T 6	15	90	0.534	968.70	296.82	0.005	2959.32	124.82	0.035	0.027	0.204	27.25	0.010	0.048	1.307
T 7	32	123	0.569	987.84	299.58	0.005	3457.78	54.55	0.033	0.029	0.241	56.45	0.014	0.043	1.400
T 8	35	129	0.524	1024.11	355.03	0.005	0.005	81.47	0.048	0.019	0.204	18.67	0.005	0.037	0.763
T 9	36	130	0.472	1155.32	368.57	0.005	3037.64	96.99	0.033	0.028	0.211	15.47	0.005	0.040	0.718
T 10	32	122	0.451	1475.64	216.36	0.005	2525.21	72.10	0.036	0.030	0.156	63.56	0.015	0.048	2.419
T11	45	136	0.376	847.23	244.00	0.005	2579.44	73.32	0.041	0.036	0.065	21.39	0.006	0.041	0.982
T12	39	130	1.653	1334.76	230.84	0.005	2341.20	132.03	0.101	0.098	0.147	79.52	0.033	0.055	3.449
T 13	40	132	1.717	1455.44	226.40	0.053	2490.15	298.88	0.041	0.032	0.258	169.33	0.062	0.048	7.035
T 14	40	133	0.944	553.74	220.12	0.005	0.005	51.78	0.029	0.023	0.147	39.31	0.007	0.036	1.644
T 15	38	130	0.993	695.91	232.12	0.005	0.005	70.37	0.025	0.021	0.178	33.67	0.012	0.039	0.873
T 16	42	135	1.067	430.12	327.42	0.005	0.005	91.25	0.026	0.020	0.153	28.99	0.006	0.043	0.875
T 17	43	130	1.011	630.59	284.78	0.005	0.005	59.05	0.036	0.032	0.216	45.02	0.013	0.047	1.272
T18	40	132	0.937	836.55	204.66	0.005	2076.86	53.81	0.038	0.026	0.143	58.25	0.021	0.052	1.444
T 19	40	133	1.071	721.76	299.20	0.005	3081.95	73.15	0.054	0.042	0.261	31.79	0.010	0.051	0.991
T20	38	130	0.967	1093.51	175.12	0.005	1847.44	70.73	0.051	0.052	0.130	56.37	0.007	0.048	3.378

Table 4. part two: *Thunnus thynnus.* Fish length (cm), weight (kg) and metal concentration (µg/g) in skeletal muscles.

Fish	Weight	Lenght	Zn	As	Se	Sr	MO	Ag	Cd	Sn	Sb	Ba	Tl	Pb	Th	U
T 1	39	130	12.545	2.614	2.794	0.473	0.019	0.031	0.084	0.005	0.005	0.058	0.005	0.020	0.075	0.005
T 2	32	125	7.345	1.427	3.780	0.136	0.037	0.031	0.158	0.005	0.005	0.014	0.005	0.008	0.067	0.005
T 3	63	150	7.639	1.624	3.073	0.143	0.016	0.055	0.314	0.005	0.005	0.017	0.005	0.006	0.064	0.005
T 4	160	210	6.426	1.886	3.662	0.276	0.012	0.006	0.049	0.005	0.005	0.024	0.005	0.011	0.049	0.005
T 5	14	88	25.795	2.158	2.326	0.570	0.016	0.012	0.183	0.005	0.005	0.023	0.005	0.008	0.059	0.005
T 6	15	90	32.243	2.291	3.354	0.911	0.025	0.005	0.395	0.005	0.005	0.026	0.005	0.008	0.062	0.005
T 7	32	123	14.193	2.273	6.280	0.345	0.040	0.011	0.195	0.005	0.005	0.020	0.005	0.010	0.061	0.005
T 8	35	129	11.008	1.830	3.455	1.031	0.014	0.005	0.043	0.005	0.005	0.010	0.005	0.005	0.047	0.005
T 9	36	130	11.503	1.850	2.880	1.253	0.016	0.005	0.028	0.005	0.005	0.012	0.005	0.006	0.055	0.005
T 10	32	122	32.931	5.584	5.640	0.336	0.036	0.033	0.478	0.005	0.005	0.018	0.005	0.009	0.067	0.005
T11	45	136	12.155	2.153	2.653	0.274	0.012	0.013	0.111	0.005	0.005	0.020	0.005	0.008	0.055	0.005
T12	39	130	39.794	2.222	4.919	0.724	0.034	0.058	0.360	0.008	0.005	0.028	0.005	0.008	0.066	0.005
T 13	40	132	60.825	2.982	9.261	1.708	0.063	0.120	0.765	0.031	0.005	0.052	0.005	0.014	0.051	0.005
T 14	40	133	9.890	5.004	3.318	0.129	0.024	0.014	0.047	0.008	0.005	0.024	0.005	0.006	0.046	0.005
T 15	38	130	10.409	4.611	2.247	0.192	0.017	0.009	0.022	0.009	0.005	0.024	0.005	0.006	0.050	0.005
T 16	42	135	7.540	2.451	1.788	0.272	0.008	0.007	0.019	0.007	0.005	0.020	0.005	0.006	0.052	0.005
T 17	43	130	10.039	3.329	2.412	0.180	0.021	0.011	0.053	0.006	0.005	0.027	0.005	0.007	0.058	0.005
T18	40	132	10.968	5.403	3.072	0.227	0.027	0.018	0.074	0.005	0.005	0.025	0.005	0.007	0.059	0.005
T 19	40	133	11.425	2.985	2.367	0.265	0.019	0.009	0.025	0.007	0.005	0.040	0.005	0.009	0.061	0.005
T20	38	130	14.722	5.828	3.377	0.335	0.028	0.055	0.053	0.005	0.005	0.030	0.005	0.007	0.060	0.005

Table 5: *Pagellus bogaraveo*. Fish length (cm), weight (kg) and metal concentration (µg/g) in skeletal muscles.

Fish	Lenght	Weight	Hg	Na	Mg	Al	K	Ca	V	Cr	Mn	Fe	Co	Ni	Cu
P 1	37	1	0.219	1842.78	304.71	0.317	3250.47	381.15	0.057	0.048	0.095	8.81	0.005	0.047	0.369
P 2	25	0.6	2.429	1834.72	250.37	0.556	3056.12	1220.34	0.079	0.067	0.156	4.37	0.006	0.059	0.124
P 3	35	2	0.954	736.11	296.58	0.208	3648.42	119.33	0.063	0.059	0.145	5.52	0.010	0.058	0.260
P 4	32	0.8	0.445	657.55	390.57	0.210	0.005	190.20	0.041	0.036	0.098	3.85	0.005	0.045	0.183
P 5	18	0.8	0.416	1363.35	353.05	0.702	0.005	355.40	0.040	0.034	0.111	7.21	0.007	0.053	0.379
P 6	19	0.78	0.982	1348.82	273.47	0.130	3517.87	307.72	0.056	0.051	0.107	8.28	0.007	0.055	0.358
P 7	19.7	0.82	0.371	1080.76	384.16	0.131	3566.76	255.17	0.061	0.058	0.082	5.38	0.007	0.064	0.252
P 8	17	0.68	0.701	1082.63	393.09	1.638	2890.32	492.35	0.068	0.044	0.149	8.09	0.012	0.058	0.426
P 9	16.9	0.65	0.336	1106.33	361.04	0.165	3215.71	898.98	0.050	0.038	0.141	6.66	0.010	0.068	0.265
P 10	39	1.2	0.148	1572.25	290.58	1.345	2744.94	652.48	0.031	0.030	0.122	5.66	0.005	0.059	0.257
P 11	39	1.3	0.362	1343.51	344.54	0.084	2855.78	362.69	0.031	0.028	0.126	4.44	0.005	0.049	0.232
P 12	38	1.1	0.963	1646.82	287.62	0.163	2790.58	956.84	0.030	0.030	0.151	5.31	0.007	0.067	0.343
P 13	36	1.2	0.813	1581.60	336.52	1.183	2736.00	170.39	0.066	0.044	0.207	17.55	0.008	0.063	0.801

Fish	Lenght	Weight	Zn	As	Se	Sr	MO	Ag	Cd	Sn	Sb	Ba	Tl	Pb	Th	U
P 1	37	1	6.034	1.864	0.923	1.633	0.040	0.005	0.005	0.013	0.005	0.046	0.005	0.016	0.071	0.005
P 2	25	0.6	3.113	1.882	0.773	6.963	0.017	0.005	0.005	0.007	0.005	0.071	0.005	0.022	0.015	0.005
P 3	35	2	3.697	12.886	0.806	0.696	0.024	0.005	0.005	0.118	0.005	0.037	0.005	0.009	0.018	0.005
P 4	32	0.8	4.259	4.796	0.821	0.972	0.014	0.006	0.005	0.133	0.005	0.030	0.005	0.010	0.014	0.005
P 5	18	0.8	4.855	4.085	0.879	1.920	0.012	0.005	0.005	0.059	0.005	0.060	0.005	0.012	0.005	0.005
P 6	19	0.78	4.538	3.821	0.803	1.690	0.008	0.005	0.011	0.009	0.005	0.043	0.005	0.014	0.005	0.005
P 7	19.7	0.82	3.815	4.682	0.540	1.627	0.007	0.005	0.006	0.216	0.005	0.054	0.005	0.011	0.005	0.005
P 8	17	0.68	4.165	4.789	0.777	2.601	0.013	0.005	0.006	0.050	0.005	0.075	0.005	0.028	0.005	0.005
P 9	16.9	0.65	4.107	4.828	0.638	5.015	0.009	0.005	0.016	0.038	0.005	0.074	0.005	0.016	0.005	0.005
P 10	39	1.2	4.156	3.022	0.909	2.310	0.005	0.005	0.005	0.025	0.005	0.043	0.005	0.011	0.005	0.005
P 11	39	1.3	4.302	2.052	0.908	1.718	0.005	0.005	0.005	0.025	0.005	0.039	0.005	0.012	0.005	0.005
P 12	38	1.1	4.101	3.271	0.888	5.759	0.005	0.006	0.005	0.006	0.005	0.077	0.005	0.021	0.005	0.005
P 13	36	1.2	7.428	4.486	1.122	1.706	0.005	0.005	0.024	0.802	0.005	0.033	0.005	0.022	0.005	0.005

Table 6. *Dentex dentex*. Fish length (cm), weight (kg), and metal concentration (µg/g) in skeletal muscles.

Fish	Lenght	Weight	Hg	Na	Mg	Al	K	Ca	V	Cr	Mn	Fe	Co	Ni	Cu
D 1	62	3.2	1.216	770.98	269.40	0.01	0.01	133.51	0.071	0.065	0.061	6.22	0.005	0.050	0.168
D 2	47	2.4	0.955	632.40	248.71	0.01	0.01	173.90	0.049	0.036	0.043	4.08	0.005	0.048	0.164
D 3	40	1	0.073	1035.37	303.21	0.904	3144.39	472.33	0.034	0.022	0.127	7.79	0.005	0.035	0.340
D 4	48	2.5	1.254	934.23	265.40	0.01	0.01	249.76	0.049	0.041	0.074	4.32	0.005	0.028	0.171
D 5	47	2.3	1.041	555.25	271.51	0.01	3570.25	86.00	0.029	0.022	0.047	3.25	0.005	0.035	0.159
D 6	42	2	1.222	523.87	265.26	0.01	0.01	67.40	0.035	0.020	0.052	3.27	0.005	0.029	0.164
D 7	46	2.3	0.812	849.52	282.35	0.01	0.01	86.67	0.031	0.021	0.072	5.63	0.005	0.033	0.228
D 8	43	2	1.230	1044.25	248.02	0.01	3114.23	98.07	0.041	0.023	0.080	8.35	0.005	0.038	0.203
D 9	45	2.5	1.201	662.95	280.69	0.01	0.01	78.52	0.028	0.018	0.055	4.31	0.005	0.070	0.178
D 10	43	1.5	0.436	683.06	308.58	0.005	0.01	101.06	0.050	0.038	0.095	8.55	0.005	0.039	0.378
D 11	44	2	0.597	860.44	280.17	0.012	0.01	1232.52	0.067	0.060	0.264	10.33	0.007	0.052	0.421
D 12	45	2.2	0.413	501.98	294.50	0.238	0.01	82.90	0.042	0.033	0.062	2.93	0.005	0.050	0.168
D 13	43	2	0.393	758.31	285.36	0.005	0.01	93.61	0.042	0.031	0.091	7.48	0.005	0.045	0.328

Fish	Lenght	Weight	Zn	As	Se	Sr	MO	Ag	Cd	Sn	Sb	Ba	Tl	Pb	Th	U
D 1	62	3.2	4.119	2.175	0.777	0.464	0.021	0.202	0.005	0.005	0.005	0.018	0.005	0.019	0.077	0.005
D 2	47	2.4	2.810	3.088	0.731	0.668	0.019	0.069	0.005	0.005	0.005	0.040	0.005	0.006	0.074	0.005
D 3	40	1	5.712	1.363	0.811	1.434	0.009	0.005	0.033	0.007	0.005	0.026	0.005	0.007	0.115	0.005
D 4	48	2.5	2.781	30.005	0.681	1.335	0.005	0.005	0.013	0.005	0.005	0.022	0.005	0.007	0.075	0.005
D 5	47	2.3	2.624	17.719	0.570	0.384	0.005	0.005	0.014	0.005	0.005	0.026	0.005	0.007	0.094	0.005
D 6	42	2	3.256	16.869	0.743	0.220	0.005	0.005	0.029	0.005	0.005	0.016	0.005	0.006	0.094	0.005
D 7	46	2.3	3.446	19.018	0.858	0.301	0.005	0.005	0.071	0.005	0.005	0.017	0.005	0.018	0.085	0.005
D 8	43	2	3.857	23.619	0.682	0.481	0.005	0.005	0.030	0.005	0.005	0.018	0.005	0.006	0.093	0.005
D 9	45	2.5	2.922	22.538	0.710	0.315	0.005	0.005	0.013	0.005	0.005	0.010	0.005	0.007	0.089	0.005
D 10	43	1.5	3.407	17.253	0.649	0.347	0.179	0.005	0.119	0.005	0.005	0.036	0.005	0.007	0.830	0.005
D 11	44	2	5.168	12.485	0.627	5.543	0.065	0.005	0.114	0.005	0.005	0.066	0.005	0.011	0.164	0.005
D 12	45	2.2	2.791	18.074	0.506	0.169	0.045	0.005	0.017	0.005	0.005	0.022	0.005	0.008	0.116	0.005
D 13	43	2	4.169	16.130	0.583	0.255	0.031	0.005	0.100	0.005	0.005	0.027	0.005	0.007	0.082	0.005

Table 7. Presence of metallic substances in fish.

For each metallic substance, the followings are reported: the estimated percentage of contaminated fish (columns 2-4 for *Dentex*, *Pagellus* and *Thunnus* respectively); Likelihood Ratio tests to compare the percentages of contaminated fish among the three species; Fisher exact tests, for specific comparisons between fish species, corrected for test multiplicity (multiple comparisons).

*statistically significant differences.

Substances	*Dentex* (n=13)	*Pagellus* (n=13)	*Thunnus* (n=20)	Likelihood Ratio	Multiple comparisons:		
				Chi-square, p-value	D vs P	D vs T	P vs T
Hg	100.0%	100.0%	100.0%				
Na	100.0%	100.0%	100.0%				
Mg	100.0%	100.0%	100.0%				
Al	23.1%	100.0%	5.0%	38.62, p<0.0001 *	p=0.00032 *	p=0.82698	p<0.0001 *
K	23.1%	84.6%	65.0%	11.27, p=0.00358 *	p=0.00405 *	p=0.02408 *	p=0.22788
Ca	100.0%	100.0%	100.0%				
V	100.0%	100.0%	100.0%				
Cr	100.0%	100.0%	100.0%				
Mn	100.0%	100.0%	100.0%				
Fe	100.0%	100.0%	100.0%				
Co	7.7%	69.2%	85.0%	22.36, p<0.0001 *	p=0.01082 *	p<0.0001 *	p>0.999
Ni	100.0%	100.0%	100.0%				
Cu	100.0%	100.0%	100.0%				
Zn	100.0%	100.0%	100.0%				
As	100.0%	100.0%	100.0%				
Se	100.0%	100.0%	100.0%				
Sr	100.0%	100.0%	100.0%				
Mo	53.8%	69.2%	100.0%	14.18, p=0.00083 *	p>0.999	p=0.00465 *	p=0.05242
Ag	15.4%	15.4%	85.0%	24.19, p<0.0001 *	p>0.999	p=0.00048 *	p=0.00048 *
Cd	84.6%	38.5%	100.0%	19.68, p<0.0001*	p=0.12422	p=0.44318	p=0.00028 *
Sn	7.7%	100.0%	35.0%	30.47, p<0.0001 *	p<0.0001 *	p=0.32311	p=0.00048 *
Sb	0.0%	0.0%	0.0%				
Ba	100.0%	100.0%	100.0%				
Tl	0.0%	0.0%	0.0%				
Pb	100.0%	100.0%	95.0%	1.69, p=0.42853			
Th	100.0%	30.8%	100.0%	29.43, p<0.0001 *	p=0.00137 *	p>0.999	p<0.0001 *
U	0.0%	0.0%	0.0%				

Table 8. Median concentrations of metallic elements.

For each metallic substance, the followings are reported: estimated median concentrations for each fish species (columns 2-4); Wald tests for a global comparison of median concentrations among species; Wald tests for specific comparisons, corrected for test multiplicity (multiple comparisons). df = degrees of freedom. [a] fish species with less than 5 contaminated fish were excluded from the analysis. *statistically significant differences.

For Al and Ag, only one species was included: thus only the median concentrations were reported. For K, Co, Sn and Th, two species were included: thus, only median concentrations and Wald test were reported.

Substances	Dentex	Pagellus	Thunnus	Wald test	Multiple comparisons:		
				F (df) p-value	D vs P	D vs T	P vs T
Hg	0.955	0.445	0.941	2.05 (2,43) p=0.14137			
Na	758.312	1348.823	841.891	5.63 (2,43) p=0.00673 *	p=0.00665 *	p=0.49762	p=0.02267 *
Mg	280.168	336.515	284.116	2.17 (2,43) p=0.12654			
Al [a]		0.210					
K [a]		3056.123	2525.207	4.21 (1,22) p=0.05222			
Ca	98.068	362.687	72.623	3.07 (2, 43) p=0.05659			
V	0.042	0.056	0.037	2.84 (2,43) p=0.06941			
Cr	0.031	0.044	0.030	3.41 (2,43) p=0.04228 *	p=0.18606	p=0.87391	p=0.06231
Mn	0.072	0.126	0.167	7.99 (2,43) p=0.00112 *	p=0.00450 *	p=0.00435 *	p=0.23079
Fe	5.626	5.662	37.634	14.75 (2,43) p<0.0001 *	p=0.98187	p<0.0001 *	p<0.0001 *
Co [a]		0.007	0.011	3.93 (1,24) p=0.05907			
Ni	0.039	0.058	0.043	10.04 (2,43) p=0.00026 *	p=0.00145 *	p=0.44256	p=0.00113 *
Cu	0.178	0.265	1.354	8.05 (2,43) p=0.00107 *	p=0.18687	p=0.00310 *	p=0.00264 *
Zn	3.407	4.165	11.464	30.43 (2,43) p<0.0001 *	p=0.05219	p<0.0001 *	p<0.0001 *
As	17.253	4.085	2.371	16.44 (2,43) p<0.0001 *	p<0.0001 *	p<0.0001 *	p=0.02711
Se	0.682	0.821	3.196	55.45 (2,43) p<0.0001 *	p=0.02358 *	p<0.0001 *	p<0.0001 *
Sr	0.384	1.718	0.306	5.69 (2,43) p=0.00643 *	p=0.06495	p=0.76411	p=0.01662 *
Mo	0.031	0.013	0.020	0.76 (2,33) p=0.47397			
Ag [a]			0.014				
Cd	0.030	0.011	0.079	1.16 (2,33) p=0.32666			
Sn [a]		0.038	0.008	1.22 (1,18) p=0.28384			
Ba	0.022	0.046	0.024	3.52 (2,43) p=0.03835 *	p=0.03224 *	p=0.62987	p=0.03224 *
Pb	0.007	0.014	0.008	4.36 (2,42) p=0.01904 *	p=0.03094 *	p=0.19648	p=0.04222 *
Th [a]	0.093		0.059	16.67 (1,31) p=0.00029 *			

Fig.2. Graphical representation of the median concentrations of metallic elements.

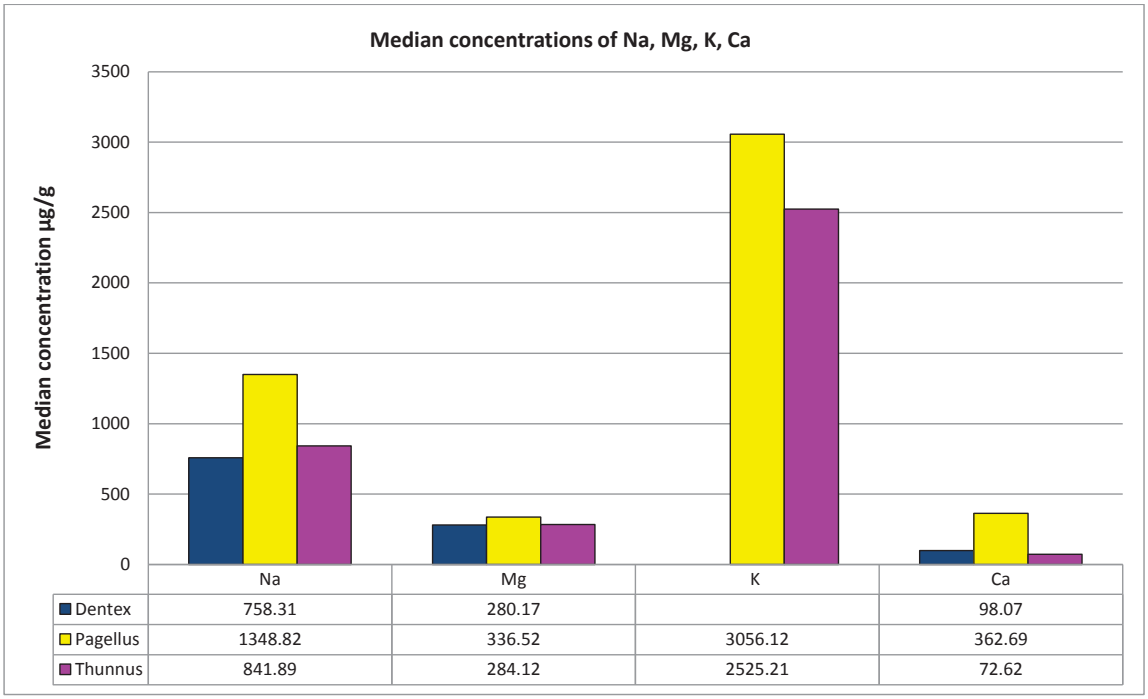

	Na	Mg	K	Ca
Dentex	758.31	280.17		98.07
Pagellus	1348.82	336.52	3056.12	362.69
Thunnus	841.89	284.12	2525.21	72.62

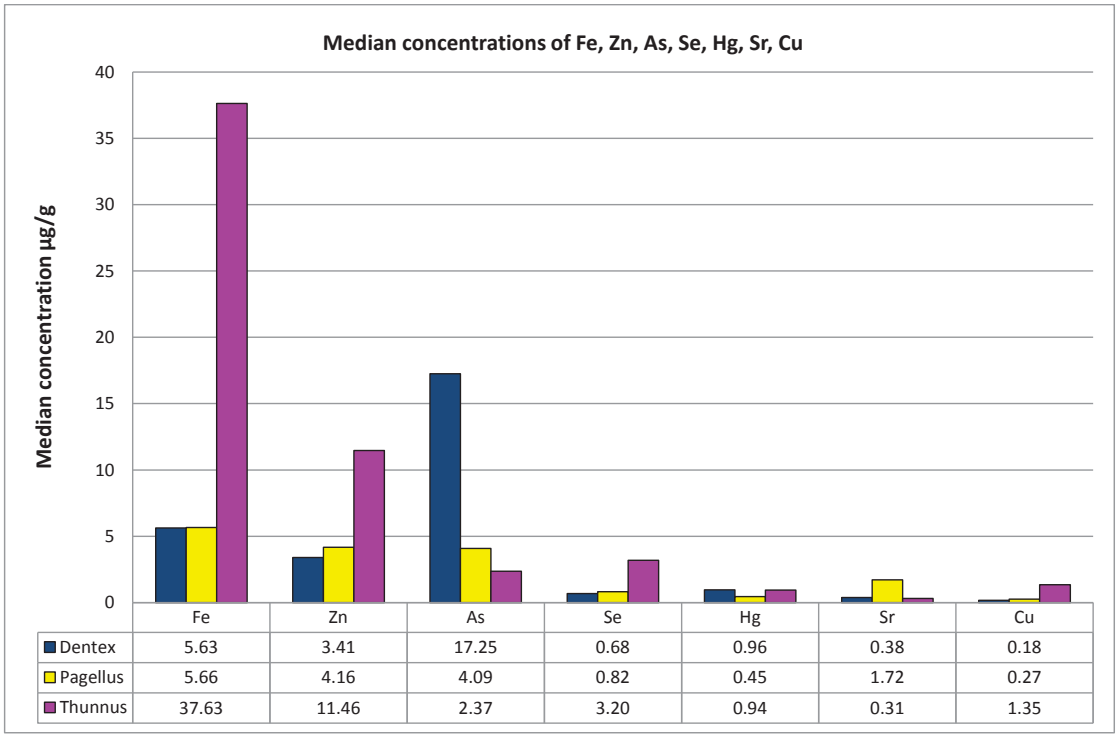

	Fe	Zn	As	Se	Hg	Sr	Cu
Dentex	5.63	3.41	17.25	0.68	0.96	0.38	0.18
Pagellus	5.66	4.16	4.09	0.82	0.45	1.72	0.27
Thunnus	37.63	11.46	2.37	3.20	0.94	0.31	1.35

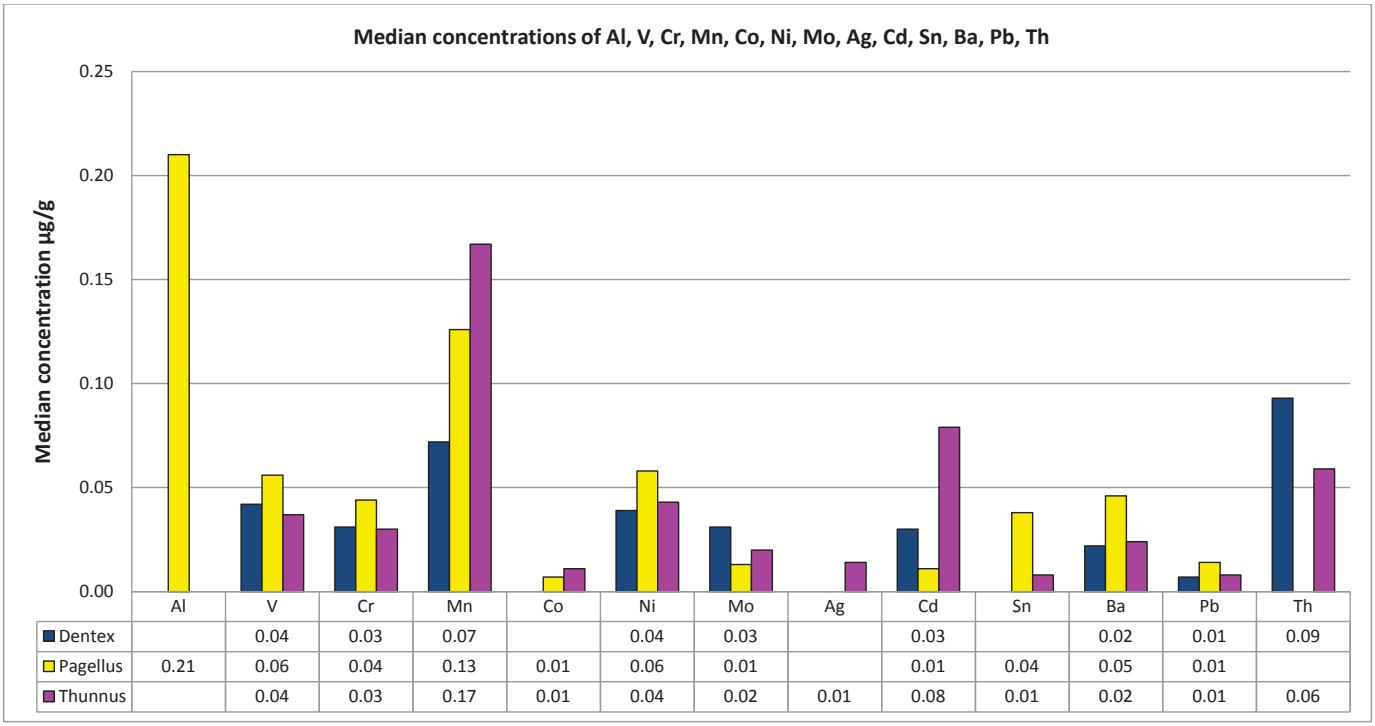

	Al	V	Cr	Mn	Co	Ni	Mo	Ag	Cd	Sn	Ba	Pb	Th
Dentex		0.04	0.03	0.07		0.04	0.03		0.03		0.02	0.01	0.09
Pagellus	0.21	0.06	0.04	0.13	0.01	0.06	0.01		0.01	0.04	0.05	0.01	
Thunnus		0.04	0.03	0.17	0.01	0.04	0.02	0.01	0.08	0.01	0.02	0.01	0.06

Table 9. Acceptable concentration levels.

For each metallic substance, the following are reported: acceptable concentration level (PTWI), Wald tests for the comparison between the median concentrations and the acceptable level, corrected for test multiplicity except in the following cases: [a] since no significant difference between species emerged in previous analysis (see: Table 8, Wald test), the comparison was performed for pooled species, [b] for Al, only one specie was included in the analysis.

* statistically significant differences.

Substances	PTWI	Wald test
Hg[a]	0.0016	pooled: t=5.48 p<0.0001 *
Al[b]	2	Pagellus: t=-10.15 p<0.0001 *
Cr	1.4	Dentex: t=-194.08 p<0.0001 * Pagellus: t=-229.99 p<0.0001 * Thunnus: t=-755.14 p<0.0001 *
Mn	1.17	Dentex: t=-63.68 p<0.0001 * Pagellus: t=-82.88 p<0.0001 * Thunnus: t=-44.32 p<0.0001 *
Ni	0.035	Dentex: t=0.86 p>0.999 Pagellus: t=8.94 p<0.0001 * Thunnus: t=2.89 p=0.01801 *
Cu	3.5	Dentex: t=-68.44 p<0.0001 * Pagellus: t=-69.46 p<0.0001 * Thunnus: t= -6.38 p<0.0001 *
Zn	7	Dentex: t=-10.21 p<0.0001 * Pagellus: t=-13.07 p<0.0001 * Thunnus: t= 5.36 p<0.0001 *
As	0.015	Dentex: t= 5.33 p<0.0001 * Pagellus: t= 5.93 p<0.0001 * Thunnus: t= 7.10 p<0.0001 *
Se	0.007	Dentex: t=18.16 p<0.0001 * Pagellus: t=19.11 p<0.0001 * Thunnus: t=13.09 p<0.0001 *
Cd[a]	0.007	pooled : t=2.72 p=0.01015 *
Sn[a]	14	pooled: t=-1180.24 p<0.0001 *
Pb	0.025	Dentex: t=-26.45 p<0.0001 * Pagellus: t=-3.82 p=0.0013 * Thunnus: t=-27.24 p<0.0001 *

3.4.4 Histopathologic indices

Overall, histopathologic indices (H-indices) were mild or moderately high (Fig.3). Considering all fish groups, the observed values ranged from a minimum of 0.01 to a maximum of 0.65 for muscle, 0.10 to 0.60 for liver, 0.11 to 0.74 for spleen, 0.02 to 0.74 for gills, 0.11 to 0.82 for kidney, and 0.00 to 0.78 for gonads. For each organ, the estimated median values for H-indices in the 3 groups are summarized in Table 10. No significant differences were found between H-indices of different species.

The concentrations of the metallic elements did not influence the muscular H-indices in all species, with the exception of Na, where the interaction between concentration of Na and fish species was statistically significant ($p=0.02960$). Specifically, the median values of muscular H-indices tend to increase with increasing Na concentration in dentices and seabreams. The action of Na tends to be different in tunas, where the variation of the median muscular H-index is less evident with increasing Na concentration.

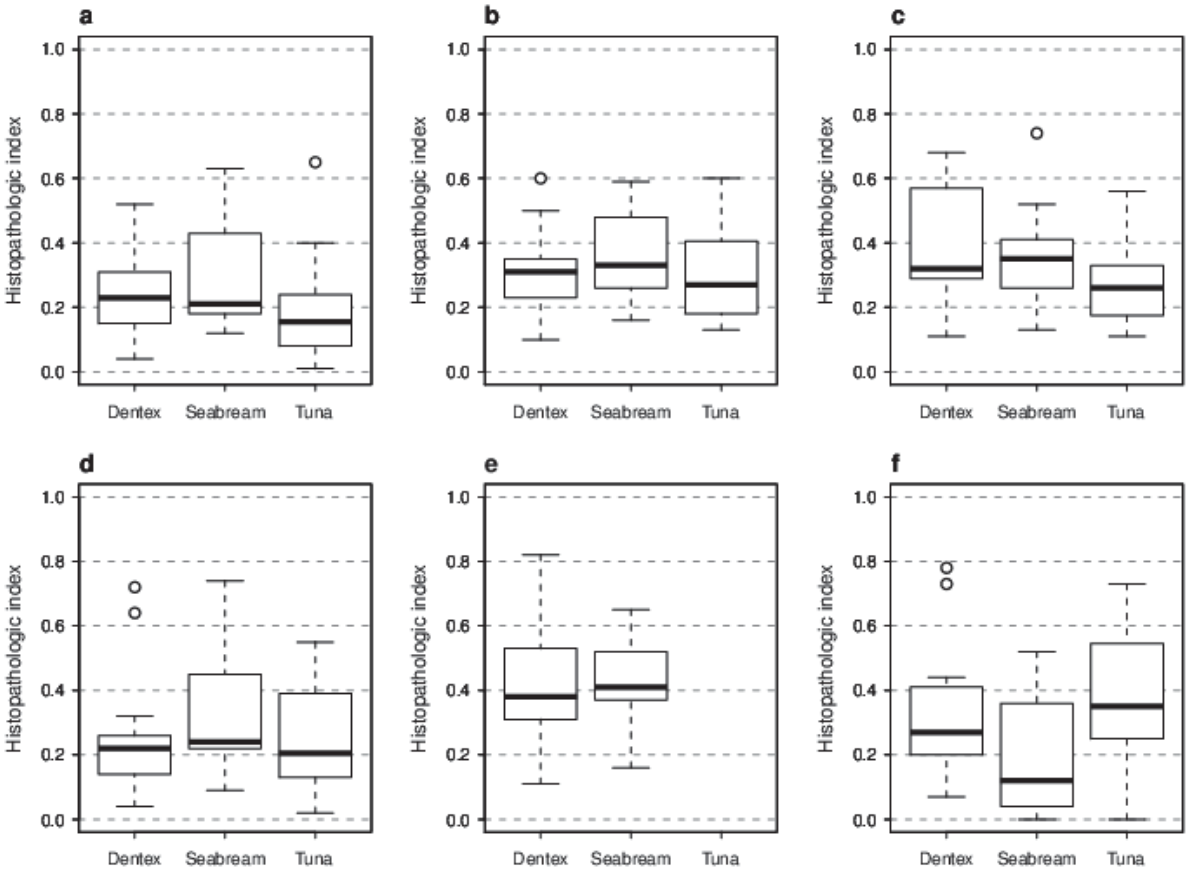

Fig.3. Sample distributions of histopathologic indices for distinct fish species.

The distributions were represented by boxplots. Panel a: muscle; b: liver; c: spleen; d: gills; e: kidney; f: gonads.

Table 10. Semi-quantitative histopathologic indices for selected organs from different fish groups. For each organ the followings are reported: estimated median values of the H-indices; comparison of the medians through the Wald test.

Organ	***Dentex***	***Pagellus***	***Thunnus***	**Wald test**
				F (df) p-value
Muscle	0.23	0.21	0.15	0.86 (2,43) p=0.43212
Liver	0.31	0.33	0.26	0.29 (2,43) p=0.74689
Spleen	0.32	0.35	0.26	1.71 (2,43) p=0.19286
Gills	0.22	0.24	0.19	0.03 (2,43) p=0.96740
Kidney	0.38	0.41		0.17 (1,24) p=0.68577
Gonads	0.27	0.12	0.34	2.14 (2,43) p=0.12978

3.4.5 Histopathology

A total of 256 samples were microscopically examined. Renal tissue was not available for tunas. A granulomatous inflammation was present in 69.5% of animals (32/46), mainly tunas (n=15), and was specifically involving gills and liver, and to a lesser extent gonads and kidneys. In the liver, anisocytosis and anisokaryosis with prominent nucleoli were evidenced in 18/46 fish (Fig. 4). In skeletal muscles, a moderate floccular degeneration and hyaline muscular changes were observed in 17/20 tunas (Fig. 5), 13/13 seabreams, and 10/13 dentices, while Zenker's necrosis was occasional in all species.

A multifocal lymphoplasmacytic interstitial myositis was observed in 11 cases (5 seabreams, 3 tunas, 3 dentices). Interestingly, a muscular parasite morphologically compatible with *Kudoa*

spp. was noted in 9 cases (1 tuna, 4 seabreams, 4 dentices). Less frequent findings included neutrophilic vasculitis, lipofuscinosis, myofibers and dystrophic mineralization in tunas.

Additionally, a prominent hypertrophy/hyperplasia of hepatic melanomacrophagic centers was detected in 31 cases (15 tunas, 8 seabreams, 8 dentices). Severe hepatic lipidosis was frequently observed both in tunas and dentices, while increased extramedullary hematopoiesis was noted in 17/13 fish.

Additionally, multifocal coagulative hepatic necrosis was evidenced mostly in tunas and dentices (Fig.6).

Renal glomeruli were within normal limit in 8 dentices and 7 seabreams, while a moderate thickening of the glomerular basement membrane was detected in the remaining cases. Furthermore, renal proximal tubules were frequently characterized by tubular epithelial degeneration and necrosis (Fig. 7), or by increased basophilia and uneven nuclei with vesicular chromatin (regeneration). Decreased hematopoietic tissue with lymphocytolysis and interstitial accumulation of eosinophilic cellular and karyorrhectic debris was evident in 17 fish.

Pathologic changes in gills included 11 cases of necrotizing branchitis with deposition of birefringent crystals, lamellar shortening, blunting and fusion (Fig. 8), and occasional cystic degeneration of the branchial epithelium. Amebic gill disease was observed in 3 fish. Other parasitic organisms were evidenced in seabreams, including Glochidium, copepods, Argulus sp. and Sphaerospora.

Splenic lymphoid follicles were decreased in number and size in approximately 50% of the examined animals. Prominent melanomacrophagic centers were observed in 63% of cases. A moderate to severe thickening and contraction of the tunica media of the splenic vessels with infiltration of foamy macrophages were noted in 5 tunas (Fig. 9). Interestingly, multifocal to coalescing splenic granulomas with intralesional nematode eggs were observed in another tuna

fish (Fig. 10). Five cases of severe necrotizing eosinophilic splenitis and panniculitis with intralesional cocci were detected in tunas and seabreams.

The ovarian tissue was composed by follicles at different stages of maturation in all female fish (Fig. 11). In particular, 9/24 females had evidence of egg yolk. The testicular examination revealed the presence of immature tubules in 9/22 fish (mainly blackspot seabream). Interestingly, severe atrophy of seminiferous tubules with loss of germ cell lineage and supporting Sertoli cells were noted in 29% of animals. Furthermore, a severe suppurative orchitis and serositis with intralesional cocci was diagnosed in a seabream.

In summary, although these findings revealed some differences in the lesional patterns between pelagic and benthopelagic fish, the overall level of histopathological injury was moderate and severe traits like neoplasms or pre-neoplastic foci were absent.

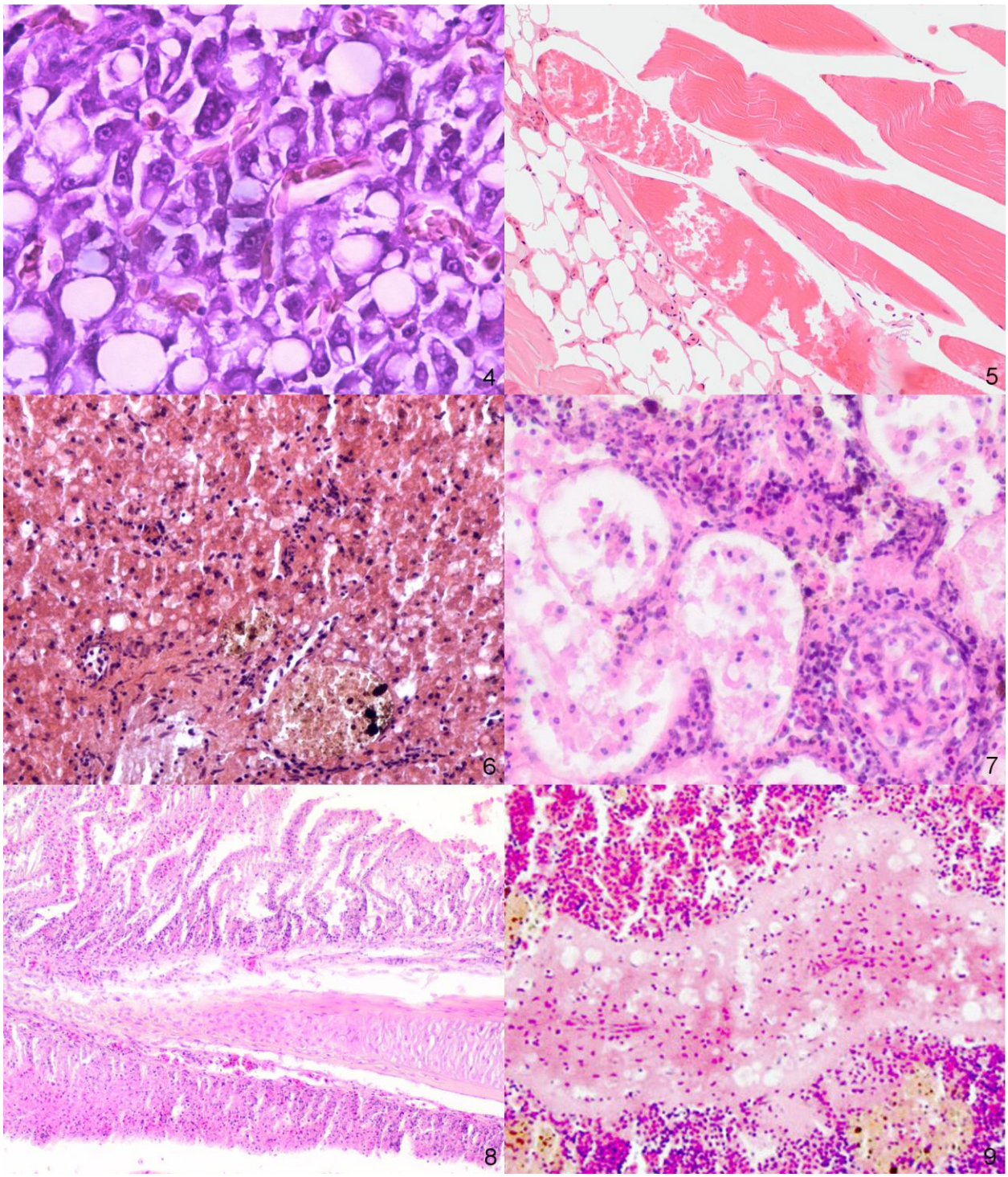
4
5
6
7
8
9

Fig.4. Liver; *Thunnus thynnus* No.13. Anisocytosis and anisokaryosis with prominent nucleoli are noted. H&E, 40x. **Fig.5.** Skeletal muscle; *Pagellus bogaraveo* No.3. Moderate floccular degeneration and Zenker's necrosis in the skeletal muscle. H&E, 40x. **Fig.6.** Liver; *Dentex dentex* No.10. The hepatic cord architecture is disrupted, and hepatocytes are characterized by loss of cellular details and pyknotic or absent nuclei. H&E, 20x. **Fig.7.** Kidney; *Pagellus bogaraveo* No.4. There is multifocal tubular degeneration and necrosis, with sloughed epithelial cells and eosinophilic cellular debris within the tubular lumina. Glomeruli exhibit thickening of the glomerular basement membrane. H&E, 40x. **Fig.8.** Gills; *Pagellus bogaraveo* No.5. Branchial lamellar shortening, blunting and fusion. H&E, 40x. **Fig.9.** Spleen; *Thunnus thynnus* No.6. Thickening of the vascular tunica media and deposition of foamy macrophages. H&E, 20x.

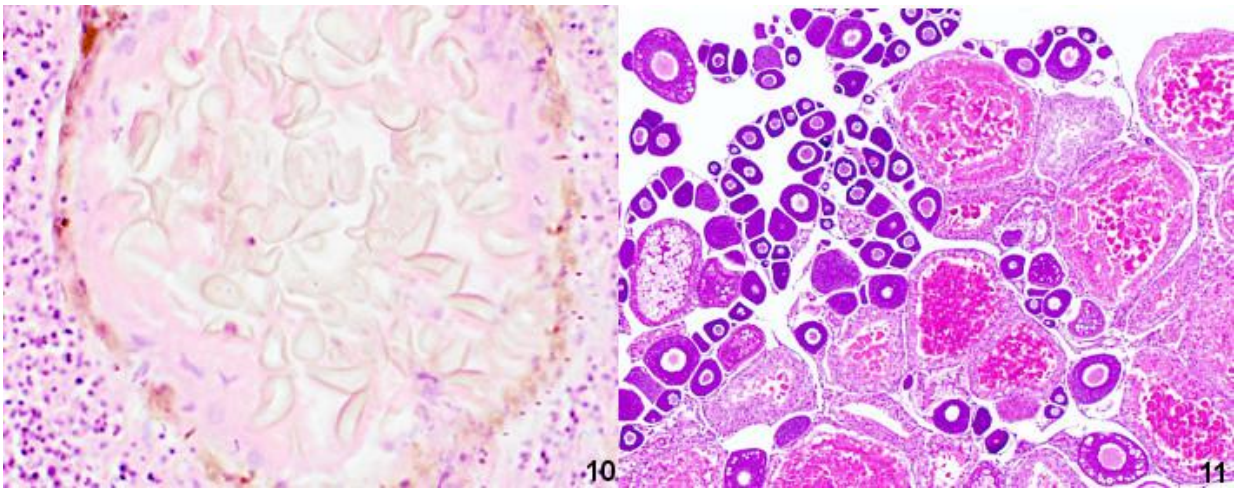

Fig.10. Spleen; *Thunnus thynnus* No.4. Focal splenic granuloma with intralesional nematode eggs. Eggs have a thick yellow capsule, and measure approximately 70-100micron in diameter. H&E, 40x. **Fig.11.** Ovary; *Pagellus bogaraveo* No.1. Ovarian follicles at multiple stages of development and maturation, with evidence of previtellogenic and vitellogenic stages. H&E, 40x.

3.5 Discussion

Research on fish contamination and human exposure is often framed in terms of a single contaminant. Given the need to define an appropriate baseline for cumulative exposure to environmental contaminants, this approach might not be most appropriate.

This study aims to encourage cross-disciplinary discussion and to establish research and monitoring priorities in order to protect the human health.

In the current study, benthopelagic and pelagic species from the Mediterranean Sea were examined as possible biomonitors of distinct environmental pollution niches. The choice of different fish species derived from the knowledge that biological and ecological factors have significant influence on metal bioaccumulation, bioavailability, and transference (Hosseini et al., 2013). Bioavailability is influenced by a complex variety of interrelated factors, such as antagonism or synergism of toxic compounds, water temperature, pH, salinity, and dissolved oxygen, and the sensitivity of the organisms depending on age and reproductive status (Ansari et al., 2004). Several studies have also indicated that the concentration of trace minerals in fish muscle may be influenced not only by external factors (food source, environment) but also by anatomical and physiological aspects (Alvarez et al., 2009). Some unexpected findings were represented by the high simultaneous levels of multiple metallic elements in the same group and the large variety of histologic lesions in fish that were randomly chosen with the only inclusion criteria of species and similar weight and lenght. Due to the homogeneously chosen small size and young age of the examined fish, the relatively high level of metals in skeletal muscle was considered a matter of concern. An immediate comparison with other caseloads was difficult due to the paucity of data regarding benthopelagic fishes as bioindicators of environmental pollution. Our results partially paralleled previous findings in *Thunnus thynnus*

from the Mediterranean Sea (Storelli, Barone, et al., 2010). However, our levels of Ca, Fe, Cu, Zn, Se, Sr, Cr, Ni, Hg, Pb, and Cd were lower than previous reports (Carvalho et al., 2005).

Marine sediments are generally considered basins for pollutants and a possible source of contamination for aquatic species (Ansari et al., 2004; Cousin and Cachot, 2014; Rahmanpour et al., 2014; Sapozhnikova et al., 2004). According to the different ecology, different levels of some metallic elements were observed in the 3 selected groups. Specifically, elements with a defined PTWI such as Hg, Cd, Se, inorganic As, Ni, and Zn, were determined to be higher with significant differences among species. This is in contrast with recent reports (Di Bella et al., 2015). Excessive levels of Se inorganic As and were present in all species.

Selenium is an essential micronutrient and cofactor for important antioxidant enzymes (Arnold et al., 2014). In humans, epidemiological studies have indicated a link between neurotoxicity and acute Se exposure, although such effect could also arise secondarily to a low-level chronic Se overexposure (Vinceti et al., 2014). Great progress on selenium toxicity in the aquatic species has been made during the last two decades. In freshwater fish, a prolonged exposure to high toxic levels has been linked to increased mortality, growth depression, reproduction impairment, and migration (Hamilton, 2004). Se has a narrow margin between dietary requirement and toxicity (Arnold et al., 2014), and may represent a potential cause for the gonadal lesions, and consequent reproductive impairment in our wild fish populations. To better support this correlation, severe histologic changes in the male genital tract were evidenced in those tunas and seabreams with the highest level of Se.

Arsenic enters rivers and is transported downstream, moving from water to sediment (Williams et al., 2006), and it tends to concentrate and persist in the upper seasoil, where benthopelagic fish (such as dentices) are located. In this study, the median concentration of total As (organic and inorganic) was higher than the PTWI set for inorganic As by the FAO/WHO in 1989.

Despite being present almost exclusively as an organic substance within marine organisms, arsenical compounds are not uniformly distributed throughout the tissues, and inorganic As could still represent 1-3.5% of the total metal (Borak and Hosgood, 2007; Storelli and Marcotrigiano, 2000). Inorganic arsenic, found mainly as arsenate and to a lesser extent as arsenite, represents the predominant toxic form of arsenic in seawater (Borak and Hosgood, 2007). Due to its toxicity and health risk for humans, the PTWI set for inorganic As is no longer considered appropriate (EFSA, 2009); however, no new tolerable intake levels have been established for food (EFSA, 2009).

An overload of Ni was recorded for *Pagellus* and *Thunnus*, with its median concentration being significantly higher than the tolerable weekly intake. Nickel has been classified as a Group I carcinogen (IARC, 1990). In rainbow trouts, Ni toxicity has been shown to induce contractions of vascular smooth muscle (Brix et al., 2004), similar to those described in our group of tunas.

Zinc has been included in the list of essential elements for its probable benefic role at low doses; however, toxicity occurs either at metabolic deficiencies or at high concentrations (Kennedy, 2011). Gills represent the main target for Zn toxicity, with consequent impairment of branchial physiology, Ca^{2+} uptake imbalance, hypocalcemia, death (Niyogi and Wood, 2006; Kori-Siakpere et al., 2008). In our study, Zn was increased above tolerable levels only in tunas. It has been observed that the level of zinc found in fish did not directly relate to the exposure concentrations. Furthermore, a recent study showed that bioaccumulation of zinc in fish is inversely related to the aqueous exposure (McGeer et al., 2003).

For Hg and Cd, our study failed to evidence significant differences among fish species from different ecosystems. However, their median concentrations in the pooled species were significantly higher than their relative PTWI. This is of great importance from the human perspective, as the main source of Hg exposure for human is represented by the ingestion of

contaminated fish, especially predators, where Hg is almost entirely present as methylmercury (MeHg). The developing human nervous system is a sensitive target for MeHg exposure (Clarkson et al. 2003). Despite MeHg at low levels is generally considered safe, an association with subclinical autoimmunity among reproductive-age females has been discovered (Somers et al., 2015).

Current research suggests that MeHg production in coastal marine sediments is one of the most important sources (Sunderland et al., 2006), where methylation is largely controlled by bacterial activity and the bioavailability of inorganic Hg (Chen et al., 2008). Recent studies indicate that MeHg concentrations are higher in pelagic than in benthic fauna, suggesting that chemical flux into the water column may be more important than biotransfer mechanisms (Chen et al., 2008). However, MeHg burdens in similar trophic-level fish have been reported to be higher in demersal than in pelagic species (Garcia-Hernandez et al. 2007).

Cadmium has been defined as a human carcinogen (Group 1) by IARC (IARC, 2012); however, there is little evidence of associations between oral exposure and increased cancer rates. Cadmium remains an important determinant of cardiovascular diseases and mortality in U.S. adults (Tellez-Plaza et al., 2012). In fish, Cd toxicity has been reported as a possible cause of decreased innate immunity (Ghiasi et al., 2010). Our finding of several infectious organisms could possibly be attributed to increased levels of this element.

For the elements without maximum dietary limits, an increased concentration of Fe, Na, Sr, Ba, and Th was documented. Despite these elements are considered less important as human toxicants, their increment could still be responsible of metabolic and organic perturbations for marine organisms with detrimental osmoregulatory failure.

Sodium chloride represents about 77% of the total dissolved solids in seawater, with calcium, magnesium, and carbonate comprising the largest proportion of the remaining solute (National

Research Council, 2005d). Marine animals are constantly trying to retain water within their bodies. Given the high number of sodium-potassium ATP-ase pumps, gills are responsible for the excretion of salts in seawater and retention of water in order to osmoregulate (National Research Council, 2005d). In our caseload, the extension and severity of the branchial lesions were more prominent in seabreams, where a Na imbalance was noted. Furthermore, the increasing Na concentration in dentices and seabreams considered herein has been significantly correlated with increasing median value of muscular H-indices.

Other elements (Al, Cr, Cu, Sn, Pb, and Mn) were found to be at or below the corresponding acceptable levels.

As previously reported, pathological changes in fish are the result of adverse biochemical and physiological alterations within the organism itself (Hinton and Lauren, 1990); thus, histopathological analysis of relevant organs is considered a useful tool to assess the overall health status of fish (Hinton and Lauren, 1990). This observation was further supported by this work where, despite the lack of gross lesions, several pathological findings were evidenced microscopically.

The wide range of sublethal changes detected across multiple organs and tissue types in fishes indicates that multiple contaminants or agents capable of causing tissue alterations are likely to be present as pollutants in the marine environment (Schlacher et al., 2007). In particular, inflammatory and degenerative lesions of the skeletal muscles represent common findings in many fish species as a host response to pathogens or natural cell turnover, and are indistinguishable from alterations caused by environmental contaminants (Feist et al., 2015; Feist and Longshaw, 2008). Lesions in the dorsal skeletal muscle were most frequently observed in tunas and to a lesser extent in the other 2 groups. Mild to moderate myofiber degeneration and necrosis paralleled previous findings in fish acutely exposed to “heavy”

metals (Kaoud and El-Dahshan, 2010). However, due to their field-collection and the presence of intralesional hemorrhages, a capture myopathy has to be considered as a possible differential diagnosis. Despite muscular alterations observed in this work remain non specific for any toxic injurious substance and the severity of muscular degeneration was not correlated to any abnormal level of toxic compound, the unusual association with perimisial reactivity and muscular regeneration should be regarded as possible consequence of chronic exposure to multiple pollutans rather than a sudden response to injury.

Because of its major role for the overall homeostasis in terms of nutrition, defense against toxicants and reproductive development, the liver is a susceptible target for a variety of toxicants (Hinton et al., 2001). A higher tolerance to hepatotoxins in fish has been attributed to different factors including a lower perfusion rate, toxic exposure limited to the basal hepatocellular membrane, and a homogenous distribution of biotransforming enzymes compared to most mammals (Wolf and Wolfe, 2005). Our findings partially paralleled previous environmental studies on microscopical hepatic changes after exposure to selected toxic compounds (Bais et al., 2012; Costa et al., 2009; Schlacher et al., 2007; Wangsongsak et al., 2007). In our caseload, hepatic lipidosis, increased extramedullary hematopoiesis, and morphological anomalies of macrophage aggregates were evidenced in all the 3 groups. Despite an extensive lipidosis was present in the majority of hepatic samples from tunas, these animals did not exhibit and increased levels of metals above the mean values reported for the entire group. Fish hepatic lipidosis is considered a general failure in lipid metabolism occurring after exposure to undifferentiated chemical compounds (Van Dyket al., 2007), and has been observed in fish exposed to metals (Giari et al., 2007), crude oil extracts, xenobiotics (Greenfield et al., 2008; Triebskorn et al., 2008), and contaminated estuarine sediments (Costa et al., 2009).

Experimental studies on livers in wild caught fish exposed to cadmium and zinc (Van Dyk et al., 2007), or to chromium, copper, nickel, lead and arsenic (Costa et al., 2009) identified hyaline droplet hepatocellular degeneration as the most conspicuous histologic change after a short term acute toxic exposure. Surprisingly, this change progressively disappeared upon long term chronic exposure to the same substances (Costa et al., 2009; Van Dyket al., 2007). In parallel, this finding was not observed in our fish species, assuming that, despite their young age, these animals can be possibly considered subject to continuous long-term exposure and chronic toxicities.

Melanomacrophagic centers are predominantly composed of cells containing lipofuscin–ceroid pigments, ferric iron and hemosiderin which have been all considered residues of the catabolism of several compounds (Ribeiro HJ et al., 2011). A correlation between fish aging and the volumetric increase of melanomacrophagic centers has been established for liver, spleen and kidney (Passantino et al., 2014). Proliferation of melanomacrophages has been also linked with starvation, increased tissue catabolism, nutritional imbalances, infectious diseases and sediment contamination (Wolf and Wolfe, 2005). In our caseload, the finding of very large and randomly distributed macrophage aggregates in liver, kidney and spleen in all groups seemed relevant, especially for relatively young animals. Given the presence of high concentrations of metals in the different species considered herein, this change was interpreted as the result of a possible cumulative effect of low but persistent doses of environmental contaminants.

In fish collected from this study, no neoplasms were detected, although an increase frequency of hepatic and splenic tumors has been reported in various fish as a result of the exposure to environmental carcinogens (Ribeiro CA et al., 2005). This could however be explained by the relative young age of the fish collected.

Gills interact directly with the aquatic environment and are therefore a useful indicator of toxic damage (Evans et al., 2005). Exposure to metallic and organic contaminants has been linked to acute lesions in gills such as aneurisms, lamellar fusion, and hypertrophy/hyperplasia of the lamellar epithelium as a defense mechanism to prevent toxicants from reaching the blood stream (Da Cuña et al., 2011; Ribeiro CA et al., 2005). As previously mentioned, severe branchial changes were observed mainly in seabreams, in which Na was reported to be significantly higher. These anomalies were most likely associate with prolonged stress and osmoregulatory disruptions rather than with an acute exposure to waterborne contaminants. Furthermore, the high number of branchial ectoparasites, and the unusual presence of birefringent crystals within the interlamellar spaces may support a hampered osmotic regulation, gas exchanges and xenobiotic metabolism, with generalized impairment of the fish health status. Atrophy of branchial mucous cells and hypertrophy of chloride cells have been previously reported, and have been correlated to environmental instability and possibly to high concentrations of petroleum aromatic hydrocarbons (PAHs) and PCBs (Costa et al., 2009; Fanta et al., 2003).

The dangerous levels of metals detected could reflect into potential damage to the immune and genital systems, and consequently reduce or damage the offspring. Major microscopic findings that could be related to chemical bioaccumulation were especially the reduction of splenic lymphoid tissue and renal hematopoietic tissue, and the severe atrophy and loss of testicular germ cells.

In the current literature, specific information regarding thickening of the tunica media of splenic arteries observed mainly in Atlantic bluefin tunas seems not to be straightforward. However, we speculate that this finding could be related to stressful conditions with impaired cardiac output and consequent hypertensive state, and possibly to the increased levels of nickel.

Furthermore, occasional thickening of the afferent glomerular arterioles and of the basement membrane of the glomerular tuft were observed in the same fish with abnormal splenic arteries, further supporting a generalized condition.

3.6 Conclusions

Chronic alterations in gills, livers, immune and reproductive systems were common in all fish species encountered, and high levels of Fe, Na, Sr, Ba, Th, Hg, Cd, Se, As, Ni, and Zn were observed in conjunction with various tissue lesions comprising testicular atrophy, renal tubular necrosis, branchitis, splenic atrophy, proliferation of melanomacrophagic centers. It is demonstrated that high levels of metals are responsible for a variety of physiological and behavioral changes in fish, and could result in human morbidity and mortality. Due to major concerns regarding fish population decrease in number and size and to the possible human chronic exposure to contaminated fish, studies addressing combined toxic effects of high levels of multiple metals should be implemented in different marine ecosystems.

Monitoring data should be collected to characterize the spatial and vertical distribution of metals in seawaters across a range of marine ecosystems.

A qualitative and quantitative histopathological approach may provide relevant information concerning alterations in field-collected or laboratory-exposed aquatic organisms. Random controls of juvenile fish from different niches should be included in the protocols for routine ecologic monitoring of seas and oceans, as they provide a valid complementary evaluation of environmental alterations. In addition, a better understanding of the general ecology of marine species is needed to properly interpret differences in toxic burden between and within species.

CHAPTER 4

Analysis of persistent organic pollutans in fish

4.1 Introduction

Antropogenic waste of persistent organic pollutants (POPs) into the marine environment has increased POP levels to a large extent in the last decades. The Mediterranean marine environment is considered one of the richest ecosystems with availability of multiple habitat niches. At the same time, it is considered one of the most vulnerable in the world as a consequence of its hydrogeographical characteristic and highly pollutant industrial activities (Koenig et al., 2013; Storelli, Losada, et al., 2010). Particularly, the impact of anthropogenic contamination of deep-sea ecosystems has been proven significant within the northwestern Mediterranean basin (Koenig et al., 2013).

Great concern has arisen during the last decade regarding the presence and concentration of POPs in the environment. Their semivolatile chemical properties and high environmental half-lives result in long-range transport and global distribution, with potential toxicity and strong tendency to bioaccumulate in living organisms (Fernández and Grimalt, 2003). The Barcelona Convention for the Protection of the Mediterranean Sea, including the Mediterranean Action Plan (MAP) and the Mediterranean Marine Pollution Monitoring and Research Program (MEDPOL), has encouraged

the implementation of monitoring programs for the evaluation of health status of the Mediterranean basin (Storelli, Losada, et al., 2010).

Amongst POPs, the worldwide contamination by persistent organochlorine pollutant compounds (OPCs) such as polychlorinated biphenyls (PCBs) and organochlorine pesticides (OCs), is of major concern due to their well known adverse effects (Kramer et al., 2012), such as neoplasms (IARC, 2013; Kramer et al., 2012), insulin resistance and diabetes (Androutsopoulos et al., 2013; Moustafalou et al., 2013), cognitive dysfunction (Bouchard et al., 2014), and elevated rate of chronic diseases such as Parkinson, Alzheimer and amyotrophic lateral sclerosis, birth defects, and reproductive disorders (Moustafalou et al., 2013).

4.1.1 Polychlorinated biphenyls

Polychlorinated biphenyls (PCBs) are poisonous and persistent organic compounds composed of 200 congeners that are stable and lipophilic. In water, they adhere to organic particles, enter the food chain after consumption by organisms, are slowly metabolized, and can be bioaccumulated even at higher trophic levels. In fish, PCBs decrease growth, cause ionic imbalance, hyperglycemia, anemia, toxicopathic lesions in tissues, such as gill, liver, and spleen, and disrupt reproduction ultimately affecting population levels (Khan, 2011).

In humans, initial epidemiological studies have indicated a link between PCBs and the development of non-Hodgkin lymphoma based on the convergence of several important factors, including the temporal correspondence between exposure to PCBs and increased incidence of lymphoid tumors, the evidence for immunotoxicity and carcinogenicity of PCBs, and the structural similarity between PCBs and dioxins, which are known as human carcinogens as well (Kramer et

al., 2012). Most research on the neurotoxic effects of PCB exposure has focused on childhood neurobehavioral impairments associated with prenatal exposure, with multiple studies reporting adverse associations between exposures and intelligence quotient and executive function, with processing speed, verbal abilities, visual recognition, memory (Boucher et al., 2009) and increased prevalence of attention deficit/hyperactivity disorder (ADHD) (Eubig et al., 2010). However, it has been shown that PCB exposure has adverse cognitive effects even at levels generally considered at low or no risk, and affecting mainly those of advanced age (Bouchard et al., 2014).

4.1.2 Organochlorine pesticides

The ecological risk assessment of pesticide use in Europe and the protection goals of related ecosystems have recently been debated by the European Food Safety Authority (EFSA). In particular, the EU Directive 2009/128/EC enforcement request Member States to adopt action plans aiming to reduce risks and impacts related to pesticide uses (Babut et al., 2013). Pesticides are well known endocrine disrupting chemicals, and are able to cross the placenta and blood–brain barrier and persist in cord blood and amniotic fluid. Therefore, there are increasing numbers of studies addressing their potential effects on the developing brain as a result of prenatal and early childhood exposure (Engel et al., 2011). Furthermore, exposure to low concentrations of some OC pesticides has been associated with metabolic dysregulation (excess adiposity and dyslipidemia) leading to prediabetic conditions (Androutsopoulos et al., 2013).

The OCs hexachlorobenzene (HCB) and dichlorodiphenyltrichloroethane (DDT) are among the most widespread POPs, and several studies have been addressed to evaluate their presence and level in fish tissues (Miranda et al., 2008). Food contamination with pesticides or their residues is

another concerning issue for human health. Agricultural and industrial activities are the most important sources of chlorinated compounds.

Common chemical feature of OCs is their high environmental persistence and high bioaccumulation in sediments and in marine and estuarine fishes. OCs represent lipophilic substances with low solubility in water; these features allow their persistence in animal organs, especially adipose tissue and nervous system. OCs interfere with the transmission of the neuronal pulse and therefore are mainly axonal neurotoxic in all mammals. In some species of fish, OCs intoxication induces behavioural abnormalities indicative of neurotoxicity and alterations of gills, liver, kidney and testes.

4.2 Fundamentals of GC-MS

Gas chromatography is a physical method of separation in which the components to be separated are distributed between two phases, one being a stationary bed of large surface area, and the other a gas that percolates through the stationary bed. The purpose of the gas chromatograph is to separate mixtures into individual components that can be detected and measured one at a time.

A typical gas chromatograph consists of an injection port, a column, carrier gas flow control equipment, ovens and heaters for maintaining temperatures of the injection port and the column, an integrator chart recorder and a detector. To separate the compounds in gas-liquid chromatography, a solution sample that contains organic compounds of interest is injected into the sample port where it will be vaporized. The vaporized samples that are injected are then carried by an inert gas, which is often used by helium or nitrogen. This inert gas goes through a glass column

packed with silica that is coated with a liquid. Materials that are less soluble in the liquid will increase the result faster than the material with greater solubility.

PCBs (except non-ortho-substituted congeners; no-PCB) and OCPs can be considered together because they are extracted and analyzed together in most cases.

The quantification of PCBs and pesticides in biological samples usually consists of three distinct steps: extraction of compounds from the sample matrix by a solvent or a combination of solvents; clean up from impurities on single or multiple columns; and finally, identification and quantification by GC with a suitable detector (MS). The combination of gas chromatography and mass spectrometry is an invaluable tool in the identification of molecules. The availability of accurate analytical standards is a fundamental requirement of an analytical program designed to quantify PCB/OCPs. Standards are available from commercial chemical supply companies as well as from agencies involved in certification of reference materials.

A GC-MS consists of the following components:

1. Injector

   It is necessary for introducing the sample at the head of the column. A calibrated microsyringe is used to deliver a sample volume in the range of a few microliters through a rubber septum and into the vaporization chamber.

2. Carrier gas

   Helium is most commonly used because of its safety, efficiency, and larger range of flow rates. Nitrogen, argon, and hydrogen are also used depending upon the desired performance and the detector being used.

3. Column

Capillary columns consist of a long tube made of glass with a small internal diameter. There are two basic forms of capillary column: a wall-coated open tubular (WCOT) column, with a thin later of the stationary phase coated along the column walls, and a support-coated open tubular (SCOT) column, where the column walls are first coated with a 30-micron-thick layer of adsorbent solid. One of the most popular types of capillary columns is the fused silica wall-coated (FSWC) open tubular column, with diameters as small as 0.1 mm and lengths as long as 100 m.

4. Column oven

Column oven houses the column and maintains a constant temperature (isothermal operation) or a variable temperature as per the requirement of analysis (temperature programming), starting at low temperature and gradually ramp to higher temperature.

5. Detector

Located at the end of the column, this device provides a quantitative measurement of the components of the mixture as they elute in combination with the carrier gas. In a GC/MS system, the sample exits the chromatography column, and passes through a transfer line into the inlet of the mass spectrometer. The sample is then ionized and fragmented, typically by an electron impact ion source. The ions flow into a mass analyzer where they are sorted according to their m/z value, or mass to charge ratio. The chromatogram will point out the retention times, and the mass spectrometer will use the peaks to determine what kind of molecules are present in the elute.

4.3 Material and methods

4.3.1 Sampling site selection

A total of 46 randomly selected wild caught fish were obtained from the FAO catch areas 37.1.1.in the Western Mediterranean Sea. Fish sampling occurred during the fall/winter and early spring 2012/2013 along the coastal area of France and Spain. Fish species selected were Atlantic bluefin tuna (*Thunnus thynnus,* n=20) captured by drift longlining, and bentopelagic fish including blackspot seabreams (*Pagellus bogaraveo,* n=13) captured by shore *angling,* and common dentices (*Dentex dentex*, n=13) captured by trammel nets. Fish were transported refrigerated on ice, grossly inspected, sacrificed by cervical sectioning, and individually labeled, weighted, measured and processed at the laboratory.

4.3.2 Microscopic evaluation

Tissue samples obtained from dorsal skeletal muscle and liver were fixed in 10% neutral-buffered formalin, routinely processed, cut onto 4 micron sections and stained with hematoxylin and eosin (HE). Sections were separately evaluated by two pathologists. A qualitative description was performed, followed by the development of a group-weighted semi-quantitative index for each organ in each fish species in order to integrate all the main microscopic anomalies into a single index (H-index). A lesional scoring system was applied based on the presence and severity of all the microscopical abnormalities. Specifically, histologic findings were scored as grade 0—absence of detectable abnormalities; grade 1—mild focal changes; grade 2—mild multifocal tissue alterations (tissue still recognizable); grade 3—moderate focal changes; grade 4—moderate multifocal changes; grade 5—fairly extensive lesions with disruption of the tissue architecture;

grade 6—severe coalescing lesions effacing the tissue architecture. The alterations were divided into 4 reaction patterns (circulatory, regressive, progressive, inflammatory), and a weight between 1 (minimal significance), 2 (moderate impact) and 3 (highest severity) was defined for each pattern, as reported in previous proposals (Bernet et al., 1999, Costa et al., 2009, Gonçalves et al., 2013). The following formula described by Gonçalves et al. (2013) was applied to calculate the H-indices:

$$I_h = \frac{\sum_1^j w_j a_{jh}}{\sum_1^j M_j}$$

where I_h is the histopathological index for the individual h; w_j represents the weight of the jth histopathological alteration; a_{jh} is the score value attributed to the j_h alteration and M_j is the attributable maximum (weight×maximum score) for the jth alteration,which normalizes I_h to a value between 0 and 1.

From each of the 3 groups, fish characterized by the lowest levels of contaminants were selected as the negative control.

4.3.3 Analytical chemistry

Chemicals and reagents

Mix solution of PCBs congeners (PCB 28; PCB 52; PCB 101; PCB 138; PCB 153 and PCB 180), PCB 209 (internal standard for PCBs), were purchased from AccuStandard (New Haven, USA). Standard solution of 16 OCs (α-HCH; Hexachlorobenzene; β-BHC; Lindane; Heptachlor; Aldrin; Heptachlor epoxide; Trans Chlordane; 4,4'-DDE; Endosulfan I; 2,4'-DDT; Endrin; 4,4'-DDD; Endosulfan II; 4,4'-DDT and Endosulfan sulfate) was purchased from Restek (Bellefonte, PA,

USA). Silica gel 60 (0.063–0.200mm) was purchased from Merck (Darmstadt, Germany) and diatomaceous hearth was purchased from Thermo-Fisher Scientific. Hexane, isooctane, ethyl acetate, acetone (special grade for pesticide residue analysis (Pestanal) and 4-nonylphenol (IS for OCs) were purchased from Fluka (Sigma-Aldrich, St. Louis, MO, USA). Working solution were prepared by diluting the stock solution in hexane for pesticides and then stored at −40°C. Mixed compound calibration solution, in hexane, was prepared from the stock solutions and used as spiking solutions as well. Matrix-matched standards were prepared by adding appropriate amounts of standards to the control matrix covering the range from 0.005 mg Kg^{-1} to 0.1 mg kg^{-1}. However, since a wide range of contaminants were included in the study, for some the MRLs were still below this concentration and for others they were well above this concentration.

Accelerated Solvent Extraction (ASE) procedure with clean-up "in line"

In order to analyse a large number of pesticides from different classes, a simple extraction and clean up in single step ("in-line") method was optimised to expand range applicability. The extraction was performed using an ASE 350 (Thermo-Fisher Scientific, Waltham, MA, USA). The extraction conditions were presented in Table 11. A 33 mL cells for accelerated solvent extraction (ASE) were used for the analysis. A representative portion (300 g) of muscle was obtained from each fish and minced, then 3 g were homogenised with an equal weight of diatomaceous earths, sodium sulphate. One mL of isooctane solution containing the three IS was added. To fill the remaining empty part of the cell diatomaceous earths were added. The cells were packed with one cellulose filter at the bottom followed by the fat retainer. The dried samples were transferred into the ASE cells. The fat retainer, solvents, solvent composition, and flush volume were previously

optimized (data not shown); temperature (80 ◦C), pressure (1500 psi), number of static cycles, and purging time (90 s with nitrogen) were fixed throughout the study. The extraction solvent was a mixture of hexane/acetone (4:1, v/v). Organic extracts were finally collected in a 66 mL vials and treated with sodium sulphate to remove any possible humidity. Afterwards, the extract was collected and dried under vacuum in a centrifugal evaporator at a temperature of 30°C. The residue was dissolved in 50 µL of isooctane and submitted to analysis by GC/MS-MS.

An uncontaminated fish sample used as control was selected for all procedure's optimization steps. For fish fortification, 3 g of the control sample was spiked by adding an appropriate volume of the standard working solution to cover the concentration range from 0.005 mg Kg^{-1} to 0.1 mg kg^{-1} in relation to pesticide MRLs realise the matrix-matched calibration curves.

Table 11. Accelerated Solvent Extraction (ASE) parameters for analysis of POPs in fish

Temperature	**Pressure**	**Static time**	**Cycles**	**Rinse volume**	**Fat retainer (neutral silica)**	**Cell Size**
(°C)	(psi)	(min)	(n°)	(%)	(g)	(mL)
80	1500	10	3	90	10	33

GC-MS/MS analysis of POPs

Triple quadrupole mass spectrometry (QqQ) in electronic impact (EI) mode was employed for the simultaneous detection and quantification of POPs in fish samples.

A GC Trace 1310 chromatograph coupled to a TSQ8000 triple quadrupole mass detector (Thermo Fisher Scientific, Palo Alto, CA, USA), was used to confirm and quantify residues in fish samples by using a fused-silica capillary column Rt-5MS Crossbond-5% diphenyl 95% dimethylpolysiloxane (35 m x 0.25 mm i.d., 0.25 μm film thickness, Restek, Bellefonte, PA, USA). The oven temperature program was: initial temperature 80 °C, hold 3 min, increased to 170 °C at 10 °C min^{-1}, then from 170 °C to 190 °C at 3 °C min^{-1}, then raised to 240 °C at 2 °C min^{-1}, then ramped to 280 °C at 3 °C $min^{-1}$and finally from 280 °C to 310 °C at 10 °C min^{-1} and held at this temperature for 5 min. The carrier gas (helium, purity higher than 99.999%) was in constant flow mode at 1.0 ml min^{-1}. A volume of 1 μL was injected using programmed temperature vaporizer injection (PTV) in splitless mode with a 1-min splitless period and the following inlet temperature programme: 80 °C (0.05 min), 14.5 °Cs^{-1} to 200 °C (1 min) and 4.5 °C s^{-1} to 320 °C (12 min – cleaning phase). A baffle liner (2 mm × 2.75 mm × 120 mm, Siltek-deactivated; Thermo Fisher Scientific) was used. The transfer line was maintained at 270 °C and the ion source at 250° C. The electron energy and the emission current were set to 70 eV and 50 μA, respectively. The scan time was 0.3 s and the peak widths of both quadrupoles were 0.7 Da full widths at half maximum. Argon was used as a collision cell gas at a pressure of 1.5 mTorr. The QqQ mass spectrometer was operated in selected reaction monitoring mode (SRM) detecting two-three transitions per analyte, Identification of pesticides was carried out by comparing sample peak

relative retention times with those obtained for standards under the same conditions and the MS/MS fragmentation spectra obtained for each compound.

The XcaliburTM processing and instrument control software program and Trace Finder 3.0 for data analysis and reporting (Thermo Fisher Scientific) were used.

Validation parameters and quality control

The method was evaluated for its repeatability, linearity, recovery, limit of detection and quantification. According to European SANCO guideline, LOQ is defined as "the lowest validated spiked level meeting the method performance acceptability criteria" (mean recovery within the range 70%-120% and RDS <20%. Values of LOQ are reported in Table 12.

Recovery of the analytes and method repeatability (expressed as relative standard deviation, R.S.D. %) studies were carried out at fortification level of 1.0 ng g^{-1} - six replicates each by adding known quantities of POPs standard solution to 3 g of homogenized fish (SANCO/12571/2013; Panseri et al, 2011).

Table 12. Recoveries (% RDS), LOQ and determination coefficient (r^2) of the method

Contaminants (POPs)	LOQ (ng g^{-1}w.weight)	Recovery % (RDS)	Determination coefficient (r^2)
Polychlorobyphenils (PCBs)			
PCB 18	0.22	98 (5)	0.9993
PCB 28	0.24	102 (7)	0.9994
PCB 31	0.15	90 (5)	0.9995
PCB 44	0.12	101 (7)	0.9997
PCB 52	0.21	103 (7)	0.9999
PCB 101	0.12	97 (4)	0.9999
PCB 118	0.09	95 (8)	0.9998
PCB 138	0.15	105 (4)	0.9999
PCB 149	0.12	98 (6)	0.9995
PCB 150	0.06	102 (4)	0.9999
PCB 154	0.18	98 (9)	0.9999
Organochlorines (OCs)			
α HCH	2.97	78 (10)	0.9959
Hexachlorobenzene	3.78	80 (12)	0.9945
β BHC	3.51	85 (12)	0.9995
Lindane (γ HCH)	2.39	96 (10)	0.9985
Heptachlor	2.84	93 (12)	0.9996
Aldrin	2.55	75 (14)	0.9991
Heptachlor epoxide	2.73	77 (14)	0.9994
Trans chlordane	4.44	92 (10)	0.9993
Endosulfan I	3.38	80 (13)	0.9992
pp' DDE	2.55	97 (12)	0.9994
Endrin	2.98	88 (11)	0.9998
Endosulfan II	3.42	90 (10)	0.9993
pp DDD	2.74	87 (14)	0.9986
op DDT	2.83	82 (14)	0.9963
Endosulfan sulfate	3.22	85 (12)	0.9921
pp' DDT	2.74	95 (12)	0.9992

4.4 Results

4.4.1 Caseload selection and inspection

A total of 46 fishes from the Western Mediterranean Sea were collected. The medium weight of the three fish categories was 1.23 kg (range 0.8-2.5 kg) for seabreams, 1.89 kg (range 0.9-3.2 kg) for dentices, and 37.45 kg (range 31-45 kg) for tunas. The medium length of seabreams was 21.71 cm (range 18-29 cm), 43.30 cm (range 38.6-50 cm) for dentices, and 133.15 cm (range 118-141 cm) for tunas. Based on the general aspect, shape, relative size, position and colour of the gonads, all fish were considered sexually mature. A total of 24 fish were female, whereas 22 were male. There was no evidence of macroscopically detectable lesions within external or internal organs.

4.4.2 Histopathology

The histopathologic muscular and hepatic findings, and corresponding H-indices for the 3 groups, are summarized in Table 13. Changes in skeletal dorsal muscles included moderate floccular degeneration and hyaline muscular changes observed in 17/20 tunas (Fig. 12), 13/13 seabreams, and 10/13 dentices, while Zenker's necrosis was occasional. A multifocal lymphoplasmacytic interstitial myositis was observed in 11 cases (5 seabreams, 3 tunas, 3 dentices). Parasites morphologically compatible with *Kudoa spp*. were noted in 9 cases (1 tuna, 4 seabreams, 4 dentices), multifocally causing enlargement and disruption of skeletal fibers. Muscular interstitial lipidosis was most frequently seen in tunas, and similarly for hemorrhage and edema of the perimuscular soft tissues. Less frequent findings included neutrophilic vasculitis, lipofuscinosis, hyperemia, regenerating myofibers and dystrophic mineralization in tunas.

In the hepatic parenchyma, multifocal coagulative hepatic necrosis was mostly evidenced in tunas and dentices (Fig. 13). Additionally, hepatic anysocytosis and anisokaryosis, and severe hepatic lipidosis were documented. There was a prominent hypertrophy/hyperplasia of hepatic melanomacrophagic centers, and the incidence of this finding in tunas was twice the one for the other fish species.

Table 13. H-indices for skeletal muscles and livers from the 3 different fish groups.

H-indices	*Thunnus thynnus*	*Pagellus bogaraveo*	*Dentex dentex*
Skeletal muscle	0.18	0.31	0.24
Liver	0.30	0.36	0.32

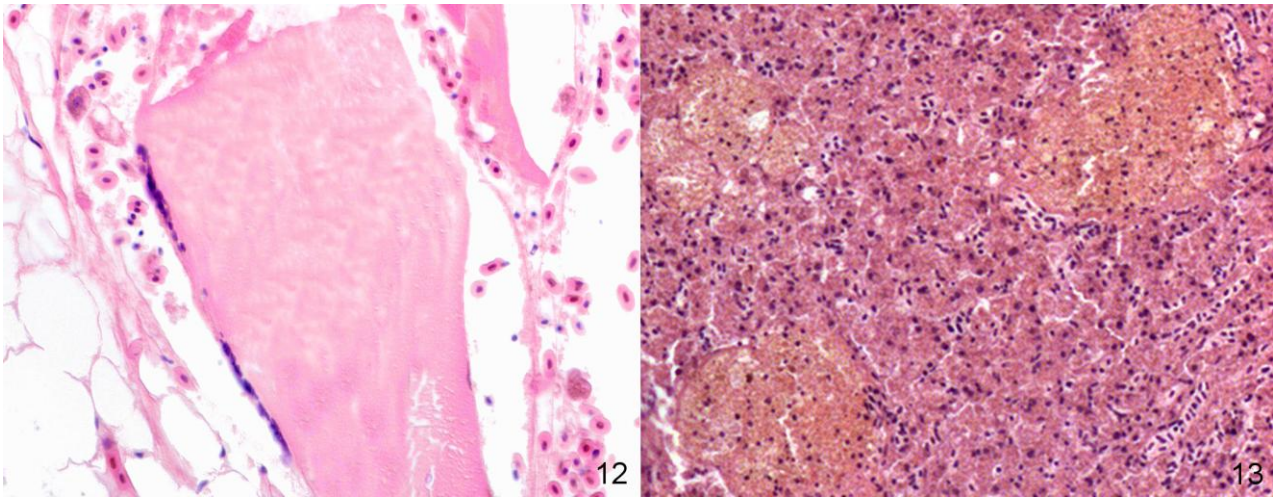

Fig.12 Skeletal muscle; *Thunnus thynnus* No.3. Floccular degeneration with hypereosinophilic homogeneous cytoplasm and loss of cross striation (hyaline degeneration) of scattered myofibers. H&E, 40x. **Fig.13** Liver; *Thunnus thynnus* No.5. Locally extensive loss of viable hepatocytes and accumulation of eosinophilic cellular and karyorrhectic necrotic debris. HE, 40x.

4.4.3 PCBs and OCs

The mean concentrations of non dioxin-like PCBs congeners and OCs in the dorsal skeletal muscles are summarized in Table 14. The concentration of PCBs was higher in samples obtained from *Pagellus bogaraveo*, closely followed by *Thunnus thynnus,* whereas muscles collected from *Dentex dentex* demonstrated the lowest concentrations.

Figures 14 and 15 depict the current total ion chromatograms (GC-MS/MS) of blank *Pagellus* sample spiked with POPs and of *Pagellus* sample naturally contaminated with POPs, respectively.

Tissue analysis for OCs revealed highest levels of sum endosulfan, sum heptachlor, and endrin aldehyde in *Thunnus thynnus*, whereas sum DDT, sum HCH, endrin, and aldrin were highest in *Pagellus bogaraveo* and *Dentex dentex* respectively.

Table 14. Mean concentrations of non dioxin-like PCBs congeners and OCs in the dorsal skeletal muscles of fish.

Polychlorobyphenils (PCBs)	***Thunnus thynnus***	***Pagellus bogaraveo***	***Dentex dentex***
PCB 18	0.022	0.132	0.15
PCB 28	0.035	0.2	0.18
PCB 31	0.101	0.103	0.085
PCB 44	0.1	0.325	0.25
PCB 52	0.061	0.375	0.045
PCB 101	0.89	0.9	0.75
PCB 118	0.212	0.233	0.12
PCB 138	1.48	2.89	1.38
PCB 149	1.93	2.75	2.2
PCB 180	2.56	3.2	2.1
PCB 194	1.44	2.25	1.35
Organochlorines (OCs)	***Thunnus thynnus***	***Pagellus bogaraveo***	***Dentex dentex***
sum DDT	132	254	110
sum HCH	3.54	7.56	2.59
sum endosulfan	27.5	10.93	8.94
sum heptachlor	14.2	10.25	5.54
endrin	3.45	2.47	3.55
endrin aldehyde	70.25	60.12	54.32
aldrin	85.44	95.55	90.45

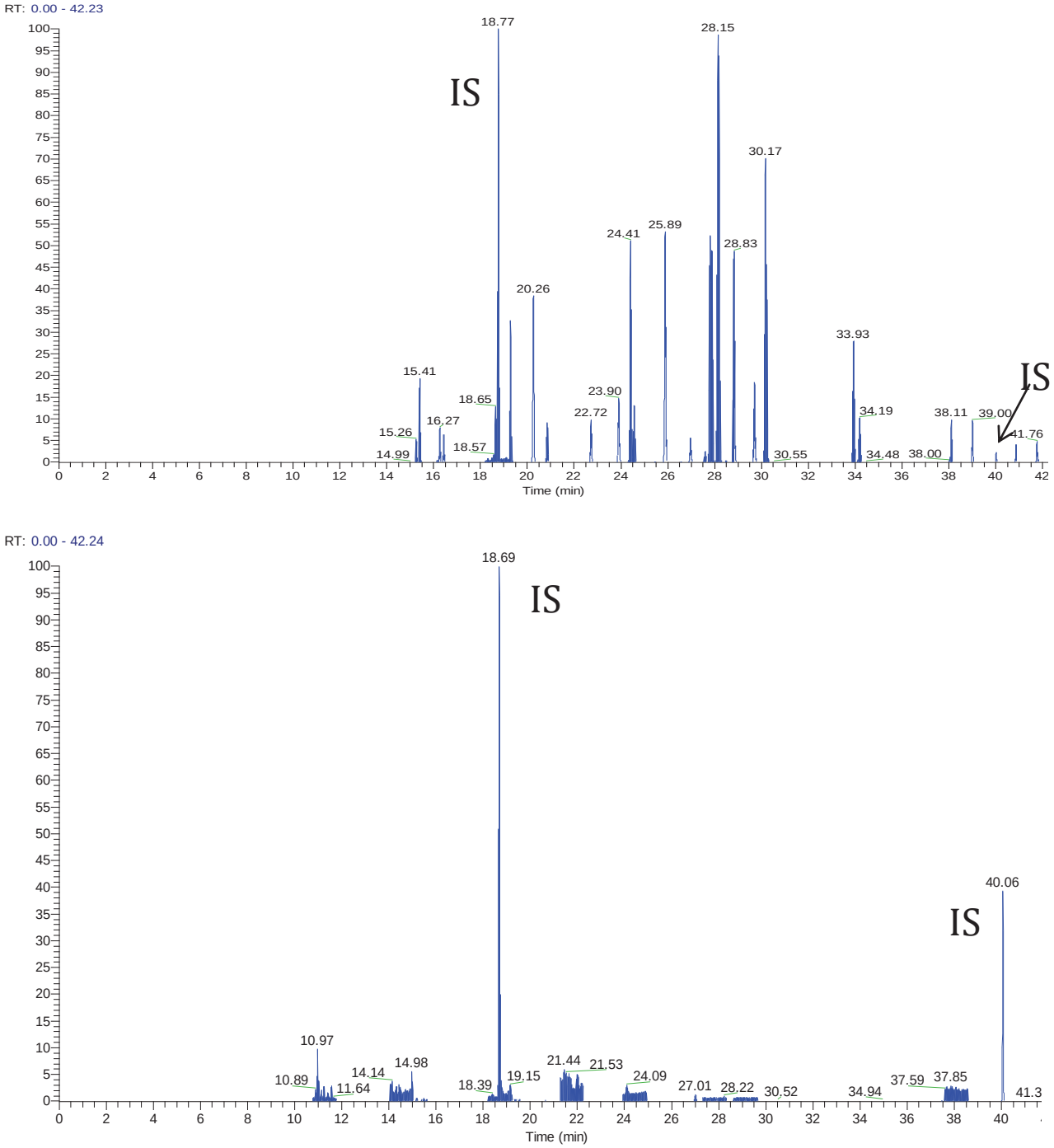

Fig.14. Current total ion chromatograms (GC-MS/MS) of blank *Pagellus* sample spiked with POPs. (IS= internal standard). **Fig.15.** Current total ion chromatograms (GC-MS/MS) of *Pagellus* sample naturally contaminated with POPs. (IS= internal standard).

4.5 Discussion

In this study, a qualitative and quantitative analysis of PCB congeners and organochlorine pesticides was carried out in muscular samples obtained from Mediterranean fish of diverse ecosystems. However, given the increasing fish demand and extensive export of fish worldwide, the impact of the results obtained in this study can be considered as a global health risk for humans. The presence of persistent anthropogenic chemicals in aquatic environments suggests concern for human toxicity, and consequent advisories to reduce human exposure to these persistent organic chemicals (Sapozhnikova et al., 2004). It was sometimes difficult to compare the total PCB and OC levels with previous studies, due to variations in the detection limits and the congeners analyzed, in addition to other laboratory parameters (Sprague et al., 2012). According to the differing field locations, behaviour and feeding habits, different levels of compounds were observed in the 3 selected groups. As predators, all these fishes can readily accumulate substances both from the water and from food. One of the most interesting findings was represented by the high levels and simultaneous presence of multiple toxicants in the same fish group, and the associated presence of histologic lesions in randomly chosen wild fish. Additionally, due to the homogeneously small size and young age of the examined fish, the relatively high level of POPs in muscles was considered a matter of concern with high risk of possible toxic effects for humans.

Polychlorinated biphenyls (PCBs) are poisonous and persistent organic compounds composed of 209 congeners that are stable and lipophilic. In water, PCBs adhere to organic particles, enter the food chain, are metabolized slowly, and bioaccumulate even at higher trophic levels (Khan, 2011). Most research on the neurotoxic effects of PCB exposure has focused on childhood neurobehavioral impairments associated with prenatal exposure. However, it has been shown that

PCB exposure has adverse cognitive effects even at levels generally considered at low or no risk, and affecting mainly those of advanced age (Bouchard et al., 2014).

In Europe, monitoring of PCB pollution has been primarily focused on water, sediments and pelagic fish of the Mediterranean Sea (Corsolini et al., 2007; Di Bella et al., 2006; Perugini et al.,2006; Storelli et al., 2008), but very few data have been reported regarding PCBs in benthic fish (Storelli et al., 2009).

Numerous studies have reported elevated concentrations of PCBs in wild fish from several aquatic environments (Barron et al. 2000; Bettinetti et al., 2012; Khan, 2011; Miranda et al., 2008; Sapozhnikova et al., 2004). Each congener has different physical activities and biological properties, according with the number and location of the chlorine atoms (Hardell et al., 2010). The levels of PCBs detected in this report, partially paralleled previous reports where similar congeners were evaluated (Ribeiro CA et al., 2005; Sapozhnikova et al., 2004). In our work, the highest levels of PCBs were detected in blackspot seabreams, which are bottom-feeding fish that live in relatively shallow water bays. Similar findings have been previously reported (Hardell et al., 2010), and provide additional evidence regarding the bottom sediment accumulation of these compounds, which contribute to increase the contaminant levels in this species. It is essential to remember that sediments are generally considered as sinks for persistent organic pollutants and a possible secondary source of contamination for aquatic species (Cousin and Cachot, 2014). Not surprisingly, the levels of several PCBs were also elevated in tunas. PCBs tend to concentrate mainly in the lipid fraction of organisms and may lead to substantial physiological burdens. The solubility in the adipose tissue and persistence of these compounds contribute to their bioaccumulation and biomagnification in the food chain (Di Bella et al., 2006). Tunas are well

known as top predators of the marine food network, and accumulate significant amounts of POPs because of their long life-span, their low biodegradation capacity and the presence of lipid-rich tissues (Di Bella et al., 2006; Sprague et al., 2012; Ueno et al., 2002).

Despite being a benthopelagic fish as well, dentices displayed lower levels of POPs within muscular samples. In fish, lipid levels within tissues can vary considerably among species, gender, and seasons (Henry, 2015), and unequal mobilization or deposition of lipid stores among tissues within an individual fish can redistribute tissue POP concentrations, especially for PCBs (Bodiguel et al. 2009). This finding in dentices could be related to changes in tissue lipid levels as a consequence of alterations in habitat or other stressful situations. In fact, *Dentex dentex* is classified by the International Union for the Conservation of Nature (IUCN) as "Vulnerable (V)" in the Red List of Threatened Species in the Mediterranean Sea (Abdul Malak et al., 2011).

The ecological risk assessment of pesticide use in Europe and the protection goals of related ecosystems have recently been debated by the European Food Safety Authority (EFSA). In particular, the EU Directive 2009/128/EC enforcement request Member States to adopt action plans aiming to reduce risks and impacts related to pesticide uses (Babut et al., 2013). Pesticides are well known endocrine disrupting chemicals, and are able to cross the placenta and blood–brain barrier and persist in cord blood and amniotic fluid. Therefore, there are increasing numbers of studies addressing their potential effects on the developing brain as a result of prenatal and early childhood exposure (Engel et al., 2011). Furthermore, exposure to low concentrations of some OC pesticides has been associated with metabolic dysregulation (excess adiposity and dyslipidemia) leading to prediabetic conditions (Androutsopoulos et al., 2013).

The OCs hexachlorobenzene (HCB) and dichlorodiphenyltrichloroethane (DDT) are among the most widespread POPs, and several studies have been addressed to evaluate their presence and level in fish tissues (Miranda et al., 2008). OCs represent lipophilic substances with low solubility in water and high persistence in adipose tissue (Miranda et al., 2008; Ribeiro CA et al., 2005). Not surprisingly, the highest global level of OCs was encountered in tunas, whose fat content in muscles is higher compared to those of the other fish species considered herein.

Despite the toxic role of PCBs and their metabolites has been investigated for nearly 50 years, there is a lack of consensus regarding the effects of these environmental contaminants on wild fish populations (Henry, 2015). The toxicologic effects of contaminants upon chronic environmental exposures are difficult to resolve within the background of numerous other environmental stressors that influence fish physiology (Schwarzenbach et al., 2006). However, several studies reported decrease growth, ionic imbalance, hyperglycemia, and anemia in fish exposed to PCB and pesticides, along with toxicopathic lesions in tissues, such as gill, liver, and spleen (Khan, 2011; Miranda et al., 2008). In some species of fish, OCs intoxication induces behavioral abnormalities indicative of neurotoxicity (Miranda et al., 2008).

Pathologic changes in fish are the result of adverse biochemical and physiological alterations within the organism itself; thus, histopathology is considered a useful tool to assess the overall health status of fish (Hinton and Lauren, 1990). Unfortunately, attributing observation of toxic effects in wild fish to specific substances requires more evidence than just the detection of these substances in fish tissues, as there are innumerable compounds associated with similar toxicopathic-related lesions (Henry, 2015). Interestingly, for both the skeletal muscle and liver, lesion occurrences and severity exhibited a tendency to increase in blackspot seabreams.

Because of its major role for the overall homeostasis in terms of nutrition and metabolism of several substances, the liver is the target organ of a variety of toxicants (Hinton, 2001). Specifically, biliary ductular hyperplasia, lymphoplasmacytic infiltration and multifocal hemosiderosis have been described in liver of benthic marine sculpins captured at tentatively decontaminated sites (Khan, 2011). In the study of Miranda et al. (2008), severe damage in the liver of *H. malabaricus* was documented and included a high incidence of necrosis, cell vacuolation, hepatic fibrosis, tumors, and inflammatory responses.

Experimental and observational studies on livers in wild fish exposed to xenobiotics have identified intracytoplasmic eosinophilic bodies in hepatocytes as the most conspicuous histologic change (Van Dyk et al., 2007; Wolf and Wolf, 2005), along with hepatic necrosis (Costa et al., 2009). Surprisingly, this change was not observed in our caseload. However, hepatic coagulative necrosis and single cell necrosis were present in the 3 groups examined.

In our caseload, hepatic lipidosis was one of the most recurrent findings, especially in tunas. A common morphologic response of the fish liver to toxicity is the loss of hepatic glycogen; however, paradoxically, toxic exposure can also result in accumulations of fat or glycogen in the liver (Wolf and Wolf, 2005). Hepatic lipidosis has been described in fish exposed to metals, crude oil extracts, and environmental mixtures of xenobiotics (Costa et al., 2009). Hepatic lipidosis has been regarded as a general failure in lipid metabolism as a result of exposure to undifferentiated compounds rather than a specific response (Van Dyk et al., 2007) which is in accordance with our observations regarding the mixed toxic burden.

In humans, epidemiological studies have indicated a link between PCBs and the onset non-Hodgkin lymphoma based on the temporal correspondence between exposure to PCBs and

increasing incidence of lymphoid tumors, the evidence for the immunotoxicity and carcinogenicity of PCBs, and the structural similarity between PCBs and dioxins, which are known as human carcinogens as well (IARC, 2013; Kramer et al., 2012).

An increase frequency of hepatic and splenic tumors has been reported in various fishes as a result of the exposure to environmental carcinogens (Ribeiro CA et al., 2005). Similarly, a significant elevation in the prevalence of hepatic preneoplastic foci has been previously described in young walleyes collected from assessment sites previously contaminated with PCBs (Barron et al., 2000). However, in fish collected from our study, no neoplasms were detected, although features of POP-driven hepatocellular dysplasia were documented. This discrepancy could be explained by the relative young age of fish considered herein.

4.6 Conclusions

The potential health risks related to fish consumption as a consequence of their content of environmental toxic contaminants is recognized worldwide. Fish meat currently represents the main source of human intake of POPs. Although the effects of POP exposure on humans are not completely understood, it is known that the immune system, reproductive tract, and endocrine system could be affected, along with the onset of neoplastic diseases. Despite the recognized danger, adequate tolerable limits for the amount of PCBs and OCs in marine organisms are not yet available. The global assessment of marine status through the use of fish from different hydrological settings as bio-indicators represent a complementary choice to evaluate the responses of marine organisms to pollutans, and to assess the maximum amount of residues without adverse effects. For these reasons, experimental and observational studies addressing combined toxic

effects of high levels of multiple contaminants should be implemented in different marine ecosystems, in order to provide valuable insights in their cumulative effects upon chronic exposure.

References

1. Abdolahpur Monikh F, Safahieh AR, Savari A, Doraghi A, 2012. Heavy metal concentration in sediment, benthic, benthopelagic, and pelagic fish species from Musa Estuary (Persian Gulf). Environ Monit Assess;185:215–222.

2. Abdul Malak D, Livingstone SR, Pollard D, Polidoro BA, Cuttelod A, Bariche M, Bilecenoglu M, Carpenter KE, Collette BB, Francour P, Goren M, Kara MH, Massutí E, Papaconstantinou C, Tunesi L, 2011. Overview of the Conservation Status of the Marine Fishes of the Mediterranean Sea. Gland, Switzerland and Malaga, Spain: IUCN.61.

3. Afonso P, McGinty N, Graça G, Fontes J, Mónica I, Totland A, Menezes G, 2014. Vertical Migrations of a Deep-Sea Fish and Its Prey. PLOS ONE;9(5):e97884.

4. Afonso P, Graça G, Berke G, Fontes J, 2012. First observations on seamount habitat use of blackspot seabream (Pagellus bogaraveo) using acoustic telemetry. J Exp Mar Biol Ecol;1:436–437.

5. Álvarez V, Medina I, Prego R, Aubourg SP, 2009. Lipid and mineral distribution in different zones of farmed and wild blackspot seabream (*Pagellus bogaraveo*). Eur J Lipid Sci Technol;111:957–966.

6. Androutsopoulos VP, Hernandez AF, Liesivuori J, Tsatsakis AM, 2013. A mechanistic overview of health associated effects of low levels of organochlorine and organophosphorous pesticides. Toxicol;307:89–94.

7. Ansari TM, Marr IL, Tariq N, 2004. Heavy metals in marine pollution prospective: a mini review. J Applied Sci;4:1-20.

8. Arnold MC, Lindberg TTY, Liu YT, Porter KA, Hsu-Kin H, Hinton DE, Di Giulio RT, 2014. Bioaccumulation and speciation of selenium in fish and insects collected from a mountaintop removal coal mining-impacted stream in West Virginia. Ecotoxicol; 23:929-938.

9. ATSDR, 2004. Toxicological profile for strontium. Agency for Toxic Substances and Disease Registry, Atlanta, GA, United States, Department of Health and Human Services, Public Health Service (http://www.atsdr.cdc.gov/toxprofiles/ tp159.html).

10. ATSDR, 1992. Toxicological profile for antimony. Agency for Toxic Substances and Disease Registry, Atlanta, GA, United States, Department of Health and Human Services, Public Health Service (http://www.atsdr.cdc.gov/toxprofiles/ tp23.html).

11. Au DWT, 2004. The application of histo-cytopathological biomarkers in marine pollution monitoring: a review. Marine Pollut Bull;48:817–834.

12. Babut M, Arts GH, Barra Caracciolo A, Carluer N, Domange N, Friberg N, Gouy V, Grung V, Lagadic L, Martin-Laurent F, Mazzella N, Pesce S, Real B, Reichenberger S, Roex EWM, Romijn K, Röttele M, Stenrød M, 2013. Pesticide risk assessment and management in a globally changing world—report from a European interdisciplinary workshop. Environ Sci Pollut Res;20:8298–8312.

13. Bais UE, Lokhande MV, 2012. Effect of cadmium chloride on histopathological changes in the freshwater fish *Ophiocephalus striatus* (Channa). Int J Zool Res; 8(1):23-32.

14. Barron MG, Anderson MJ, Cacela D, Lipton J, Teh SJ, Hinton DE, Zelikoff JT, Dikkeboom AL, Tillitt DE, Holey M, Denslow N, 2000. PCBs, liver lesions, and

biomarker responses in adult walleye (*Stizostedium vitreum vitreum*) collected from Green Bay, Wisconsin. J Great Lakes Res;26:250-271.

15. Bernet D, Schmidt H, Meier W , Wahli T, 1999. Histopathology in fish: proposal for a protocol to assess aquatic pollution. J Fish Dis;22, 25–34.

16. Bettinetti R, Quadroni S, Manca M, Piscia R, Volta P, Guzzella L, Roscioli C, Galassi S, 2012. Seasonal fluctuations of DDTs and PCBs in zooplankton and fish of Lake Maggiore (Northern Italy). Chemosphere;88:344-351.

17. Bodiguel X, Maury O, Mellon-Duval C, Roupsard F, Le Guellec AM, Loizeau V, 2009. A dynamic and mechanistic model of PCB bioaccumulation in the European hake (*Merluccius merluccius*). J Sea Res;62:124-134.

18. Borak J, Hosgood HD, 2007. Seafood arsenic: Implications for human risk assessment. Regulat Toxicol Pharmacol;47:204–212.

19. Borja A, Galparsoro I, Irigoien X, Iriondo A, Menchaca I, Muxika I, Pascual M, Quincoces I, Revilla M, Germán Rodríguez J, Santurtún M, Solaun O, Uriarte A, Valencia V, Zorita I, 2011. Implementation of the European Marine Strategy Framework Directive: a methodological approach for the assessment of environmental status, from the Basque Country (Bay of Biscay). Mar Pollut Bull;62(5):889-904.

20. Borja A, Elliott M, Carstensen J, Heiskanen AS, Van de Bund W, 2010. Marine management – Towards an integrated implementation of the European Marine Strategy Framework and the Water Framework Directives. Mar Pollut Bull;60:2175-2186.

21. Bouchard MF, Oulhote Y, Sagiv SK, Saint-Amour D, Weuve J, 2014. Polychlorinated biphenyl exposures and cognition in older U.S. adults: NHANES (1999–2002). Environ Health Perspect;122:73–78.

22. Boucher O, Muckle G, Bastien CH, 2009. Prenatal exposure to polychlorinated biphenyls: a neuropsychologic analysis. Environ Health Perspect;117:7–16.

23. Brix KV, Keithly J, Deforest DK, Laughlin J, 2004. Acute and chronic toxicity of nickel to rainbow trout (*Oncorhynchus mykiss*). Environ Toxicol Chem;23:2221-2228.

24. Cade BS, Noon BR, 2003. A gentle introduction to quantile regression for ecologists. Front Ecol Environ;1(8):412-420.

25. Canli M, Atli G. The relationships between heavy metal (Cd, Cr, Cu, Fe, Pb, Zn) levels and size of six Mediterranean fish species, 2003. Environ Pollut;121:129–136.

26. Carvalho ML, Santiago S, Nunes ML, 2005. Assessment of the essential element and heavy metal content of edible fish muscle. Anal Bioanal Chem;382:426–432.

27. Chen CY, Serrell N, Evers DC, Fleishman BJ, Lambert KF, Weiss J, Mason RP, Bank MS, 2008.Meeting report: methylmercury in marine ecosystems-from sources to seafood consumers. Environ Health Perspect;116:1706–1712.

28. Clarkson TW, Magos L, Myers GJ, 2003. The toxicology of mercury-current exposures and clinical manifestations. N Engl J Med;349:1731–1737.

29. Cohen AJ, Roe FJ, 2000. Review of risk factors for osteoporosis with particular reference to a possible aetiological role of dietary salt. Food Chem Toxicol;38(2):237-253.

30. Cohen T, Hee SS, Ambrose RF, 2001. Trace metals in fish and invertebrates of three California coastal wetlands. Mar Pollut Bull;42(3):224-232.

31. Corsolini S, Sarà G, Borghesi N, Focardi S, 2007. HCB, *p,p¢*-DDE and PCB ontogenetic transfer and magnification in bluefin Tuna (*Thunnus thynnus*) from the Mediterranean Sea. Environ Sci Technol;41:4227-4233.

32. Costa PM, Caeiro, S, Lobo J, Martins M, Ferreira AM, Caetano M, Vale C, DelValls TÁ, Costa MH, 2011. Estuarine ecological risk based on hepatic histopathological indices from laboratory and in situ tested fish. Mar Pollut Bull;62:55–65.

33. Costa PM, Diniz MS, Caeiro S, Lobo J, Martins M, Ferreira AM, Caetano M, Vale C, DelValls TA, Costa MH, 2009. Histological biomarkers in liver and gills of juvenile *Solea senegalensis* exposed to contaminated estuarine sediments: a weighted indices approach. Aquatic Toxicol; 92:202–212.

34. Costa PM, Carreira S, Costa MH, Caeiro S, 2013. Development of histopathological indices in a commercial marine bivalve (*Ruditapes decussatus*) to determine environmental quality. Aquat Toxicol;126:442–454.

35. Cousin X, Cachot J, 2014. PAHs and fish exposure monitoring and adverse effects from molecular to individual level. Environ Sci Pollut Res; 21:13685–13688.

36. Cuevas N, Zorita I, Costa PM, Franco J, Larreta J, 2015. Development of histopathological indices in the digestive gland and gonad of mussels: Integration with contamination levels and effects of confounding factors. Aquatic Tox;162:152–164.

37. Da Cuña RH, Rey Vázquez G, Piol MN, Guerrero NV, Maggese MC, Lo Nostro FL, 2011. Assessment of the acute toxicity of the organochlorine pesticide endosulfan in Cichlasoma dimerus (Teleostei, Perciformes). Ecotoxicol Environ Saf; 74(4):1065-1073.

38. Denkhaus E, Salnikow K, 2014. Nickel essentiality, toxicity, and carcinogenicity. Cri Rev Oncol/Hematol;42:35–56.

39. Di Bella G, Licata P, Brizzese A, Naccari C, Trombetta D, Lo Turco V, Dugo G, Richetti A, Naccari F, 2006. Levels and congener pattern of polychlorinated biphenyl

and organochlorine pesticide residues in bluefin tuna (*Thunnus thynnus*) from the Straits of Messina (Sicily, Italy). Environ Int;32:705–710.

40. Di Bella G, Potortì AG, Lo Turco V, Bua D, Licata P, Cicero N, Dugo G, 2015. Trace elements in Thunnus thynnus from Mediterranean Sea and benefit–risk assessment for consumers. Food Add Contam: Part B;8(3):175-181.

41. Duffus JH, 2002. Heavy metals - a meaningless term? Pure Appl Chem;74:793–807.

42. EFSA (European Food Safety Authority), 2009. EFSA Panel on Contaminants in the Food Chain (CONTAM) - Scientific Opinion on Arsenic in Food. The EFSA J; 7(10):1351-1550.

43. Engel SM, Wetmur J, Chen J, Zhu C, Barr DB, Canfield RL, Wolff MS, 2011. Prenatal exposure to organophosphates, paraoxonase 1, and cognitive development in childhood. Environ Health Perspect; 119(8):1182-8.

44. Eubig PA, Aguiar A, Schantz SL, 2010. Lead and PCBs as risk factors for attention deficit/hyperactivity disorder. Environ Health Perspect;118(12):1654-67.

45. EU Directive 2009/128/EC of the European Parliament and of the Council of 21 October 2009 establishing a framework for Community action to achieve the sustainable use of pesticides (text with EEA relevance). OJ L 309, pp.71-86.

46. EU Directive 2008/629/EC Commission regulation of 2 July 2008 amending Regulation (EC) No 1881/2006 setting maximum levels for certain contaminant in foodstuffs. OJ L 173, pp.6-9.

47. EU Directive 2008/56/EC of the European Parliament and of the Council of 17 June 2008 establishing a framework for Community action in the field of marine environmental policy (Marine Strategy Framework Directive). OJ L 164, pp.19-40.

48. EU Directive 2006/1881/EC Commission regulation setting maximum levels for certain contaminant in foodstuffs. OJ L 364, pp.5-24.

49. Evans DH, Piermarini PM, Choe KP, 2005. The multifunctional gill: dominant site of gas exchange, osmoregulation, acid–base regulation, and excretion of nitrogenous waste. Physiol Rev; 85:97-177.

50. Fanta E, Rios FS, Romão S, Vianna AC, Freiberger S, 2003. Histopathology of the fish *Corydoras paleatus* contaminated with sublethal levels of organophosphorus in water and food. Ecotoxicol Environ Saf;54:119-130.

51. Feist SW, Lang T, Stentiford GD, Road B, Nothe T, 2004. ICES techniques in marine environmental sciences biological effects of contaminants: use of liver pathology of the European flatfish dab (*Limanda limanda L.*) and flounder (*Platichthys flesus L.*) for monitoring. ICES Tech Mar Environ Sci;38:1-42.

52. Feist SW and Longshaw M, 2008. Histopathology of fish parasite infections – importance for populations. J Fish Biol; 73:2143–2160.

53. Feist SW, Stentiford GD, Kent ML, Ribeiro Santos A, Lorance P, 2015. Histopathological assessment of liver and gonad pathology in continental slope fish from the northeast Atlantic Ocean. Mar Environ Res; 106:42-50.

54. Fernández P and Grimalt JO, 2003. On the Global Distribution of Persistent Organic Pollutants. Chimia;57(9).

55. Fowler BA, Selene CH, Chou J, Jones RL, Chen CJ, 2007. Chapter 19: Arsenic. In: Handbook on the Toxicology of Metals. Nordberg GF, Fowler BA, Nordberg M, Friberg L (Eds.), 3rd edition, Academic Press, London, UK, pp.367-406.

56. Garcia-Hernandez J, Cadena-Cardenas L, Betancourt-Lozano M, Garica-de-la-Parra LM, Garcia-Rico L, Marquez-Farias F, 2007. Total mercury content found in edible

tissues of top predator fish from the Gulf of California, Mexico. Toxicol Environ Chem;89:507–522.

57. Ghiasi F, Mirzargar SS, Bdakhshan H, Shamsi S, 2010. Effects of low concentrations of cadmium on the level of lysozyme in serum, leukocyte count and phagocytic index in *Cyprinus carpio* under the wintering conditions. J Fish Aq Sci;5: 113– 119.

58. Giari L, Manera M., Simoni E, Dezfuli BS, 2007. Cellular alterations in different organs of European seabass *Dicentrarchus labrax* exposed to cadmium. Chemosphere; 67:1171-1181.

59. Gomez-Sanchez EP, 2015. Salt-sensitive hypertension: food for thought. Hypertension;65(2):283-4.

60. Gonçalves C, Martins M, Costa MH, Caeiro S, Costa PM, 2013. Ecological risk assessment of impacted estuarine areas: integrating histological and biochemical end points in wild Senegalese sole. Ecotoxicol Environ Saf;95:202–211.

61. Greenfield BK, Teh SJ, Ross JRM, Hunt J, Zhang GH, Davis JA, Ichikawa G, Crane D, Hung SSO, Deng DF, Teh FC, Green PG, 2008. Contaminant concentrations and histopathological effects in Sacramento splittail (*Pogonichthys macrolepidotus*). Arch Environ Contam Toxicol; 55:270-281.

62. Grosell M, 2011. Copper. In: Homeostasis and Toxicology of Essential Metals. Wood CM, Farrell AP, Brauner C (Eds). Fish Physiology, Vol. 31A, Academic Press, Elsevier Inc, New York, USA, pp.53–133.

63. Goulet R, Fortin C, Spry DJ, 2011. Uranium. In: In: Homeostasis and Toxicology of Non-Essential Metals. Wood CM, Farrell AP, Brauner CJ (Eds). Fish Physiology, (Eds.). Vol. 31B. Academic Press, Elsevier Inc, New York, USA, pp.391–428.

64. Hamilton SJ, 2004. Review of selenium toxicity in the aquatic food chain. Sci Total Environ;326:1-31.

65. Hardell S, Tilander H, Welfinger-Smith G, Burger J, Carpenter DO, 2010. Levels of polychlorinated biphenyls (PCBs) and three organochlorine pesticides in fish from the Aleutian Islands of Alaska. PLoS ONE 5(8):e12396.

66. Henry TB, 2015. Ecotoxicology of polychlorinated biphenyls in fish—a critical review. Crit Rev Toxicol; DOI: 10.3109/10408444.2015.1038498

67. Hinton DE, Baumann PC, Gardner GR, Hawkins WE, Hendricks JD, Murchelano RA, Okihiro MS, 1992. Histopathologic biomarkers. Biochemical, physiological, and histological markers of anthropogenic stress. In: Biomarkers. Lewis Publishers, Boca Raton, pp. 155–209.

68. Hinton DE, Lauren DL, 1990. Liver ultrastructural alterations accompanying chronic toxicity in fishes: potential biomarkers of exposure. In: McCarthy JF, Shugart LR (Eds.), Biomarkers of Environmental Contamination. CRC Press, Boca Raton, pp. 17–57.

69. Hinton DE, Segner H, Braunbeck T, 2001. Toxic responses of the liver. In: D. Schlenk D, Benson WH (Eds.), Target Organ Toxicity in Marine and Freshwater Teleosts, Taylor & Francis, London, pp. 224–68.

70. Hogstrand C, 2011. Zinc. In: Homeostasis and Toxicology of Essential Metals. Wood CM, Farrell AP, Brauner CJ (Eds.). Fish Physiology, Vol. 31A, Academic Press, Elsevier Inc, New York, USA, pp.135–200.

71. Hogstrand and Wood, 1997. The toxicity of silver to marine fish. Proceedings, 4th International Conference on the Transport, Fate and Effects of Silver in the Environment, University of Wisconsin, Madison, August 25-28,1996, pp.109-111.

72. Hosseini M, Nabavi SM, Parsa Y, 2013. Bioaccumulation of trace mercury in trophic levels of benthic, benthopelagic, pelagic fish species, and sea birds from Arvand River, Iran. Biol Trace Elem Res; 156(1-3):175-180.

73. IARC (International Agency for Research on Cancer), 1990. Chromium, nickel and welding. IARC monographs on the evaluation of carcinogenic risks to humans. Vol. 49.

74. IARC (International Agency for Research on Cancer), 1993. Beryllium, cadmium, mercury, and exposure to the glass manufacturing industry. IARC monographs on the evaluation of carcinogenic risks to humans. Vol. 58.

75. IARC (International Agency for Research on Cancer), 2006. Inorganic and organic lead compounds. IARC monographs on the evaluation of carcinogenic risks to humans. Vol. 87.

76. IARC (International Agency for Research on Cancer), 2012. Cadmium and cadmium compounds. IARC monographs on the evaluation of carcinogenic risks to humans. Vol. 100C.

77. IARC (International Agency for Research on Cancer), 2013. Carcinogenicity of polychlorinated biphenyls and polybrominated biphenyls. IARC monographs on the evaluation of carcinogenic risks to humans. Vol. 107.

78. Johnson A, Carew E, Sloman KA, 2007. The effects of copper on the morphological and functional development of zebrafish embryos. Aquatic Toxicol;84:431–438.

79. Kaoud HA, El-Dahshan AR, 2010. Bioaccumulation and histopathological alterations of the heavy metals in *Oreochromis niloticus* fish. Nat Sci;8(4):147-156.

80. Kennedy CJ, 2011. The toxicology of metals in fishes. In: Farrell AP (Ed.), Encyclopedia of Fish Physiology - From Genome to Environment, Academic Press, San Diego, CA; USA, pp.2061–2068.

81. Khan RA, 2011. Chronic Exposure and decontamination of a marine sculpin (*Myoxocephalus scorpius*) to polychlorinated biphenyls using selected body indices, blood values, histopathology, and parasites as bioindicators. Arch Environ Contam Toxicol;60:479–485.

82. Koenig S, Huertas D, Fernández P, 2013. Legacy and emergent persistent organic pollutants (POPs) in NW Mediterranean 2 deep-sea organisms. Sci Tot Environ;443:358-66.

83. Koenker R, 2005. Quantile regression (No. 38). Cambridge university press, Cambridge, UK.

84. Kori-Siakpere O, Ubogu EO, 2008. Sublethal haematological effects of zinc on the freshwater fish, *Heteroclarias sp.* (Osteichthyes: Clariidae). Afr J Biotechnol; 7(12):2068–2073.

85. Kramer S, Hikel SM, Adams K, Hinds D, Moon K, 2012. Current status of the epidemiologic evidence linking polychlorinated biphenyls and non-Hodgkin lymphoma, and the role of immune dysregulation. Environ Health Perspect;120:1067–1075.

86. Krewski D, Yokel RA, Nieboer E, Borchelt D, Cohen J, Harry J, Kacew S, Lindsay J, Mahfouz AM, Rondeau V, 2007. Human health risk assessment for aluminium, aluminium oxide, and aluminium hydroxide. J Toxicol Environ Health B Crit Rev;10(1):1-269.

87. Lorance P, 2011. History and dynamics of the overexploitation of the blackspot seabream (Pagellus bogaraveo) in the Bay of Biscay. ICES J Mar Sci;68:290–301.

88. Mager EM, 2011. Laed. In: Homeostasis and Toxicology of Non-Essential Metals. Wood CM, Farrell AP, Brauner CJ (Eds). Fish Physiology, (Eds.). Vol. 31B. Academic Press, Elsevier Inc, New York, USA, pp.185–236.

89. Marengo M, Durieux EDH, Marchand B, Francour P, 2014. A review of biology, fisheries and population structure of *Dentex dentex* (Sparidae). Rev Fish Biol Fisher;24(4):1065-1088.

90. McGeer JC, Niyogi S, Scott Smith D, 2011. *Cadmium*. *In:* Homeostasis and Toxicology of Non-Essential Metals. Wood CM, Farrell AP, Brauner CJ (Eds). Fish Physiology, (Eds.). (Eds.).Vol. 31B. Academic Press, Elsevier Inc, New York, USA, pp.125–184.

91. Menezes GM, Sigler MF, Silva HM, Pinho MR, 2006. Structure and zonation of demersal fish assemblages off the Azores archipelago (mid-Atlantic). Mar Ecol Progr Ser;324:241–260.

92. Miranda AL, Roche H, Randi MA, Menezes ML, Ribeiro CA, 2008. Bioaccumulation of chlorinated pesticides and PCBs in the tropical freshwater fish *Hoplias malabaricus*: histopathological, physiological, and immunological findings. Environ Int; 34(7):939-949.

93. Mok JS, Kwon JY, Son KT, Choi WS, Kang SR, Ha NY, Jo MR, Kim JH, 2014. Contents and risk assessment of heavy metals in marine invertebrates from Korean coastal fish markets. J Food Prot; 77(6):1022-1030.

94. Morato T, Sola E, Grós MP, Menezes G, 2001. Feeding habits of two congeners species of seabreams, *Pagellus bogaraveo* and *Pagellus acarne*, off the Azores (Northeastern Atlantic) during spring of 1996 and 1997. Bull Mar Sci;69:1073-1087.

95. Mostafalou S, Abdollahi M, 2013. Pesticides and human chronic diseases: evidences, mechanisms, and perspectives. Toxicol Appl Pharmacol;268:157–177.

96. Muthukumaravel K, Paulay MG, 2007. Toxic effect of cadmium on the electrophoretic protein patterns of gill and muscle of *Oreochromis mossambicus*. E-J Chem;14(2):284-286.

97. National Research Council (NRC), 2005a. Arsenic. In: Mineral Tolerance of Animals, 2nd revised edition. The National Academies Press, Washington DC, USA, pp.31-45.

98. National Research Council (NRC), 2005b. Calcium. In: Mineral Tolerance of Animals, 2nd revised edition. The National Academies Press, Washington DC, USA, pp.97-114.

99. National Research Council (NRC), 2005c. Magnesium. In: Mineral Tolerance of Animals, 2nd revised edition. The National Academies Press, Washington DC, USA, pp.224-234.

100. National Research Council (NRC), 2005d. Potassium. In: Mineral Tolerance of Animals, 2nd revised edition. The National Academies Press, Washington DC, USA, pp.306-320.

101. National Research Council (NRC), 2005e. Sodium Chloride. In: Mineral Tolerance of Animals, 2nd revised edition. The National Academies Press, Washington DC, USA, pp.357-371.

102. National Research Council (NRC), 2005f. Tin. In: Mineral Tolerance of Animals, 2nd revised edition. The National Academies Press, Washington DC, USA, pp.386-397.

103. National Research Council (NRC), 2005g. Vanadium. In: Mineral Tolerance of Animals, 2nd revised edition. The National Academies Press, Washington DC, USA, pp.398-412.

104. Niyogi S, Wood CM, 2006. Interaction between dietary calcium supplementation and chronic waterborne zinc exposure in juvenile rainbow trout, *Oncorhynchus mykiss*. Comp Biochem Physiol Part C: Toxicol Pharmacol;143:94–102.

105. Noël L, Dufailly V, Lemahieu N, Vastel C, Guérin T, 2005. Simultaneous Analysis of Cadmium, Lead, Mercury, and Arsenic Content in Foodstuffs of Animal Origin by Inductively Coupled Plasma/Mass Spectrometry after Closed Vessel Microwave Digestion: Method Validation. Journal of AOAC International;88(6):1811-1821.

106. Nordberg, GF, Nogawa K, Nordberg M, Friberg L, 2007. Chapter 23: Cadmium. In: Handbook on the Toxicology of Metals. Nordberg GF, Fowler BA, Nordberg M, Friberg L (Eds.), 3rd edition, Academic Press, London, UK, pp.445-486.

107. Olojo EAA, Olurin KB, Mbaka G, Oluwe-Mimo AD, 2004. Histopathology of the gill and liver tissues of the African catfish *Clarias gariepinus* exposed to lead. Afr J Biotechnol;4(1):117-122.

108. Panseri S, Soncin S, Chiesa LM, Biondi PA, 2011. A headspace solid-phase microextraction gas-chromatographic mass-spectrometric method (HS-SPME-GC/MS) to quantify hexanal in butter during storage as marker of lipid oxidation. Food Chem;127(2):886-9.

109. Passantino L, Santamaria N, Zupa R, Pousis C, Garofalo R, Cianciotta A, Jirillo E, Acone F, Corriero A, 2014. Liver melanomacrophage centers as indicators of Atlantic bluefin tuna, *Thunnus thynnus* well-being. J Fish Dis; 37:241–250.

110. Perugini M, Giammarino A, Olivieri V, Di Nardo W, Amorena M, 2006. Assessment of edible marine species in the Adriatic Sea for contamination from polychlorinated biphenyls and organochlorine insecticides. J. Food Protect;69:1144-1149.

111. Peter AL, Viraraghavan T, 2005. Thallium: a review of public health and environmental concerns. Environ Int;31:493-501.

112. Plum LM, Rink L, Haase H, 2010. The essential toxin: impact of zinc on human health. Int J Environ Res Public Heatlth;7: 1342-1365.

113. Poston TM. 1982. The bio accumulation potential of thorium and uranium in rainbow trout Salmo-nairdneri. Bull Environ Contam Toxicol;28:682-690.

114. Rahmanpour S, Ashtiyani SML, Ghorghani NF, 2014. Biomonitoring of heavy metals using bottom fish and crab as bioindicators species, the Arvand River. Published online before print November 20, 2014, doi:10.1177/0748233714554410

115. Raimundo J, Pereira P, Caetano M, Cabrita MT, Vale C, 2011. Decrease of Zn, Cd and Pb concentrations in marine fish species over a decade as response to reduction of anthropogenic inputs: the example of Tagus estuary. Mar Pollut Bull;62(12):2854-2858.

116. Reid SD, 2011. Molybdenum and chromium. In: Homeostasis and Toxicology of Essential Metals. Wood CM, Farrell AP, Brauner CJ (Eds). Fish Physiology, Vol 31A, Academic Press, Elsevier Inc, New York, USA, pp.375–415.

117. Ribeiro CA, Vollaire Y, Sanchez-Chardi A, Roche H, 2005. Bioaccumulation and the effects of organochlorine pesticides, PAH and heavy metals in the Eel (*Anguilla anguilla*) at the Camargue Nature Reserve, France. Aquat Toxicol; 74(1):53-69.

118. Ribeiro HJ, Procopio MS, Gomes JMM, Vieira FO, Russo RC, Balzuweit K, Chiarini-Garcia H, Santana Castro AC, Rizzo E, Dias Corrêa J, 2011. Functional dissimilarity of melanomacrophage centres in the liver and spleen from females of the teleost fish *Prochilodus argenteus*. Cell Tissue Res; 346:417-425.

119. Rooker JR, Secor DH, Demetrio G, Kaufman AJ, Rios AB, Ticina V, 2008. Evidence of trans-Atlantic movement and natal homing of bluefin tuna from stable isotopes in otoliths. Mar Ecol Prog Ser;368:231-239.

120. Salvadó JA, Grimalt JO, López JF , Durrieu de Madron X, Pasqual C, Canals M, 2013. Distribution of organochlorine compounds in superficial sediments from the Gulf of Lion, northwestern Mediterranean Sea. Progress in Oceanography;118:235-248.

121. SANCO/12571/2013. Guidance document on analytical quality control and validation procedures for pesticide residues analysis in food and feed (2014).

122. Sapozhnikova Y, Bawardi O, Schlenk D, 2004. Pesticides and PCBs in sediments and fish from the Salton Sea, California, USA. Chemosphere;55(6):797-809.

123. Schlacher TA, Mondon JA, Connolly RM, 2007. Estuarine fish health assessment: evidence of wastewater impacts based on nitrogen isotopes and histopathology. Mar Pollut Bull; 54(11):1762-1776.

124. Schwarzenbach RP, Escher BI, Fenner K, Hofstetter TB, Johnson CA, von Gunten U, Wehrli B, 2006. The challenge of micropollutants in aquatic systems. Science; 313:1072-1077.

125. Somers EC, Ganser MA, Warren JS, Basu N, Wang L, Zick SM, Park SK, 2015. Mercury exposure and antinuclear antibodies among females of reproductive age in the United States: NHANES. Environ Health Perspect;123:792–798.

126. Sprague M, Dick JR, Medina A, Tocher DR, Bell JG, Mourente G, 2012. Lipid and fatty acid composition, and persistent organic pollutant levels in tissues of migrating Atlantic bluefin tuna (*Thunnus thynnus, L.*) broodstock. Environ Pollut;171:61-71.

127. Stentiford GD, Longshaw M, Lyons BP, Feist SW, 2003. Histopathological biomarkers in estuarine fish species for the assessment of biological effects of contaminants. Mar Environ Res;55:137–159.

128. Storelli MM, Barone G, Cuttone G, Giungato D, Garofalo R, 2010. Occurrence of toxic metals (Hg, Cd and Pb) in fresh and canned tuna: public health implications. Food Chem Toxicol;48(11):3167-70.

129. Storelli MM, Casalino E, Barone G, Marcotrigiano GO, 2008. Persistent organic pollutants (PCBs and DDTs) in small size specimens of bluefin tuna (*Thunnus thynnus*) from the Mediterranean Sea (Ionian Sea). Environ Int;34:509-513.

130. Storelli MM, Losada S, Marcotrigiano GO, Roosens L, Barone G, Neels H, Covaci A, 2009. Polychlorinated biphenyl and organochlorine pesticide contamination signatures in deep-sea fish from the Mediterranean Sea. Environ Res; 109:851-856.

131. Storelli MM, Marcotrigiano GO, 2000. Organic and inorganic arsenic and lead in fish from the South Adriatic Sea, Italy. Food Addit Contam;17(9):763-768.

132. Storelli MM, Perrone VG, 2010. Detection and quantitative analysis of organochlorine compounds (PCBs and DDTs) in deep sea fish liver from Mediterranean Sea. Environ Sci Pollut Res Int;17(4):968-76.

133. Sunderland EM, Gobas FAPC, Branfireun BA, Heyes A, 2006. Environmental controls on the speciation and distribution of mercury in coastal sediments. Mar Chem;102:111–123.

134. Tellez-Plaza M, Navas-Acien A, Menke A, Crainiceanu CM, Pastor-Barriuso R, Guallar E, 2012. Cadmium exposure and all-cause and cardiovascular mortality in the U.S. general population. Environ Health Perspect;120:1017–1022.

135. Thomas, R., 2008. Practical guide to ICP-MS – a tutorial for beginners (2nd Ed) CRC Press, Boca Raton, Florida. 347 p.

136. Triebskorn R, Telcean I, Casper H, Farkas A, Sandu C, Stan G, Colarescu O, Dori T, Kohler HM, 2008. Monitoring pollution in River Mures, Romania, part II: metal accumulation and histopathology in fish. Environ Monit Assess;141:177-188.

137. Tucker JW Jr, 2012. The rearing environment In: Marine Fish culture. Springer Science + Business Media DV, pp 49-148.

138. Ueno D, Iwata H, Tanabe S, Ikeda K, Koyama J, Yamada H, 2002. Specific accumulation of persistent organochlorines in bluefin tuna collected from Japanese coastal waters. Marine Poll Bull;45:254–261.

139. Ungaro, 2008. Field manual on macroscopic identification of maturity stages for the Mediterranean fishery resources. GCP/RER/ITA/MSM-TD-21. MedSudMed Technical Documents No 21: 34 pp.

140. Van der Oost RM, Beyer J, Vermulen NPE, 2003. Fish bioaccumulation and biomarkers in environmental risk assessment: a review. Environ Toxicol Pharmacol;13:57-149.

141. Van Dyk JC, Pieterse GM, Van Vuren JHJ, 2007. Histological changes in the liver of *Oreochromis mossambicus* (Cichlidae) after exposure to cadmium and zinc. Ecotoxicol Environ Saf;66:432-440.

142. Vera-Candioti J, Soloneski S, Larramendy ML, 2011. Acute toxicity of chromium on *Cnesterodon decemmaculatus* (Pisces: Poeciliidae). Theoria;20:81–88.

143. Vinceti M, Mandrioli J, Borella P, Michalked B, Tsatsakise A, Finkelstein Y, 2014. Selenium neurotoxicity in humans: bridging laboratory and epidemiologic studies. Toxicology Letters;230:295–303.

144. Voegborlo RB, Adimado AA, Ephraim JH, 2007. Total mercury distribution in different tissues of frigate tuna (*Auxis thazard thazard*) from the Atlantic Coastal Waters of Ghana, Gulf of Guinea. Environ Monit Assess;132(1-3):503-508.

145. Wangsongsak A, Utarnpongsa S, Kruatrachue M, Ponglikitmongkol M, Pokethitiyook P, Sumranwanich T, 2007. Alterations of organ histopathology and metallolhionein mRNA expression in silver barb, *Puntius gonionotus* during subchronic cadmium exposure. J Environ Sci;19:1341–1348.

146. Williams AG, Scheckel KG, Tolaymat T, Impellitteri CA, 2006. Mineralogy and characterization of arsenic, iron, and lead in a mine waste-derived fertilizer. Environ Sci Technol;40:4874-4879.

147. Wolf JC, Wolfe MJ, 2005. A brief overview of nonneoplastic hepatic toxicity in fish. Tox Pathol;33:75–85.

Appendix

6.1 Additional research projects

During my PhD at the University of Milan, I was involved in additional research projects regarding small animal medicine. In particular, our group focused on feline hypertrophic cardiomyopathy, feline upper respiratory tract lymphoma and feline nasal inflammatory processes. The preliminary findings and final results derived from these projects have been presented at international congresses, and finally lead to two publications reported in the section "PUBLICATIONS IN PEER-REVIEWED JOURNALS".

A brief explanation of the projects is following:

- **Pathogenesis of feline hypertrophic cardiomyopathy: comparison of myocardial lesions in prolonged survivors and in cats experiencing sudden death**

  Hypertrophic cardiomyopathy (HCM) is one of the most common causes of sudden death in young men. HCM is characterized by a wide spectrum of clinical manifestations raising problems in its early diagnosis and prognostication. Considerable advances in the understanding of molecular pathways involved in human HCM have not been paralleled by correlations with the clinical phenotype. HCM is the most common feline myocardial disease bearing genetic, clinical and pathological resemblance with the human counterpart. More so, clinico-pathological abnormalities described in juvenile cats resemble those documented in young men. Sudden death represents a common and unpredictable complication of human and

feline HCM. The identification of lesions and the early recognition of patients at greatest risk of sudden death is one of the major fields of investigation in man and one of the major aims of this research for cats.

Hypothesis/Objectives: Adult cats affected by HCM are characterized by two distinct clinical courses, cats with a prolonged clinical history that respond to therapy and survive years with HCM and cats of less than 1,5 year experiencing sudden death without previously detectable clinical signs and diagnosed with HCM at necropsy.

The hypothesis of the current work is that in sudden death and longer survival HCM cats there are differences in myocardial lesional and growth factor expression profiles, and that these differences can be correlated with the different clinical course. Specifically, juvenile sudden death HCM cats may bear earlier and more prominent lesions. Thus the objective of this work is to investigate myocardial gross, microscopic and ultrastructural lesions in the two study populations and in control age-matched non-diseased cats, and evaluate immunohistochemical expression of proliferation index and growth factors involved in angiogenesis and fibrogenesis.

Expected Results: In sudden death cats, the presence of more severe myocardial changes (increased fibrosis, angiogenesis, increased number of cardiomyocytes with differing proliferation index and TEM abnormalities), is envisaged. The expected increase in growth factor expression in sudden death cats may cause early myocardial hypertrophy and fibrosis and may explain the difference in lesional and clinical severity in the two study groups.

Potential Impact for Animal Health: The finding of possible derangements of growth and vascular factors expression may highlight potential clinical markers predicting the outcome and may aid in the understanding of the pathogenesis of HCM.

- **Feline upper respiratory tract lymphoma: cytology, histology and phenotype, FeLV expression and their correlation with prognosis**

  Lymphomas are among the most common feline malignancies representing more than 50% of all tumors in cats. The upper respiratory tract (URT) is considered a relatively rare site of lymphoma, accounting for less than 1% of all feline tumors. In previous studies, the evaluation of the three distinct presentations of URT lymphoma defined as nasal, nasopharyngeal or lymphoma simultaneously developing in both locations (combined lymphomas) as distinct clinical-pathological and prognostic entities seems not available. In humans, chronic inflammation is now generally accepted as a risk factor for the development of a variety of cancers, including hematopoietic malignancies. Associations involving bacterial and viral infections with human lymphoma development are well documented and mostly regard B-cell lymphomas of mucosal-associated lymphoid tissue (MALT). Epstein–Barr virus (EBV) infection is an example of lymphotropic virus with tumorigenic activity.

  Hypothesis/Objectives: Lymphomas arising in the nasal cavities, nasopharynx, or involving both locations represent distinct pathologic entities with different response to therapy, variable relapse rates and different survivals. Feline leukemia virus (FeLV) might be involved in feline URT lymphoma development when FeLV reactivation and transformation of harboring cells is favored by trauma or inflammation.

Expected Results: The evaluation of cytology, histology, phenotype, FeLV tissue antigens, and follow up data of three different URT lymphomas will confirm the prognostic role of the clinical and pathological variables. The presence of lymphoplasmacytic inflammation in cats experiencing a neoplastic transformation of lymphoid cells will document the putative role of inflammation and lymphomagenesis in cats.

6.2 Publications in peer-reviewed journals

1. Spalla I, Locatelli C, Riscazzi G, **Santagostino SF**, Cremaschi E, Brambilla P. Survival in cats with primary and secondary cardiomyopathies. Accepted on J Fel Med Surg.

2. **Santagostino SF**, Mortellaro CM, Buchholz J, Lugli M, Forlani A, Ghisleni G, Roccabianca P. Primary angiocentric/angioinvasive T-cell lymphoma of the tympanic bulla in a FeLV positive cat. Accepted on J Fel Med Surg.

3. Forlani A, Roccabianca P, Palmieri C, Sarli G, Stefanello D, **Santagostino SF**, Randi C, Avallone G. Pathological characterization of primary splenic liposarcoma in three dogs. Accepted on Vet Quarterly

4. **Santagostino SF**, Mortellaro CM, Boracchi P, Avallone G, Caniatti M, Forlani A, Roccabianca P. Feline upper respiratory tract lymphoma: site, cyto-histology, phenotype, FeLV expression and prognosis. Vet Pathol 2015; 52: 250-259.

5. Forlani A, Palmieri C, **Santagostino SF**, Queliti R, Roccabianca P. Pulmonary alveolar proteinosis/phospholipidosis in a English Bulldog. Accepted on JAVMA.

6. Amati M, Venco L, Roccabianca P, **Santagostino SF**, Bertazzolo W. Pericardial lymphoma in seven cats. J Fel Med Surg 2013; 16(6):507-512.

6.3 National and international oral presentations

1. **Santagostino SF,** Carotenuto A, Roccabianca P, Bonacini S,Caniatti M, Borghi L, Mortellaro CM. How to get profitable biopsies from nasopharyngeal space-occupying lesions in cats: 13 cases (2012-2015). 12th VES Meeting, 2015, Santa Barbara, USA.

2. Mortellaro CM, **Santagostino SF**, Caniatti M, Roccabianca P. Nasopharyngeal lymphomas vs. lymphoplasmacitic nasopharyngitis in cats: the endoscopist-pathologist alliance to meet the challenge. 10th VES Meeting, 2013, Key Largo, USA.

3. Forlani A, Caniatti M, **Santagostino SF**, Vicini B, Luraschi C, Roccabianca P. Correlation between cytology and histopathology in the diagnosis of splenic neoplasms in dogs. The 31st ESVP/ECVP Meeting, 2013, London, UK.

4. **Santagostino SF**, Mortellaro CM, Avallone G. Caniatti M, Forlani A, Roccabianca P. Feline nasal lymphoma: cytologic, histologic and immunohistochemical evaluation. IX AIPVet Congress, 2012, Perugia, Italy.

6.4 National and international poster presentations

1. Santagostino SF, Engiles JB, Turek BJ, Sánchez MD. Hemophilic polyarthropathy in a dog: clinico-pathologic findings. 2015 ACVP/ASVCP/STP Meeting, Minneapolis, MN, USA.

2. Carotenuto AM, **Santagostino SF,** Roccabianca P, Borghi L, Mortellaro CM. Endoscopic-guided palliative debulking of nasopharyngeal neoplasms in cats: 2 cases. 12th VES Meeting, 2015, Santa Barbara, USA.

3. Walsh AL, **Santagostino SF**, Durham AC. Xanthogranulomatous coelomitis with acid-fast positive bacteria in a pigeon.2014 ACVP/ASVCP Meeting, Atlanta, GA, USA.

4. Loria KO, **Santagostino SF**, Sanchez M, Sirivelu MP. Feline pulmonary adenosquamous carcinoma: comparison of cytologic and histologic findings. 2014 ACVP/ASVCP Meeting, Atlanta, GA, USA.

5. **Santagostino SF**, Forlani A, Roccabianca P, Fedrizzi G, Malandra R, Ranghieri V, Zaffra N, Ghisleni G. Metal exposure and toxicology in selected fish species from the Mediterranean Sea: risk assessment for human consumption. 2ndESTP, ESVP, ECVP Meeting, 2014, Berlin, DE.

6. Ghisleni G, Ferrari MG, **Santagostino SF**, Forlani A. NK-cell large granular lymphocyte leukemic lymphoma in a dog. European Canine Lymphoma Group, 2013, Lugano, CH.

7. Santagostino SF, Mortellaro CM, Forlani A, Ghisleni G., Roccabianca P. Primary angiocentric/angioinvasive T-cell lymphoma of the tympanic bulla in a FeLV positive cat. The 31st ESVP/ECVP Meeting, 2013, London, UK.

8. Forlani A, Avallone G, **Santagostino SF**, Roccabianca P. Epidemiology of neoplastic diseases in ferret: a 10 years study. The 31st ESVP/ECVP Meeting, 2013, London, UK.

9. Forlani A, Palmieri C, **Santagostino SF**, Queliti R, Roccabianca P. Massive pulmonary alveolar lipoproteinosis in an English Bulldog. 31st ESVP and ECVP Meeting, 4-7 Sept 2013, London, UK.

Original Article

Journal of Feline Medicine and Surgery
1–9

DOI: 10.1177/1098612X15588797
jfms.com

Survival in cats with primary and secondary cardiomyopathies

Ilaria Spalla[1], Chiara Locatelli[1], Giulia Riscazzi[1], Sara Santagostino[2], Elena Cremaschi[1] and Paola Brambilla[1]

Abstract

Objectives Feline cardiomyopathies (CMs) represent a heterogeneous group of myocardial disease. The most common CM is hypertrophic cardiomyopathy (HCM), followed by restrictive cardiomyopathy (RCM). Studies comparing survival and outcome for different types of CM are scant. Furthermore, little is known about the cardiovascular consequences of systemic diseases on survival. The aim of this retrospective study was to compare survival and prognostic factors in cats affected by HCM, RCM or secondary CM referred to our institution over a 10 year period.

Methods The study included 94 cats with complete case records and echocardiographic examination. Fifty cats presented HCM, 14 RCM and 30 secondary CM.

Results A statistically significant different survival time was identified for cats with HCM (median survival time of 865 days), RCM (273 days) and secondary CM (<50% cardiac death rate). In the overall population and in the primary CM group (HCM + RCM), risk factors in the multivariate analysis, regardless of the CM considered, were the presence of clinical signs, an increased left atrial to aortic root (LA/Ao) ratio and a hypercoagulable state.

Conclusions and relevance Primary CMs in cats share some common features (ie, LA dimension and hypercoagulable state) linked to feline cardiovascular physiology, which influence survival greatly in end-stage CM. The presence of clinical signs has to be regarded as a marker of disease severity, regardless of the underlying CM. Secondary CMs are more benign conditions, but if the primary disease is not properly managed, the prognosis might also be poor in this group of patients.

Accepted: 6 May 2015

Introduction

Cardiomyopathies (CMs) are a heterogeneous group of myocardial disease that can primarily affect the heart (primary CM) or that are part of a generalised systemic illness (secondary CM).[1,2]

Hypertrophic cardiomyopathy (HCM) is the most common feline CM, and is characterised by a hypertrophied (>6 mm in diastole), non-dilated left ventricle (LV) in the absence of another systemic or cardiac disease able to mimic similar wall thickening.[1–5]

HCM is characterised by a wide phenotypic spectrum, with diffuse hypertrophy (symmetrical and concentric hypertrophy of the LV), or asymmetric hypertrophy involving the interventricular septum (IVS) or the left ventricular free wall (LVFW) or isolated segments in the LV, including the papillary muscle.[4–8]

The presence of a documented systemic illness that is responsible for LV wall thickening identifies a secondary CM.[2,9–11]

Little is known about the prevalence and the consequences of cardiac abnormalities in cats affected by hyperthyroidism and systemic hypertension, and no study has investigated the outcome of these patients with a particular focus on the cardiovascular system.

Hyperthyroidism is a systemic disease that determines a 'high output state' as a consequence of a general decrease in peripheral vascular resistance and an increase in cardiac output associated with sinus

[1]The Cardiology Unit; Department of Veterinary Sciences and Public Health (DIVET), Università degli Studi di Milano, Milan, Italy
[2]The Pathology Unit; Department of Veterinary Sciences and Public Health (DIVET), Università degli Studi di Milano, Milan, Italy.
Part of this study was presented as a poster communication at the 22nd ECVIM-CA Congress, Maastricht (NL), 6–8 September 2012.

Corresponding author:
Ilaria Spalla DVM, PhD, Department of Veterinary Sciences and Public Health (DIVET), Università degli Studi di Milano, 20122 Milan, Italy
Email: illispa@hotmail.com

tachycardia.[9,11] Systemic hypertension can induce an increase in LV diastolic thickness by the increase in afterload associated with the disease.[10]

Restrictive cardiomyopathy (RCM), which accounts for 20% of referred feline CMs, is defined by the presence of restrictive mitral inflow Doppler pattern, stiff, non-hypertrophied LV with biatrial enlargement. Two echocardiographic patterns can be identified: the myocardial form and the endomyocardial form.[2,3,12]

Since most of the published work in feline cardiology refers to HCM,[6–8,13–16] with only one study[3] presenting the clinical and echocardiographic features of idiopathic feline CM, and no study focused on the effect of secondary CM on survival, the aim of our study is to provide data about population characteristics, survival time and prognostic factors in cats affected by the most common CMs in our referral institution: HCM, RCM and secondary CM.

Materials and methods

The clinical archive of the cardiology unit was reviewed for cats diagnosed with CM. Inclusion criteria were any patient with a complete case record (owner data, patient signalment and anamnesis, complete clinical findings and cardiac investigation), a follow-up available (telephone call or echocardiographic re-check at our institution) and a definitive diagnosis of HCM, RCM or secondary CM. Complete cardiac investigation included a detailed anamnesis and signalment, clinical findings and a complete echocardiography. Doppler technique was used to assess systemic blood pressure (BP) in all patients as recommended by the American College of Veterinary Internal Medicine guidelines.[17] When BP was >160 mmHg on serial repeated measurements, the cat was classified as affected by systemic hypertension. A complete blood count and biochemical blood analysis were performed, including thyroxine (T4), and treatment with ace inhibitor and/or calcium channel blocker was started as recommended.[17] All cats older than 10 years of age had their T4 levels tested.[18]

If the patient presented with a clinical history or with clinical findings related to the presence of hyperthyroidism (polyphagia, progressive weight loss), T4 levels and a screening blood test were performed regardless of the patient's age.

Cats diagnosed with dilated CM, arrhythmogenic CM or unclassified CM; congenital heart disease or infiltrative disease; or those with incomplete case records or no information regarding follow-up were excluded from the analysis.

The final diagnosis of CM was determined by echocardiography (M-mode, B-mode and Doppler echocardiography). Criteria for echocardiographic diagnosis were established as follows.

Primary HCM: Cats were diagnosed with HCM when diastolic left ventricular wall thickness was >6 mm in the absence of any other cardiac or systemic illness that might mimic the same echocardiographic feature. The measurement was obtained by M-mode and/or B-mode images, where available.

A detailed characterisation of LV hypertrophy was provided for each case: symmetrical (if both IVS and LVFW were >6 mm and IVS/LVFW ratio was 0.7–1.3[8,19]) or asymmetrical (if the hypertrophied LV segment was localised at IVS, LVFW or at the papillary muscle only). The IVS asymmetric phenotype was characterised by a IVS/LVFW ratio of >1.3, while LVFW phenotype was associated with a IVS/LVFW ratio of <0.7.[8,19] Papillary muscle hypertrophy was defined when no increase in IVS or LVFW in diastole was identified and when papillary muscle area[20] was >0.8 cm^2.

Secondary CM: Cats were diagnosed with secondary CM when a complete echocardiography was performed in a patient with BP or T4 levels above the reference values and echocardiographic abnormalities were detected.

RCM: Echocardiographic diagnosis of RCM was based on the presence of a marked left atrial or biatrial dilation (left atrial to aortic root [LA/Ao] ratio >2)[4] without concomitant myocardial hypertrophy (LV wall thickness <6 mm), in the presence of a restrictive pattern on transmitral pulsed wave Doppler trace.

Left atrial enlargement was defined by a LA/Ao ratio on B-mode greater than 1.5.[4] Cats with a LA/Ao ratio between 1.5 and 2.0 were identified as having mild to moderate LA enlargement, while cats with a LA/Ao ratio >2.0 were considered to have severe LA enlargement.[4]

Systolic anterior motion of the mitral valve (SAM) was defined as a midsystolic displacement of the anterior septal leaflet into the left ventricular outflow tract (LVOT) causing dynamic obstruction of blood flow, with an acceleration of LVOT flow and the presence of a jet of mitral regurgitation.[4]

Echocardiographic signs of a hypercoagulable state included the presence of spontaneous echocardiographic contrast ('smoke effect') or the direct visualisation of intracardiac thrombi in the left atrium or auricle.

Owners or referring veterinarians were contacted in order to obtain information about long-term follow-up.

If the cat was alive, a re-check was offered. If the cat had died, an attempt was made to classify the event as cardiac related or not. Euthanasia due to worsening of heart failure was considered cardiac related if no other cause of death was obvious. Cats still alive or that had died or were euthanised for reasons unrelated to cardiac disease were censored in the statistical analysis. Subjects lost to follow-up were included in the survival analysis up until the last time point at which they were known to be alive and then were thereafter censored in the analysis.

Statistical analysis

Data were analysed using a computerised statistics software (SPSS Statistics for Windows v17), and in all cases

$P < 0.05$ was set to indicate statistical significance. Basic descriptive statistical analyses were performed using Microsoft Excel. The Shapiro–Wilk test was used to verify variables' normal distribution. If the distribution was normal, a *t*-test was used to compare the means of two continuous variables; the Mann–Whitney U-test was used with non-normally distributed variables. Data with normal distribution are expressed as mean ± SD. For data not normally distributed, median and ranges are given.

Survival was calculated as the days between diagnosis and death or last visit/telephone contact.

The Kaplan–Meier method was used to estimate survival function and plot time to event curves in the different groups. A log-rank test with right censoring was used to determine whether a significant difference existed between groups.

Schoenfeld residuals and time dependent covariates were used to test the assumption of proportional hazards (the hazard in one group is a constant proportion of the hazard in the other group). Univariate and multivariate Cox proportional hazard analysis were performed in order to determine the effect of any variable on survival.

Variables were added to the multivariable model in a manual stepwise manner, including first all variables statistically significant in the univariate analysis, and then excluding those not reaching statistical significance one by one, until all the variables included were statistically significant. Univariate and multivariate Cox proportional hazard analysis were performed in the overall population (HCM, RCM and secondary CM) and in primary CM (HCM and RCM). Variables assessed for their effect on outcome in each group were CM, breed, sex, age at presentation, presence of clinical signs, presence of heart murmur, presence of SAM, echocardiographic hypertrophy pattern, indexed LA/Ao ratio, presence of echocardiographic signs of hypercoagulable state. Hazard ratio (HR) and 95% confidence intervals (CI) were calculated.

Results

From March 2003 to March 2013, 124 cats were diagnosed with HCM, RCM or secondary CM. Of these, 23 were lost to follow-up after the first visit, and seven were excluded for incomplete case record (n = 4) and incomplete BP and T4 in cats older than 10 years of age (n = 3).

The final study population comprised 94 patients: 50 patients with an echocardiographic diagnosis of HCM, 14 cats diagnosed with RCM and 30 cats with secondary CM due to systemic hypertension (n = 17) and hyperthyroidism (n = 13).

Breed population included mostly domestic shorthair cats (n = 60), followed by Persian (n = 20), longhair cats (n = 10; four Norwegian Forest Cats, three Maine Coons, two Ragdolls and one Birman) and four Siamese cats. Male cats were slightly predominant but not over-represented in the population, as 53% were male (n = 50) and 47% were female (n = 44).

Age at diagnosis varied widely, with a median age of 10 years (0.8–21 years). However, the median age for cats with HCM was statistically different (7.2 years, range 0.8–15 years, $P < 0.001$) from cats with RCM (10.3 years, range 4–16 years) and cats with secondary CM (14.6 years, range 7–21 years).

Most cats in the study (n = 57) had a cardiac murmur at cardiac auscultation. Nevertheless, the presence of a heart murmur varied in the three groups of CM: 76% (n = 38) of cats with HCM had a cardiac murmur, while few cats (n = 5, 35%) in the RCM group had a cardiac murmur; 47% of cats with secondary CM had a cardiac murmur (Table 1).

The majority of the overall population presented with one or more clinical signs (n = 57, Table 2). The presence of clinical signs varied between the three groups. All cats with RCM presented with clinical signs, cats with HCM showed a higher prevalence of symptomatic patients compared with asymptomatic ones, and cats with secondary CM were equally distributed in the two categories.

On echocardiographic evaluation, five patterns of LV morphology were identified (Table 1). All cats with HCM had a variable degree of LV hypertrophy. Most of the cats presented with an asymmetric echocardiographic pattern (52% of cats with HCM), localised in most patients at the IVS (n = 21) and to a lesser extent to the LVFW (n = 5). A concentric symmetrical pattern was identified in 38% of patients (n = 19), while only 10% of patients had hypertrophied papillary muscles but no evidence of increased wall thicknesses in diastole.

All cats with RCM showed IVS and LVFW <6 mm, atrial enlargement and a restrictive pattern at pulsed wave transmitral Doppler flow.

Cats with secondary CM presented with a wide spectrum of echocardiographic pattern: 41% (n = 9) of cats had symmetrical hypertrophy, 27% (n = 8) and 23% (n = 7) had asymmetrical hypertrophy of the LVFW and IVS respectively, two cats presented absence of hypertrophy with LV dilation (6%) and only one cat (3%) presented with isolated papillary muscle hypertrophy.

Most of the cats with hypertensive heart disease showed concentric (n = 8, 47%) and IVS hypertrophy (n = 5, 30%), while few of them presented with isolated LVFW (n = 3, 17%) and papillary muscle hypertrophy (n = 1, 6%). Cats with hyperthyroidism showed a more variable echocardiographic pattern, with four (32%) cats with concentric and seven cats with asymmetrical LV hypertrophy (53%, most LVFW hypertrophy). Two cats (15%) presented no hypertrophy but LV dilation with preserved fractional shortening and ejection fraction.

Table 1 Population characteristics at presentation

	Overall population	HCM	RCM	Secondary CM
Age at diagnosis (years)	10 (0.8–21)	7.2 (0.8–15)	10.3 (4–16)	14.6 (7–21)
Sex	50♂/44♀	32♂/18♀	4♂/10♀	14♂/16♀
Breed	Domestic shorthair 60 (65%) Persian 20 (21%) Norwegian Forest Cat 4 (4%) Siamese 4 (4%) Maine Coon 3 (3%) Ragdoll 2 (2%) Birman 1 (1%)	Domestic shorthair 25 (50%) Persian 16 (32%) Maine Coon 3 (6%) Norwegian Forest Cat 2 (4%) Ragdoll 2 (4%) Birman 1 (2%) Siamese 1 (2%)	Domestic shorthair 8 (58%) Persian 3 (21%) Siamese 2 (14%) Norwegian Forest Cat 1 (7%)	Domestic shorthair 27 (91%) Persian 1 (3%) Norwegian Forest Cat 1 (3%) Siamese 1 (3%)
Heart murmur	37 (39%)	38 (76%)	5 (35%)	14 (50%)
Arrhythmias during auscultation	4 (4%)	1 (2%)	0	3 (10%)
Clinical signs	53 (54%)	29 (58%)	14 (100%)	10 (33%)
SAM	40 (43%)	31 (62%)	0 (0)	9 (30%)
Echocardiographic pattern of hypertrophy	Symmetric hypertrophy 30 (32%) Asymmetrical IVS 28 (30%) Asymmetrical LVFW 13 (14%) Asymmetrical PapMuscle 6 (6%) RCM phenotype 14 (15%) No hypertrophy 3 (3%)	Symmetric hypertrophy 19 (38%) Asymmetrical IVS 21 (42%) Asymmetrical LVFW 5 (5%) Asymmetrical PapMuscle 5 (5%) RCM phenotype 0 (0)	Symmetric hypertrophy 0 Asymmetrical IVS 0 Asymmetrical LVFW0 Asymmetrical PapMuscle 0 RCM phenotype 14 (100%)	Symmetric hypertrophy 13 (41%) Asymmetrical IVS 7 (23%) Asymmetrical LVFW 8 (27%) Asymmetrical PapMuscle 1 (3%) No hypertrophy 2 (6%)
LA/Ao ratio	Normal 38 (40%) Mild to moderate 38 (40%) Severe 17 (20%)	Normal 24 (48%) Mild to moderate 17 (34%) Severe 9 (18%)	Normal 0 Mild to moderate 9 (64%) Severe 5 (36%)	Normal 14 (50%) Mild to moderate 12 (40%) Severe 3 (10%)
Hypercoagulable state on echocardiography	11 (12%)	7 (14%)	3 (27%)	1 (3%)

HCM = hypertrophic cardiomyopathy; RCM = restrictive cardiomyopathy; CM = cardiomyopathy; SAM = systolic anterior motion of the mitral valve; IVS = interventricular septum; LVFW = left ventricle free wall; LA/Ao = left atrial to aortic root; PapMuscle = papillary muscle

SAM was identified in 40 patients. It was more common in cats with HCM (n = 31) compared with secondary CM, equally distributed between hypertensive and hyperthyroid cats (n = 9). No cat with RCM had SAM.

In the overall population, left atrial dimensions were normal in 40% of patients and were above reference range in 60% of patients. LA/Ao ratio was mildly to moderately enlarged in 40% of patients, while only 20% of patients had severe LA enlargement.

Most of the cats with HCM and secondary CM had normal and mild to moderate left atrial enlargement, while most of the cats with RCM showed severe left atrial enlargement (Table 1).

Echocardiographic signs of a hypercoagulable state (smoke effect or direct thrombi visualisation in the left auricle or in the left atrium) were identified in 12% of patients, mainly cats with HCM and RCM (Table 1).

Univariate and multivariate analysis was performed in the overall population and in patients with primary CM (Table 3). Cardiac-related death occurred in 43% of cats, with different death rates depending on the CM: most of the cats with RCM died of cardiac related death (86%), 44% of cats with HCM and only 20% of cats with secondary CM died of cardiac related death (Figure 1).

The poorest survival was found in cats with RCM (median survival 273 days), followed by cats with HCM (median survival 865 days). Cats with secondary CM showed the best survival time, not reaching the final endpoint (cardiac death) in around 80% of the total. Most of the cats died of non-cardiac-related causes, and a few of them were alive at last follow-up.

The presence of clinical signs was associated with decreased survival both in the overall population and in the primary CM group (Figure 1). Left atrial enlargement was associated with decreased survival regardless of the underlined CM (Figure 1).

Echocardiographic signs of hypercoagulable state were shown to decrease markedly survival (Figure 1).

Table 2 Clinical signs at presentation

Reason for presentation	Overall population	HCM	RCM	Secondary CM
Dyspnoea/CHF	38	19	12	7
Arterial thromboembolism	8	5	2	1
Syncope	7	5	0	2
Other (arrhythmias with no syncopal episodes)	4	1	0	3
Total	57 (61%)	30 (60%)	14 (100%)	13 (43%)

CHF = congestive heart failure; HCM = hypertrophic cardiomyopathy; RCM = restrictive cardiomyopathy; CM = cardiomyopathy

Cats with the RCM phenotype (median survival time 273 days), with symmetrical concentric hypertrophy (median survival time 273 days) and LVFW hypertrophy (median survival time 127 days) showed poorer survival compared with cats with asymmetrical IVS or papillary muscle hypertrophy (both groups had <50% of patients reaching the final endpoint; Figure 1).

The presence of clinical signs at presentation, left atrial enlargement and the echocardiographic identification of an hypercoagulable state were all negative prognostic factors in the multivariate analysis in the overall population (Table 3).

When considering primary CM only, the presence of left atrial enlargement and the identification of a hypercoagulable state were negative prognostic factors in the multivariate analysis

Discussion

CMs affecting feline patients include a heterogeneous group of myocardial disease with wide phenotypical variability. Since the last study on idiopathic CMs was published,[3] population characteristics and disease epidemiology have changed, with a strong decrease in dilated CM.

Furthermore, there is limited information about cardiovascular abnormalities in cats with systemic hypertension and hyperthyroidism, with most of the published work dating back 10 years ago.[21–24]

The present study is the first to present data from a feline referral population in Italy. HCM is the most common CM diagnosed at our institution (53% of the population included), followed by secondary CM (32% of the population included) and RCM (15%).

The main cat breed is the domestic shorthair cat, which is the most common cat breed in Italy. A more pronounced breed variability was found in the HCM group, where half of the cats were pedigree cats, with a high prevalence of Persian cats and some longhair breed cats (Maine Coon, Norwegian Forest Cat, Ragdoll and Birman), while most of the cats with RCM and secondary CM were domestic shorthairs.

Age at diagnosis in the overall population and in cats with HCM, RCM and secondary CM was higher than previously reported (mean age for HCM cats 7.2 years vs 4.8–6.5 years in previous studies[3,13–15]). The population of cats referred to our institution and diagnosed with HCM is older than previous studies because not so many Maine Coon and Ragdoll cats were present in our population. It has been highlighted by different studies that Maine Coon and Ragdoll cats have an early onset HCM, with cats of 1–2 years of age affected by aggressive HCM forms that eventually lead to death.[15,25]

In contrast, Persian and domestic shorthair cats have an older onset HCM, and this might reflect the results in our population.[8]

Sex distribution is different between CMs. Cats with HCM are predominantly males (64%), while cats with RCM show female predisposition (71%). These findings agree with previous HCM studies, which found a male predisposition,[3,13–15] while sex predisposition for RCM cats was similar to our results in the study by Ferasin et al.[3] No sex predisposition was found for secondary CM.

A different survival rate was identified in cats affected by CM, with the worse outcome associated with cats diagnosed with RCM, followed by HCM, while few cats died of cardiac-related death in the secondary CM group.

HCM is still the most commonly diagnosed primary CM, with wide echocardiographic appearance, as previously identified by some clinical and anatomopathological studies.[2,6–8]

Hypertrophy distribution was variable in cats with HCM, as the asymmetrical IVS form was the most commonly encountered (42% of all cats with HCM), followed by the concentric symmetrical form (38%). Few cats presented with LVFW or papillary muscle hypertrophy (10% each). Our results identify a different hypertrophy distribution compared with other clinical studies, where the concentric symmetrical form was the most frequently encountered (Brizard et al[7] 61% and Trehiou-Sechi[8] 34%). Although this finding was statistically significant only in the univariate analysis, the degree and the localisation of hypertrophy affects survival, as cats with asymmetrical IVS or papillary muscle HCM live longer than those with concentric symmetrical hypertrophy and asymmetrical LVFW hypertrophy.

Interestingly, the worst outcome was identified for asymmetrical LVFW HCM. This finding might be explained by the fact that hypertrophy of LVFW might

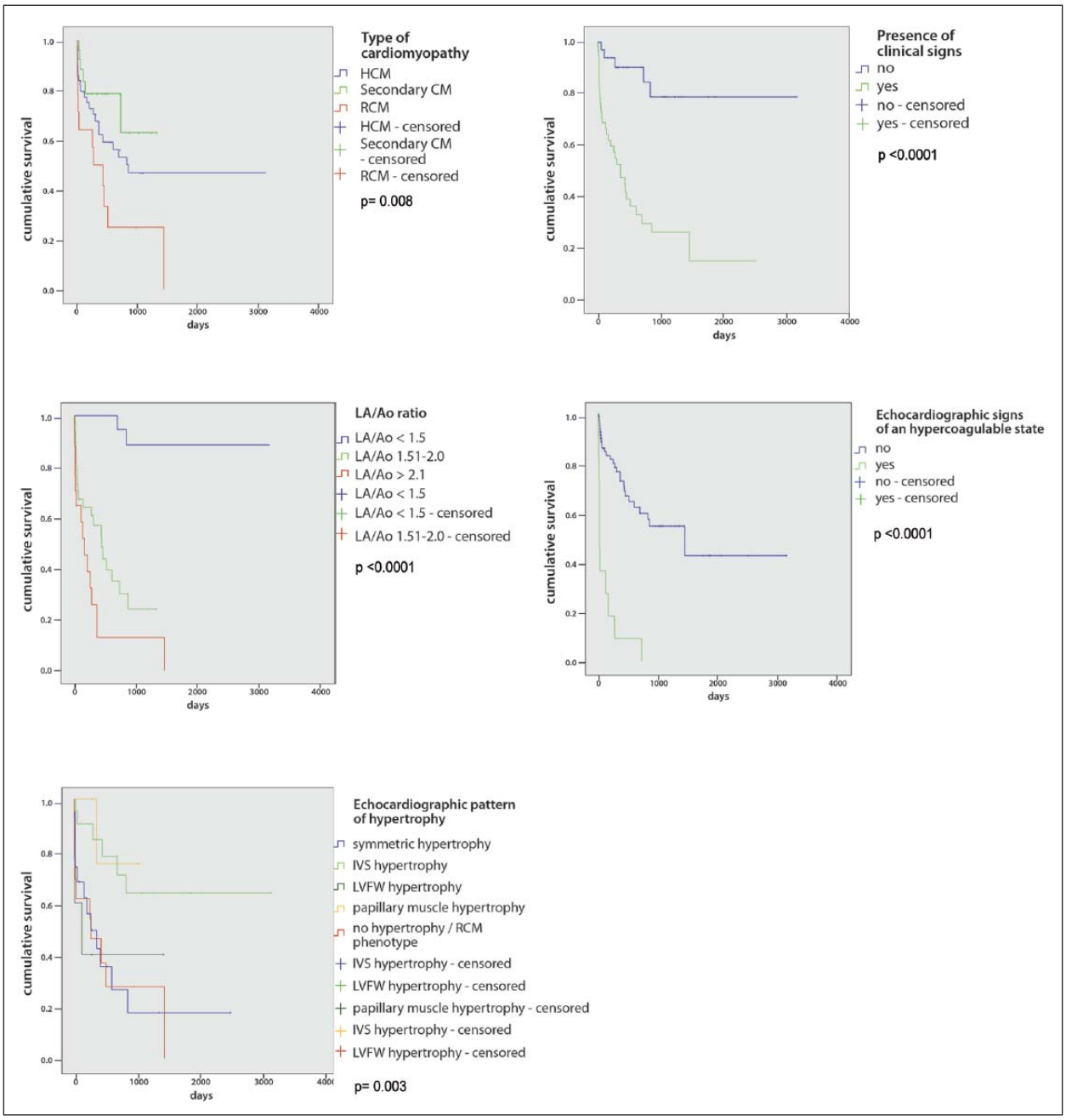

Figure 1 Kaplan–Meier survival curves in the overall population regarding type of cardiomyopathy, presence of clinical signs, left atrial to aortic root (LA/Ao) ratio and echocardiographic signs of a hypercoagulable state; a different survival time was identified in every category, as depicted. In the hypertrophic cardiomyopathy (HCM) and restrictive cardiomyopathy (RCM) group, a different survival time was observed depending on the echocardiographic pattern of hypertrophy. Log-rank *P* value is shown in each graph. CM = cardiomyopathy; IVS = interventricular septum; LVFW = left ventricular free wall

be associated with an absence of murmur (only one cat with LVFW hypertrophy had a heart murmur) and delayed diagnosis associated with the onset of clinical signs (all cats had one or more clinical signs). Unfortunately, this category was limited to only a few patients, and this could be associated with a selection bias. Hence, further studies are needed to support this hypothesis.

Symmetric HCM is associated with diffuse myocardial LV hypertrophy, and this could determine more severe diastolic dysfunction, which could favour the onset of clinical signs and early myocardial impairment.

The lack of hypertrophy is not a protective factor in cats with CM either, as cats with an RCM echocardiographic phenotype have poor survival. The same might be hypothesised for cats with HCM that show the 'burnt

Table 3 Univariate and multivariate analysis in the overall population and in cats with hypertrophic cardiomyopathy (HCM) and restrictive cardiomyopathy (RCM)

	Univariate analysis	Confidence intervals	*P* value	Multivariate analysis	Confidence intervals	*P* value
Overall population						
Presence of clinical signs	2.61	1.632–4.183	<0.001	2.38	1.163–3.187	0.003
LA/Ao ratio	37.03 (severe LA enlargement vs normal LA) 1.92 (severe LA vs moderate LA)	8.400–166.660 0.988–3.770	<0.001	3.65 (LA enlargement vs normal LA)	1.601–4.210	<0.001
Presence of echocardiographic signs of hypercoagulable state	2.00	1.572–2.549	<0.001	1.81	1.279–2.137	<0.001
Cardiomyopathy	2.28 (HCM vs secondary CM) 3.84 (RCM vs secondary CM)	1.127–4.629 1.434–10.309	0.014	NS		
Presence of heart murmur	0.72	0.524–0.988	0.042	NS		
Echocardiographic pattern of hypertrophy	2.80 (asymmetrical vs symmetrical HCM) 7.14 (RCM vs asymmetrical HCM)	1.915–12.500 0.926–55.555	0.09	NS		
HCM+RCM						
LA/Ao ratio	27.78 (severe LA enlargement vs normal) 1.49 (severe vs moderate LA enlargement)	6.289–125.000 0.727–3.105	<0.001	5.35 (enlargement vs normal LA)	1.813–6.250	<0.001
Echocardiographic signs of hypercoagulable state	2.31	1.714–3.109	<0.001	2.01	1.348–2.524	<0.001
Echocardiographic pattern of hypertrophy	4.60 (symmetrical vs asymmetrical HCM) 6.40 (RCM vs asymmetrical HCM)	1.692–12.500 0.822–50.000	0.013	NS		
Cardiomyopathy	0.76 (HCM vs RCM)	0.602–0.964	0.024	NS		
Presence of heart murmur	0.58	0.412–0.820	0.002	NS		
Clinical signs	2.74	1.509–4.964	0.001	NS		
Presence of SAM	0.70	0.498–0.997	0.048	NS		

LA/Ao = left atrial to aortic root; LA = left atrium; CM = cardiomyopathy; SAM = systolic anterior motion of the mitral valve; NS = not statistically significant

out' echocardiographic morphology, where myocardial thinning is related to severe myocardial ischemia and myocardial death.[4] However, no burnt out morphology was identified in our case series.

The protective effect of asymmetrical IVS hypertrophy has also been related to SAM pathogenesis and to the association of a heart murmur, thus providing clinical tools to perform early diagnosis.[15] As a matter of fact, most of the cats with IVS hypertrophy presented with a heart murmur (81%).

SAM can be considered a protective factor only if primary CMs are analysed, as well as the presence of a heart murmur. Both these findings can be considered protective, because they could favour early diagnosis in an asymptomatic patient.

Different pathophysiological mechanisms are responsible for myocardial hypertrophy in cats with secondary CM compared with primary HCM. Systemic hypertension induces an increase in LV thickness, mainly as a result of an attempt of the LV to normalise LV wall stress and cope with the increase in chronically elevated afterload.[10] LV hypertrophy and mass are prognostic markers in hypertensive human patients and antihypertensive therapies reduce LV mass, thus reducing the risk for cardiovascular events and death.[10] The increase in thyroid hormone concentration induces a positive chronotropic effect, an increase in β-adrenergic response and a reduction in systemic vascular resistance, which will in turn determine a so-called 'high output state' of the heart.[11]

The echocardiographic appearance of cats with systemic hypertension showed a predominant concentric and IVS hypertrophy pattern, as also identified in previous studies,[22–24] while cats with hyperthyroidism did not show a prevalent echocardiographic pattern, with a similar number of cats showing symmetrical, asymmetrical IVS or LVFW hypertrophy.

Because there is no clear distinction between the echocardiographic appearance of cats with primary or secondary hypertrophy, the importance of excluding concomitant systemic illnesses during diagnostic workout should be emphasised, as in most cases its recognition determines regression of cardiac disease and/or reduced risk for cardiovascular events.

In a few select cases, however, cardiac remodelling secondary to a systemic illness that is not properly managed can still lead to cardiac worsening and eventually death. It is not clear whether these patients have a primary CM associated with a systemic illness that exacerbates primary CM or whether cats with a secondary CM die of cardiac-related death as a consequence of unsuccessful response to systemic therapy and clinical worsening.

RCM is a less commonly encountered CM and is thought to be similar to human RCM for its echocardiographic phenotypical appearance. However, in veterinary studies,[2,12] infiltrative disease was not reported to be as common as it is in human patients (50% of RCM cases in human medicine[1]). So our knowledge concerning the etiopathogenesis of RCM in cats still appears to be unclear.

RCM is the second most common primary CM in cats, although its frequency is much lower than HCM and secondary CM combined (15% of the population studied). The prognosis is poor, with most of the cats dying of cardiac-related death less than 1 year after first diagnosis. Nevertheless, our case series showed longer median survival time compared with previous studies, with a median survival time of 7 months.

As all the cats in the RCM group were symptomatic, this finding might explain poor survival and does not help to clarify the etiopathogenesis, as no subclinical phase was identified in our case series or in other studies.[2,3,12] What might determine fibrosis and LV stiffness exactly remains unclear. Further studies are needed to categorise this condition better and to slow the progression of the disease.

Independently from the underlined CM, negative prognostic markers in the overall population are the presence of clinical signs, left atrial enlargement and echocardiographic signs of an hypercoagulable state. The presence of clinical signs is considered to be associated with the presence of congestive heart failure (CHF) and thus supports the hypothesis that cats with CHF do not live as long as a consequence of severe myocardial impairment. Asymptomatic cats failed to reach a survival probability of $<50\%$ by the end of the study. Hence, the absence of clinical signs is also a protective factor in our study.

Left atrial enlargement has always been considered as a poor prognostic factor in all previous HCM studies,[3,13–16] and is also confirmed in our study, regardless of CM classification. Left atrial enlargement might be a marker of long-standing, progressing CM and thus might explain the onset of clinical signs and might be responsible for the increased risk of hypercoagulable state. LA enlargement might thus be considered as a marker of disease severity, regardless of the underlined CM.

A hypercoagulable state was not common in our population, but proved fatal in most of the cats by markedly reducing survival (median survival time 7 days). The majority of cats with a hypercoagulable state had arterial thromboembolism or a direct echocardiographic visualisation of LA thrombi. Those presenting with smoke effect but no thrombi showed a better outcome with longer survival times: up to 732 days after diagnosis compared with 123 days for cats with echocardiographic confirmation of LA thrombi. Arterial thromboembolism is therefore a marker of severe cardiovascular impairment.[4,26]

Limitations of this study were mainly related to its retrospective nature. No systematic treatment protocols were performed, some clinical (T4 measurement) and echocardiographic data (ie, transmitral pulsed wave Doppler pattern) were not systematically assessed in our

archive. The distribution of CMs might reflect some bias related to the referral centre where the study was carried out, and the possibility that some cats classified as affected by secondary CM might have a primary CM as well, exacerbated by systemic disease. Finally, owner-related information could have biased the results due to misinterpretation of clinical signs or failure to recognise cardiac-related death.

Conclusions

HCM and RCM are the most commonly diagnosed primary CMs in our cohort of patients. Secondary CMs are commonly reported as a cause for cardiac investigation due to the presence of clinical signs or clinical abnormalities during general clinical examination and echocardiographic study. The present survival study showed an overall risk of death in cats with clinical signs, LA enlargement and echocardiographic signs of a hypercoagulable state, regardless of the underlying CM. Secondary CMs are associated with few cases of cardiac deaths. Asymptomatic HCM patients showed longer survival times. Cats with RCM generally have a poor prognosis in the short and long term.

Acknowledgements The authors would like to thank Marco Colombo for technical image assistance and all the referring vets and cat owners that made possible this study.

Conflict of interest The authors do not have any potential conflicts of interest to declare.

Funding This research received no grant from any funding agency in the public, commercial or not-for-profit sectors.

References

1 Elliot P, Andersson B, Arbustini E, et al. **Classification of the cardiomyopathies: a position statement from the European Society of Cardiology Working Group on Myocardial and Pericardial Diseases**. *Eur Heart J* 2006; 29: 270–276.
2 Ferasin L. **Feline myocardial disease part 1: classification, pathophysiology and clinical presentation**. *J Feline Med Surg* 2009; 11: 3–13.
3 Ferasin L, Sturgess CP and Cannon MJ. **Feline idiopathic cardiomyopathy: a retrospective study of 106 cats (1994–2001)**. *J Feline Med Surg* 2003; 5: 151–159.
4 Coté E, Macdonald K, Meurs K, et al. Feline cardiology. 1st ed. Somerset, NJ: Wiley-Blackwell, 2011.
5 Boon J. Veterinary echocardiography. 2nd ed. Chichester: Wiley-Blackwell, 2011, pp 37–255.
6 Peterson EN, Moise NS and Brown CA. **Heterogeneity of hypertrophy in feline hypertrophic heart disease**. *J Vet Intern Med* 1993; 7: 183–189.
7 Brizard D, Amberger C, Hartnack S, et al. **Phenotypes and echocardiographic characteristics of an European population of domestic shorthair cat with idiopathic hypertrophic cardiomyopathy**. *Schweiz Arch Tierheilkd* 2009; 151: 529–538.
8 Trehiou-Sechi E, Tissier R, Gouni R, et al. **Comparative echocardiographic and clinical features of hypertrophic cardiomyopathy in 5 breeds of cats: a retrospective analysis of 344 cases (2001–2011)**. *J Vet Intern Med* 2012; 26: 532–543.
9 Syme HM. **Cardiovascular and renal manifestations of hyperthyroidism**. *Vet Clin North Am Small Anim Pract* 2007; 37: 723–743.
10 Santos M and Shah AM. **Alterations in cardiac structure and function in hypertension**. *Curr Hypertens Rep* 2014; 16: 428–438.
11 Klein I and Ojamaa K. **Thyroid hormone and the cardiovascular system**. *N Engl J Med* 2001; 344: 501–509.
12 Fox P, Basso C, Thiene G, et al. **Spontaneously occurring restrictive nonhypertrophied cardiomyopathy in the domestic cats: a new animal model of human disease**. *Cardiovasc Pathol* 2014; 23: 28–34.
13 Atkins CE, Gallo AM, Kurzman ID, et al. **Risk factors, clinical signs and survival in cats with a clinical diagnosis of idiopathic hypertrophic cardiomyopathy: 74 cases (1985–1989)**. *J Am Vet Med Assoc* 1992; 201: 613–618.
14 Rush JE, Freeman LM, Fenollosa LK, et al. **Population and survival characteristics of cats with hypertrophic cardiomyopathy: 260 cases (1990–1999)**. *J Am Vet Med Assoc* 2002; 220: 202–207.
15 Payne JR, Luis Fuentes V, Boswood A, et al. **Population characteristic and survival in 127 referred cats with hypertrophic cardiomyopathy (1997 to 2005)**. *J Small Anim Pract* 2010; 51: 540–547.
16 Payne JR, Borgeat K, Connolly DJ, et al. **Prognostic indicators in cats with hypertrophic cardiomyopathy**. *J Vet Intern Med* 2013; 27: 1427–1436.
17 Brown S, Atkins C, Bagley R, et al. **ACVIM consensus statement: guidelines for the identification, evaluation, and management of systemic hypertension in dogs and cats**. *J Vet Intern Med* 2007; 21: 542–558.
18 Pittari J, Rodan I, Beekman G, et al. **American Association of Feline Practitioners: senior care guidelines**. *J Feline Med Surg* 2009; 11: 763–778.
19 Fifer MA and Vlahakes GJ. **Management of symptoms in hypertrophic cardiomyopathy**. *Circulation* 2008; 117: 429–439.
20 Adin DB and Diley-Poston L. **Papillary muscle measurements in cats with normal echocardiograms and cats with concentric left ventricular hypertrophy**. *J Vet Intern Med* 2007; 21: 737–741.
21 Weichselbaum R, Feeney D and Jessen C. **Relationship between selected echocardiographic variables before and after radioiodine treatment in 91 hyperthyroid cats**. *Vet Radiol Ultrasound* 2005; 46: 506–513.
22 Chetboul V, Lefebre HP, Pinhas C, et al. **Spontaneous feline hypertension: clinical and echocardiographic abnormalities and survival rate**. *J Vet Internal Med* 2003; 17: 89–95.
23 Snyder P, Salek D and Jones GL. **Effect of amlodipine on echocardiographic variables in cats with systemic hypertension**. *J Vet Internal Med* 2001; 15: 52–56.
24 Nelson L, Reidesel E, Ware W, et al. **Echocardiographic and radiographic changes associated with systemic hypertension in cats**. *J Vet Intern Med* 2002; 16: 418–425.
25 Lefbom BK, Rosenthal SL, Tyrrell WDJ, et al. **Severe hypertrophic cardiomyopathy in 10 young Ragdoll cats**. *J Vet Intern Med* 2001; 15: 308.
26 Luis Fuentes V. **Arterial thromboembolism: risks, realities and a rational first-line approach**. *J Feline Med Surg* 2012; 14: 459–470.

Case Report

jfms OPEN REPORTS

Journal of Feline Medicine and Surgery Open Reports
1–5

DOI: 10.1177/2055116915593966
jfmsopenreports.com
SAGE

Primary angiocentric/angioinvasive T-cell lymphoma of the tympanic bulla in a feline leukaemia virus-positive cat

Sara F Santagostino[1], Carlo M Mortellaro[1], Julia Buchholz[2], Margherita Lugli[1], Annalisa Forlani[1], Gabriele Ghisleni[1] and Paola Roccabianca[1]

Abstract

Case summary A 5-year-old neutered female feline leukaemia virus (FeLV)-positive domestic shorthair cat with a 5 month history of otitis media was referred for head tilt, stertor and dyspnoea. Computed tomography scan revealed soft tissue opacities inside the right tympanic bulla, with bone remodelling, and concurrent nasopharyngeal and intracranial invasion. Endoscopically guided bioptic samples were collected from the nasopharynx and middle ear. Histology revealed dense sheets of round, large, neoplastic cells, often surrounding or invading vascular walls. Neoplastic cells expressed CD3, FeLV p27 and gp70 antigens. A middle ear angiocentric/angioinvasive T-cell lymphoma was diagnosed. After improvement of clinical conditions following radiation therapy, the cat died unexpectedly. At necropsy, hepatic and splenic spread was detected.

Relevance and novel information Primary middle ear tumours are rare and their diagnosis is often delayed as clinical signs mimic more common otological conditions. Multiple bioptic specimens are pivotal for a definitive diagnosis. The young age of the cat, serology and immunohistochemistry revealed a possible transforming role of FeLV.

Accepted: 6 April 2015

Introduction

Lymphoma is considered the most common neoplasm in cat.[1] Before the introduction of feline leukaemia virus (FeLV) testing and vaccination, primary mediastinal and multicentric forms were reported,[2] while a shift towards intestinal and extranodal lymphoma subtypes is currently being observed.[1] While nasopharyngeal polyps are common and well documented in juvenile cats,[3,4] neoplasms arising from the middle ear are considered rare,[5] and only three cases of feline primary middle ear lymphoma have been reported.[6–8] This report details a cat affected by otitis media developing neurological signs caused by the presence of a middle ear and nasopharyngeal lymphoma.

Case description

A 5-year-old, spayed female, FeLV-positive, domestic shorthair cat with a previous 5 month history of otitis media not responsive to the pharmacological therapy with dexamethasone (0.5 mg/kg q24h) and amoxiclavulanic acid (25 mg/kg q12h), was referred to the University of Milan for persistent clinical signs, which included anysocoria, right head tilt, stertor and dyspnoea.

On physical examination, major clinical signs also included dysphagia, dysphonia and gagging. Myosis of the right pupil was present. A brownish, dense material oozed from the external ear canal. Body temperature,

[1]Department of Veterinary Science and Public Health, Faculty of Veterinary Medicine, University of Milan, Milan, Italy
[2]Animal Oncology and Imaging Center, Zurich, Switzerland

This case was presented as a poster at the 31st European Society of Veterinary Pathology/European College of Veterinary Pathologists meeting held in London in September, 2013.

Corresponding author:
Sara F Santagostino DVM, Department of Veterinary Science and Public Health, Section of Veterinary and Avian Pathology, Faculty of Veterinary Medicine, University of Milan, Via Celoria 10, 20133 Milan, Italy
Email: sara.santagostino@unimi.it

pulse and respiration were within normal limits. No clinically relevant alterations of some parameters were recorded by complete cell blood count (CBC) and serum biochemistry (Table 1). Serology with a commercially available enzyme-linked immunosorbent assay test (SNAP FeLV test; IDEXX) was repeated and FeLV was confirmed. A computerised tomography (CT) scan of the tympanic bullae and nasal cavities was performed. The tympanic bullae were characterised by complete bilateral loss of the normal air content. Focal soft tissue attenuation within the medial portion of the right external ear canal was recorded. A homogeneously hyperdense soft tissue opacity with enlargement of the ventromedial aspect of the right tympanic bulla, and multifocal bone lysis and remodelling of the tympanic osseous margins were documented, along with focal lysis of the right temporal bone and a local 1.5 mm opacity within the right piriform lobe (Figure 1a). Additionally, loss of the normal choanal air content and of the right ethmoid labyrinth, with deformity of the right nasopharyngeal wall and complete obliteration of the nasopharyngeal lumen caused by a 4.1 mm extension of soft tissue attenuation, were detected. There was a mechanical effect of the mass onto the hyoid apparatus and larynx, without detectable destructive/reactive processes. No anomalies were documented within the maxillary and frontal sinuses, and the sphenoid recesses. A subsequent total body CT scan was negative for thoracic and/or abdominal organ abnormalities.

An endoscopic evaluation of the nasopharynx with a flexible paediatric fibrobronchoscope evidenced total obstruction of the nasopharynx by a pink, smooth, trilobated soft tissue mass located in close contact with the opening of the Eustachian tube.

Otoscopical examination with a rigid scope (2.7 mm in diameter, 19.0 mm in length) evidenced a mass within the horizontal ear canal, emerging from the middle ear and protruding through a perforated tympanum (Figure 1b). Four perendoscopic bioptic specimens of 2–4 mm in diameter were obtained from the nasopharynx and the middle ear, and submitted for cytology and histopathology.

In accordance with diagnostic imaging and endoscopic evaluations, differential diagnoses for the rhinopharyngeal condition included nasopharyngeal polyp, lymphoplasmacytic rhinopharyngitis, neoplasia and cryptococcal granuloma, and a middle ear polyp or a middle ear tumour were considered for the middle ear condition.

Microscopic examination of tissue samples obtained from both anatomical sites revealed the presence of an unencapsulated, poorly demarcated, densely cellular neoplasm composed of sheets of round cells, surrounding and multifocally invading blood vessel walls (angiocentrism) (Figure 1c). The neoplastic cells were large, measuring 25–28 µm in diameter, with distinct cell borders, a moderate amount of pale eosinophilic and finely vacuolated cytoplasm, and large round nuclei (2.0–2.5 times the diameter of an erythrocyte) with occasional central round nucleoli (Figure 1d).

Table 1 Complete blood count (CBC) and serum biochemistry panel

Test	Result	Reference interval
CBC		
RBC ($\times 10^6$/µl)	6.15	5.0–11.20
Haemoglobin (g/dl)	10.0	10.6–15.6
Haematocrit (%)	34.4	31.7–48.0
MCV (fl)	55.9	36.7–55.0
MCH (pg)	16.3	12.3–17.3
MCHC (g/dl)	29.1	30.1–35.6
RDW (%)	18.3	16.7–22.9
Platelets ($\times 10^3$/µl)	323	175–500
WBC ($\times 10^3$/µl)	4.13	4.04–18.70
Automated differential ($\times 10^3$/µl)		
Segmented neutrophils	2.45	2.3–14.0
Band neutrophils	0.00	0.0–0.0
Lymphocytes	0.5	0.8–6.1
Monocytes	0.11	0.0–0.7
Eosinophils	0.00	0.0–1.5
Basophils	0.00	0.0–0.1
Chemistry – Canine/feline standard panel		
Glucose (mg/dl)	135	67–168
BUN (mg/dl)	45.8	15–60
Creatinine (mg/dl)	1.9	1.0–2.0
Sodium (mmol/l)	151.0	146–157
Potassium (mmol/l)	4.8	3.5–4.8
Chloride (mmol/l)	110	116–126
Total protein (g/dl)	6.08	6.0–8.6
ALT (U/l)	15	<80
AST (U/l)	27	<40
ALP (U/l)	45	<145
GGT (U/l)	6	5.19
Total bilirubin (mg/dl)	0.3	0.1–0.8

RBC = red blood cells; MCV = mean cell volume; MCH = mean cell haemoglobin; MCHC = mean cell haemoglobin concentration; RDW = red blood cell distribution width; WBC = white blood cells; BUN = blood urea nitrogen; ALT = alanine aminotransferase; AST = aspartate aminotransferase; ALP = alkaline phosphatase; GGT = γ-glutamyl transpeptidase

Mitotic figures ranged from 2 to 4 per high-power field.

Immunohistochemistry was performed with primary antibodies recognising CD3ε (1:20 dilution, rat monoclonal, clone CD3-12 Rat IgG1, human cross-reactive with feline; Serotec), CD20 (1:400 dilution, rabbit polyclonal, human cross-reactive with feline; NeoMarkers), FeLV p27 (1:100 dilution, mouse monoclonal, clone PF12J-10A; Custom Monoclonal International) and FeLV gp85/70 (1:200 dilution, mouse monoclonal, clone C11D8; Custom Monoclonal International).

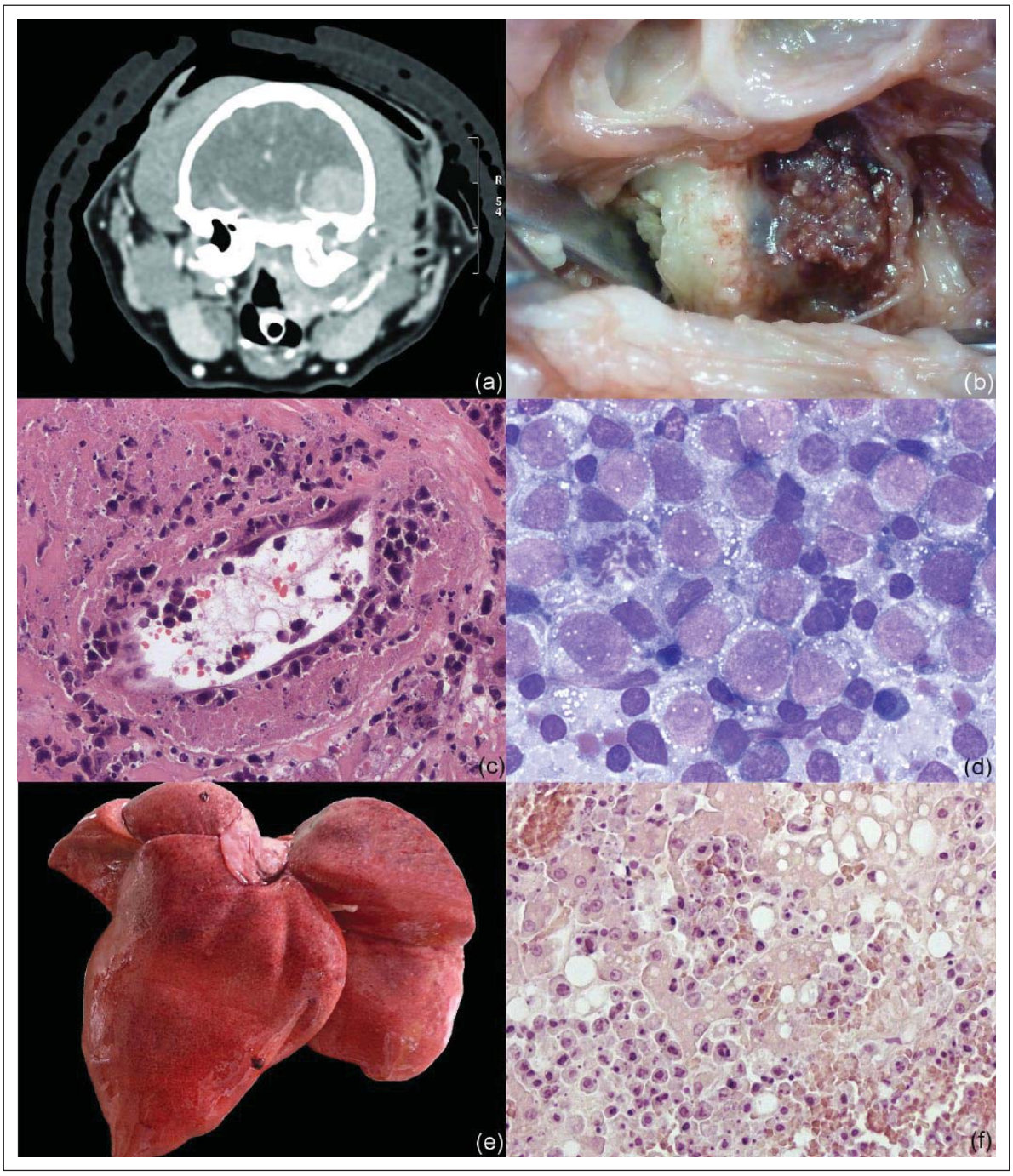

Figure 1 (a) Transverse computed tomography of the head. A soft tissue mass enlarges the medial aspect of the right tympanic bulla, with extension to the external ear canal. There is a concurrent strongly contrast-enhancing extension within the right piriform lobe and retropharyngeal space. (b) Right tympanic bulla. The ventromedial compartment is obliterated by a soft red proliferating mass. There is remodelling of the tympanic osseous margins with lysis and osteophyte formation. (c) Right tympanic bulla, diffuse large cell lymphoma and angiocentric/angioinvasive pattern. Neoplastic cells with irregularly distinct cell boundaries are disrupting and infiltrating a blood vessel. Haematoxylin and eosin (× 40). (d) Right tympanic bulla, diffuse large cell lymphoma and plasmacytoid morphology with brushing. Large, discrete lymphoid cells with scant blue vacuolated cytoplasms, round nuclei and 1–2 prominent nucleoli. Scattered small mature lymphocytes are visible. May Grünwald–Giemsa (× 40). (e) Severe diffuse hepatomegaly. (f) Histological section of the liver. The hepatic parenchyma is obscured and replaced by dense sheets of atypical lymphoid neoplastic cells with severe anisocytosis and nuclear pleomorphism

For all antibodies, antigen retrieval was achieved by heating slides in citrate buffer at pH 6.0 in a commercial pressure cooker Decloaker (Biocare Medical, Walnut Creek, CA, USA) for 10 mins.

Approximately 70% of neoplastic cells were intensely cytoplasmic CD3-positive while CD20 was diffusely negative. Cytoplasmic FeLV gp70 (capsidic glycoprotein) and cytoplasmic p27 (core protein) positivity were observed. A diffuse large cell angiocentric/angioinvasive T-cell lymphoma was diagnosed.

Routine clinical staging results, including chest and abdominal radiographs, serum biochemistry, CBC and abdominal ultrasound, were without clinically relevant alterations, and a stage I lymphoma was confirmed. Given the life-threatening dyspnoea, the cat was submitted for an extensive surgical debulking of the nasopharynx, followed by a radiation protocol of 10 fractions of 3.2 Gy each for the brain and six fractions of 6 Gy each for the middle ear. The cat was irradiated with a 6 MV Varian Linac with MLC (multileaf collimator). A single injection of L-asparaginase was administered after the first half of the radiation protocol. The cat was initially stable but died suddenly 7 days after the last radiation.

A full necropsy was granted by the owners.

At post-mortem examination the nasopharynx was free of disease. There was marked thickening of the right tympanic bone in association with multifocal osteolysis. The ventromedial compartment of the tympanic bulla was obliterated by the neoplastic tissue. A focal central nervous system (CNS) invasion was detected, with compression atrophy of the piriform lobe and adhesion of the neoplastic tissue to the base of the skull. Microscopically, the nasopharyngeal submucosa was variably infiltrated by neutrophils and small lymphocytes. However, following surgical debulking and radiation therapy, no neoplastic cells were evidenced at this time via multiple examined sections. Liver (Figure 1e) and spleen were diffusely pale red, enlarged, with massive infiltration of neoplastic cells with increased cellular pleomorphism (Figure 1f).

Scattered neoplastic cells were also microscopically evidenced in the right piriform lobe.

Death was ascribed to progression of the CNS extension (the cat developed convulsions approximately 1 week after radiation therapy) and multiorgan failure secondary to massive and widespread neoplastic invasion.

Discussion

To our knowledge, a primary tympanic lymphoma extending to the nasopharynx and CNS, followed by internal organ invasion seems not to have been previously reported. The diagnosis of a primary tumour of middle ear origin was derived from the anatomical distribution of the lesions, with concurrent tympanic rupture and the observation of morphologically similar neoplastic cells in both nasopharyngeal and middle ear compartments. In small animals, reports of neoplasia involving middle ear structures are rare.[9] Occasional reports of primary middle ear neoplasia in cats include squamous cell carcinoma (SCC) and rarely carcinomas, lymphomas and fibrosarcomas.[10]

The diagnosis of primary middle ear tumours is not considered straightforward. It is often delayed as clinical signs mimic some more common otological conditions such as inflammatory nasopharyngeal polyps, chronic otitis media, chronic proliferative otitis externa with middle ear involvement and, less frequently, cholesterol granulomas.[4,10,11]

Furthermore, the clinical signs of patients with middle ear tumours are often aspecific and most likely related to vestibular system abnormalities, concurrent otitis media/externa or nasopharyngeal secondary involvement.[12]

In this case, primary origin from the middle ear was confirmed by clinical presentation and anatomical distribution of lesions demonstrated by diagnostic imaging techniques. Indeed, the lesion observed in this cat was confined to the ventromedial compartment of the tympanic bulla, while the dorsolateral compartment of the bulla was devoid of neoplastic lesions. Owing to the characteristic anatomy of the feline middle ear, the ventromedial compartment of the tympanic bulla seems not to be commonly involved in feline auricular diseases.[13–15] This peculiar location, along with the previous clinical history and clinical signs of otitis media, and the onset of respiratory signs only secondarily, were highly suggestive of a primary ongoing process arising from the ventromedial compartment of the middle ear.

Little information regarding clinical signs, FeLV status and phenotype from previous reports of middle ear lymphoma could be retrieved.[6,8] A large T-cell lymphoma with metastasis to the regional lymph nodes has been described to involve the tympanic bulla of a cat.[7] Thus, comparison with other cases was not possible.

This cat had a long history of persistent inflammation, diagnosed by the referring veterinarian. A persistent inflammation has been associated with the subsequent development of a wide range of malignancies, and is accepted as a risk factor for the development of a variety of cancers, including lymphomas, in humans and cats.[16,17]

During chronic inflammation, lymphoid cell proliferation and gene rearrangements of T- and B-cell receptors increase with increasing production of normal but also autoreactive cells or cells with genetic mutations.[18] The relationship between lymphoma and FeLV has also long been studied. Overall, approximately 70% of cats with lymphoma have FeLV antigenaemia.[19] The rate of FeLV serological positivity has been correlated with the anatomical form of lymphoma.[5] However, owing to their rarity, no data are available for nasal or ear lymphomas. This cat was serologically positive for FeLV

and neoplastic cells expressed FeLV proteins. The expression of p27 indicates that viral infection has occurred, and FeLV gp70 expression denotes viral particle assembly confirming viral integration, replication and productive infection.[20] Thus, positivity to FeLV antigens suggested a possible role of FeLV in lymphoma development.

Lymphoid proliferation induced by persistent inflammation favours FeLV reactivation and replication within infected cells, increasing the probability of neoplastic transformation.

Angiocentricity has been described for a subset of subcutaneous lymphomas in cats,[21] where viable lymphoid neoplastic cells formed a rim around functional vessels, as reported in this case. The induction of the expression of specific homing and tethering molecules by vascular cells might have contributed to the angiocentric growth. Additionally, neoplastic lymphoid cells often invaded the vessel's wall, causing necrosis as part of general tissue invasion in our case.

Conclusions

Tumours of the auricular structures are important causes of otic morbidity and mortality, and should be considered in any case of non-responsive otitis. A high index of clinical suspicion along with proper imaging techniques, multiple deep, adequately sized biopsies and immunohistochemistry are usually required for a definitive diagnosis.

Funding The authors received no specific grant from any funding agency in the public, commercial or not-for-profit sectors for the preparation of this case report.

Conflict of interest The authors do not have any potential conflicts of interest to declare.

References

1 Vail DM. **Feline lymphoma and leukemia**. In: Withrow SJ, Vail DM and Page RL (eds). Withrow and MacEwen's small animal clinical oncology. 5th ed. St Louis, MO: WB. Saunders, 2013, pp 638–653.
2 Louwerens M, London CA, Pedersen NC, et al. **Feline lymphoma in the post-feline leukemia virus era**. *J Vet Intern Med* 2005; 19: 329–335.
3 Anderson DM, Robinson RK and White RA. **Management of inflammatory polyps in 37 cats**. *Vet Rec* 2000; 147: 684–687.
4 Sadrzadeh H, Abtahi SM and Fathi AT. **Infectious pathogens and hematologic malignancy**. *Discov Med* 2012; 14: 421–433.
5 Jacobs RM, Messick JB and Valli VE. **Tumors of the hemolymphatic system. Lymphoid tumors**. In: Meuten DJ (ed). Tumors in domestic animals. 4th ed. Ames, IA: Iowa State Press, 2002, pp 119–198.
6 Carpenter JC, Andrews LK and Holzworth J. **Tumors and tumor-like lesions**. In: Holzworth J (ed). Diseases of the cat. Philadelphia, PA: WB Saunders, 1987, pp 565–569.
7 De Lorimier LP, Alexander SD and Fan TM. **T-cell lymphoma of the tympanic bulla in a feline leukemia-virus negative cat**. *Can Vet J* 2003; 448: 987–989.
8 Trevor PB and Martin RA. **Tympanic bulla osteotomy for treatment of middle-ear disease in cats: 19 cases (1984–1991)**. *J Am Vet Med Assoc* 1993; 202: 123–128.
9 Little CJL, Pearson GR and Lane JG. **Neoplasia involving the middle ear cavity of dogs**. *Vet Rec* 1989; 124: 54–57.
10 Fan TM and de Lorimier LP. **Inflammatory polyps and aural neoplasia**. *Vet Clin North Am Small Anim Pract* 2004; 34: 489–509.
11 Meicher K and von Bomhard W. **Patient characteristics, histopathological findings and outcome in 97 cats with extranodal subcutaneous lymphoma (2007–2011)**. *Vet Comp Oncol*. Epub ahead of print 10 January 2014. DOI: 10.1111/vco.12081.
12 Cole LK. **Otoscopic evaluation of the ear canal**. *Vet Clin North Am Small Anim Pract* 2004; 34: 397–410.
13 LeCouteur RA. **Feline vestibular diseases – new developments**. *J Feline Med Surg* 2003; 5: 101–108.
14 Muilenburg RK and Fry TR. **Feline nasopharyngeal polyps**. *Vet Clin North Am Small Anim Pract* 2002; 32: 839–849.
15 Sula MM, Njaa BL and Payton ME. **Histologic characterization of the cat middle ear: in sickness and in health**. *Vet Pathol* 2014; 51: 951–967.
16 Ferreri AJ, Ernberg I and Copie-Bergman C. **Infectious agents and lymphoma development: molecular and clinical aspects**. *J Intern Med* 2009; 265: 421–438.
17 Njaa BL, Cole LK and Tabacca N. **Practical otic anatomy and physiology of the dog and cat**. *Vet Clin Small Anim* 2012; 42: 1109–1126.
18 Chan JKC, Aozasa K and Gaulard P. **DLBCL associated with chronic inflammation**. In: Swerdlow SH, Campo E, Harris NL, et al. (eds). WHO Classification of tumors of hematopoietic and lymphoid tissues. 4th ed. Lyon: IARC Press, 2008, pp 245–246.
19 Jackson M, Wood S, Misra V, et al. **Immunohistochemical identification of B and T lymphocytes in formalin-fixed, paraffin-embedded feline lymphosarcomas: relation to feline leukemia virus status, tumor site, and patient age**. *Can J Vet Res* 1996; 60: 199–204.
20 Suntz M, Failing K, Hecht W, et al. **High prevalence of nonproductive FeLV infection in necropsied cats and significant association with pathological findings**. *Vet Immunol Immunopathol* 2010; 136: 71–80.
21 Sula MJ. **Tumors and tumorlike lesions of dog and cat ears**. *Vet Clin Small Anim* 2012; 42: 1161–1178.

Veterinary Quarterly

ISSN: 0165-2176 (Print) 1875-5941 (Online) Journal homepage: http://www.tandfonline.com/loi/tveq20

Pathological characterization of primary splenic myxoid liposarcomas in three dogs

A. Forlani, P. Roccabianca, C. Palmieri, G. Sarli, D. Stefanello, S. Santagostino, C. Randi & G. Avallone

To cite this article: A. Forlani, P. Roccabianca, C. Palmieri, G. Sarli, D. Stefanello, S. Santagostino, C. Randi & G. Avallone (2015) Pathological characterization of primary splenic myxoid liposarcomas in three dogs, Veterinary Quarterly, 35:3, 181-184, DOI: 10.1080/01652176.2015.1049384

To link to this article: http://dx.doi.org/10.1080/01652176.2015.1049384

Accepted online: 08 May 2015.Published online: 04 Jun 2015.

Veterinary Quarterly, 2015
Vol. 35, No. 3, 181–184, http://dx.doi.org/10.1080/01652176.2015.1049384

CASE SERIES

Pathological characterization of primary splenic myxoid liposarcomas in three dogs

A. Forlani[a]*, P. Roccabianca[a], C. Palmieri[b], G. Sarli[c], D. Stefanello[a], S. Santagostino[a], C. Randi[d] and G. Avallone[c]

[a]*Dipartimento di Scienze Veterinarie e Sanità Pubblica, School of Veterinary Medicine, University of Milano, Via Celoria 1020133 Milano, Italy;* [b]*School of Veterinary Science, The University of Queensland, Gatton Campus, Queensland, Australia;* [c]*Dipartimento di Scienze Mediche Veterinarie, School of Veterinary Medicine, University of Bologna, Ozzano dell'Emilia, Italy;* [d]*Ambulatorio Veterinario San Rocco, Cardano al Campo, Italy*

(*Received 19 December 2014; accepted 5 May 2015*)

Non-angiomatous-non-lymphomatous sarcomas (NANLs) represent 23%–34% of canine primary splenic sarcomas. Splenic liposarcomas account for 2%–6% of NANLs but myxoid variants are rarely reported and information on their behaviour is fragmentary. An 8-year-old male crossbreed (case 1), a 12-year-old female French bulldog (case 2), and an 11-year-old crossbreed (case 3) underwent splenectomy after the detection of a splenic nodule. Histology, histochemistry, immunohistochemistry, and transmission electron microscopy (TEM) were performed. Bundles of spindle-to-polygonal cells containing occasional cytoplasmic oil-red-O positive vacuoles embedded in an Alcian blue-positive extracellular matrix were observed. Aggregates of round cells were detected in cases 1 and 3. All tumours were vimentin positive and actin, desmin, Factor VIII, and S100 negative. The TEM evidenced different maturational stages of adipose cells (lipoblasts, intermediate, and undifferentiated). All the cases developed hepatic metastases and were euthanized. Disease free interval was 2 months in cases 1 and 3, and 21 months in case 2. The presence of a neoplastic embolus in case 1 and areas of round cell differentiation in cases 1 and 3 represented the sole prognostic indices.

Keywords: dog; electron microscopy; histochemistry; immunohistochemistry; myxoid liposarcoma; spleen

Angiosarcoma and lymphoma are the most common primary canine splenic tumours, while the so-called splenic non angiomatous-non lymphomatous sarcomas (NANLs) are uncommon neoplasms with uncertain characterization (Weinstein et al. 1989; Spangler & Culbertson 1992; Spangler et al. 1994; Day et al. 1995). The canine NANLs account for 23% to 34% of primary splenic neoplasms, and most frequently include fibrosarcoma, leiomyosarcoma, and undifferentiated sarcoma, while liposarcomas (LPS) are rare (Weinstein et al. 1989; Spangler & Culbertson 1992; Spangler et al. 1994; Day et al. 1995). LPS are infrequent soft tissue neoplasms with a reported incidence lower than 0.5% of cutaneous and subcutaneous canine and feline tumours (Goldschmidt & Shofer 1992). Primary splenic LPS have been included in large caseloads of mesenchymal tumours of the canine spleen accounting for 2%–6% of NANLs and, consequently, specific information regarding LPS histotypes and their biology are fragmentary (Weinstein et al. 1989; Spangler & Culbertson 1992; Spangler et al. 1994; Day et al. 1995). In man, LPS are characterized by four histological subtypes: atypical lipomatous tumour/well-differentiated, myxoid, dedifferentiated, and pleomorphic, each bearing a distinctive prognosis (Chang et al. 1989; Goldblum et al. 2013). Well-differentiated LPS, the most common variant of LPS in man, are locally aggressive but rarely metastasize, while the less frequent dedifferentiated LPS have a high recurrence rate and metastasize frequently (Goldblum et al. 2013). The second most common type is the myxoid variant, that develops metastases in up to 58% of cases (Goldblum et al. 2013).

In dogs, three histotypes of soft tissue LPS have been described: well differentiated, myxoid, and pleomorphic (Hendrick et al. 1998). Pleomorphic LPS seems to be the most aggressive variant, although a distinctive behavioural pattern has not been conclusively demonstrated (Baez et al. 2004; Gross et al. 2005). The aim of this report is to describe the pathological and clinical features of three cases of canine primary splenic myxoid LPS.

Three dogs, two male crossbreed, 8- and 11-years-old (case 1 and 3), respectively, and a 12-year-old female spayed French bulldog (case 2), underwent abdominal ultrasonography after chronic vomiting (cases 1 and 3) and for a check after several months of the prednisone therapy administered to control a severe atopic dermatitis (case 2). Ultrasonography revealed a single splenic mass and the dogs underwent splenectomy. Splenic masses were 15×15 cm in diameter (case 1), 6.5×7 cm (case 2), 15×10 cm (case 3), white to light tan, glistering, greasy, and mucoid on the cut surface.

Tissue samples from the three masses were formalin-fixed, paraffin-embedded and routinely processed for histology. Alcian (pH 3.1)–Periodic Acid Schiff (PAS) stain was performed on selected sections. Formalin-fixed specimens were also snap-frozen in liquid nitrogen and cryostat sections were stained with oil red-O. Immunohistochemistry was performed in all cases on poly-lysine coated slides using the avidin–biotin–peroxidase method and specific

*Corresponding author. Email: giancarlo.avallone@gmail.com; giancarlo.avallone@unibo.it

primary mouse monoclonal antibodies against vimentin (Dako, clone 3B4, dilution 1:2000), smooth muscle actin (Dako, clone 1A4, dilution 1:2000), desmin (Novocastra, clone DE-R-II, dilution 1:200), and rabbit polyclonal antibodies anti-factor VIII-related antigen (Dako, Cat. N° A0082, dilution 1:200), and S100 (Dako, Cat. N° Z0311, dilution 1:10000). Heat-induced antigen retrieval (microwave, 10 minutes, pH 6 citrate buffer) was applied for immunohistochemistry for vimentin, smooth muscle actin, desmin, and factor VIII-related antigen. No antigen retrieval was applied for S100. For transmission electron microscopy (TEM), tissue fragments from cases nos. 1 and 2 were fixed in 2.5% glutaraldehyde, post-fixed in 1% OsO_4, and embedded in epoxy resin. Thin sections (70 nm) from selected areas of interest were stained with lead citrate and uranyl acetate. No additional samples from case 3 were available for the ultrastructural analysis.

Microscopically, all tumours were composed of haphazardly arranged, spindle-to-stellate cells embedded in a pale eosinophilic matrix. Cells were 15−25 μm in diameter, with a high nucleus/cytoplasmic ratio (N/C), variable amount of pale cytoplasm rarely containing sharply demarcated, clear cytoplasmic vacuoles. Nuclei were round to oval, with granular to vesicular chromatin and an occasionally visible central, round, nucleolus. In case 1, the neoplasm was infiltrative, non-encapsulated and multifocally characterized by large lacunae lined by neoplastic cells and filled with lightly eosinophilic material (Figure 1(a)). Rare multinucleated neoplastic cells and multifocal areas of necrosis were present. In more than 20% of the tumour (semiquantitative evaluation of all the haematoxylin and eosin-stained sections available at intermediate magnification), cells were round shaped, with higher N/C ratio and small amount of cytoplasm. One mitotic figure was identified in 10 high power fields (HPF). After serial sectioning, a single neoplastic intravascular embolus was detected. In case 2, the tumour was well demarcated, partially encapsulated, expansile, multilobular, and confined within the splenic parenchyma. A plexiform network of thin-walled capillaries branching at 45 to 90 degree angles was the typical histological findings. Occasional lacunae similar to case 1 were observed. Differentiated lipocytes were observed in 20% of the mass. Necrosis and haemorrhages were absent and mitoses were 16 in 10 HPF. In case 3, the tumour was non-encapsulated, focally infiltrative, and characterized by large lacunae similar to case 1. Round cell areas occupied more than 20% of the examined neoplasm. Large areas of necrosis were detected and 18 mitotic figures were observed in 10 HPF. The extracellular matrix and the material within the lacunae were Alcian blue-positive and PAS-negative, consistent with acidic mucins (Figure 1(b)). Lipocytes, lipoblasts, and scattered

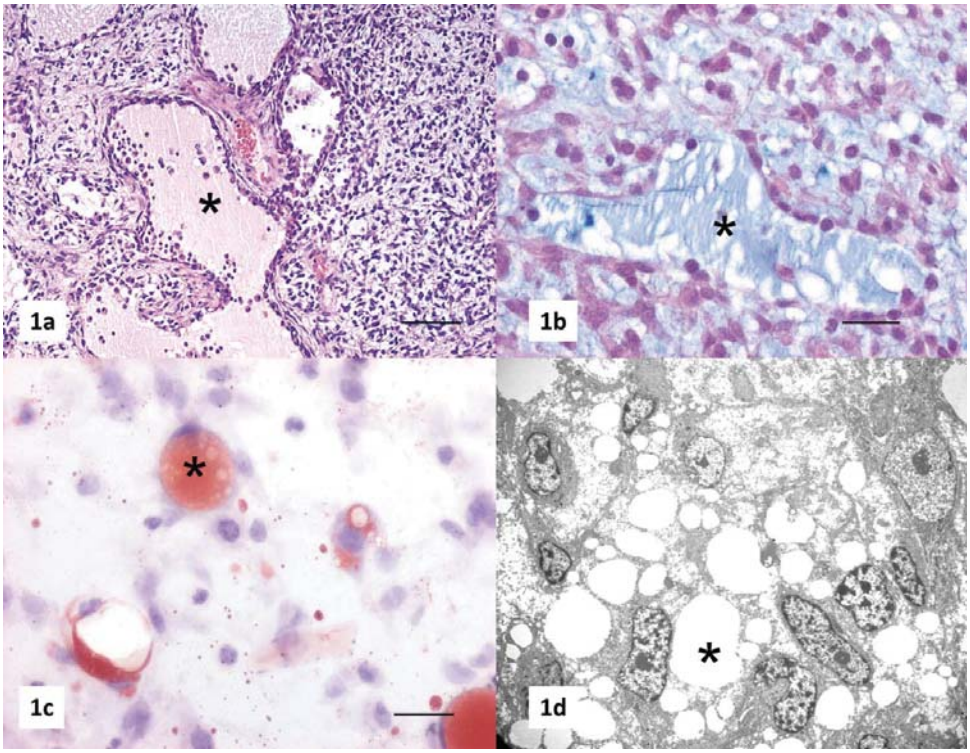

Figure 1. (a) Splenic mass from an 8-year-old male crossbreed dog (case 1). The neoplasm is composed by stellate to round cells lining large lacunae filled with lightly eosinophilic material (asterisk). Haematoxylin and eosin. Bar = 120 μm. (b) Splenic mass from an 8-year-old male crossbreed dog (case 1). The neoplasm is composed by stellate cells with optically empty cytoplasmic vacuoles. Note the lacunae lined by neoplastic cells and the Alcian blue-stained extracellular matrix (asterisk). Alcian blue. Bar = 50 μm. (c) Splenic mass from a 12-year-old female French bulldog (case 2). The intracytoplasmic vacuoles within neoplastic cells are Oil-red-O positive (orange colour) (asterisk), confirming the lipid content of neoplastic cells. Oil-red-O. Bar = 50 μm. (d) Aggregate of lipoblastic cells containing high number of electronlucent intracytoplasmic lipid droplets (asterisk). TEM, uranyl acetate and lead citrate. Original magnification = 3000x.

neoplastic spindle cells contained oil red-O positive cytoplasmic vacuoles (Figure 1(c)). Neoplastic cells were vimentin positive and smooth muscle actin, desmin, Factor VIII-related antigen and S100 negative. According to the histology and soft tissue sarcomas, grading all tumours were diagnosed as grade II myxoid LPS

TEM performed on cases 1 and 2 identified three types of neoplastic cells: primitive undifferentiated mesenchymal cells, intermediate cells, and fully developed lipoblasts. Intermediate cells and lipoblasts were respectively the most and the less represented cell types. Neoplastic cells were embedded in an amorphous matrix occasionally coating and clinging on the cells. Undifferentiated cells were round to polygonal to spindle, had few intracytoplasmic organelles, no lipid vacuoles and a poorly developed basal lamina or basal lamina remnants. Intermediate cells were spindle to stellate with variable numbers of mitochondria and rough endoplasmic reticulum (RER) and without sufficient lipid vacuoles to be considered lipoblasts. In the early stages of development, they were frequently seen in apposition to capillaries. A basal lamina encircled intermediate cells, especially those nearest to the capillary walls. Lipoblasts were round to polygonal, had numerous mitochondria, scant RER, and a poorly formed basal lamina or scarce basal lamina remnants. Their cytoplasm contained variably sized lipid vacuoles with different electrondensity (Figure 1(d)). The combination of all these results confirmed the diagnosis of grade II myxoid LPS in both cases.

All the cases developed hepatic metastases detected by ultrasonography and were euthanized because of poor prognosis. Disease-free interval was 2 month in cases 1 and 3, and 21 months in case 2. Case 1 underwent necropsy that confirmed multiple metastases in the liver and in the sternal lymph node.

To the best of our knowledge, this study represents the most comprehensive pathological characterization of canine splenic myxoid LPS. Moreover, no data on the biological behaviour of these neoplastic conditions have been previously reported in dogs. Canine LPS arises most frequently in the subcutis, and histological grade is considered prognostic (Dennis et al. 2011). However, grade was not predictive of the aggressive behaviour in case 1. A study by Baez et al. (2004) on 56 cases of canine LPS highlighted that dogs undergoing wide surgical excision had significantly longer survival times than dogs undergoing marginal excision (Baez et al. 2004). However, splenectomy did not correlate with the clinical outcome in the current cases. The most important prognostic factor for NANLs is mitotic index, and more than 9 mitoses in 10 HPF have been correlated with shorter survival times (Spangler et al. 1994). However, in case 1, the mitotic index was lower than the cutoff set by the grading system for NANLs, and this parameter did not envisage the aggressive behaviour. Conversely, case 2 was characterized by a longer survival time despite a mitotic index higher than 9. The correlation between the mitotic index and prognosis has not been well defined for visceral LPS and, as observed in our cases, the number of mitoses in splenic LPS may not be prognostically significant compared to other NANLs. This represents a novel finding since few splenic LPS (2%−6% of NANL) have been included in previous caseloads and in none of them the relevance of the histological grade can be clearly inferred (Weinstein et al. 1989; Spangler & Culbertson 1992; Spangler et al. 1994; Day et al. 1995). Additionally, it should be emphasized that the two cases with shorter survival time were characterized by a large round cell component (case 1 and 3). This histological feature is considered highly predictive of metastasis and poor prognosis in myxoid LPS in man (Goldblum et al. 2013). A prognostic study on a larger number of cases should be performed in order to confirm these observations. Further parameters indicative of an aggressive behaviour in cases 1 and 3 were the larger size, the infiltrative growth, the randomly scattered areas of necrosis, and the presence of a neoplastic embolus (case 1).

In case 2, the clear demarcation from the normal parenchyma, the partial encapsulation, and the presence of well-differentiated lipocytes were distinctive and could be considered indicative of a more differentiated and less aggressive tumour. In all cases, the application of ancillary diagnostic techniques was pivotal to confirm the diagnosis. The diagnostic hallmark of human myxoid LPS in soft tissues is the detection of a specific FUS-DDIT3 fusion oncogene, resulting from a t(12,16)(q13,p11) chromosome translocation (Goldblum et al. 2013). However, no data are available regarding the cytogenetic anomalies in canine LPS. Therefore, the diagnosis was exclusively and conclusively based on the histological, immunohistochemical, histochemical, and ultrastructural features. Immunohistochemistry ruled out the two most common types of splenic sarcoma (haemangiosarcoma and leiomyosarcoma), while histochemistry and TEM identified the lipogenic origin of neoplastic cells with the myxoid component. Additionally, TEM identified characteristic intermediate cells in apposition to vessels, so paralleling the differentiation gradient described in the human myxoid LPS that suggests the derivation of these types of tumour from undifferentiated perivascular cells, as occurs during the normal development of the white adipose tissue (Battiflora and Nunez-Alonso 1980). The gross morphology, multiple sampling, and sectioning for histological, histochemical, and immunohistochemical stains as well as TEM should be combined to achieve the correct diagnosis and subtype in canine undifferentiated splenic sarcomas. The prognostic significance of mitotic index, grade, and subtype should be evaluated on a larger number of visceral LPS and sarcomas to provide insights on and identify the most accurate factors for their correct grading.

Acknowledgements

We thank Prof Malcolm Jones and Dr Erica Lovas (School of Veterinary Science, The University of Queensland, Gatton campus, Gatton, Queensland, Australia) for the electron microscopy assistance.

Disclosure statement

No potential conflict of interest was reported by the authors.

References

Baez JL, Hendrick MJ, Shofer FS, Goldkamp C, Sorenmo KU. 2004. Liposarcomas in dogs: 56 cases (1989-2000). J Am Vet Med Assoc. 224:887–891.

Battifora H, Nunez-Alonso C. 1980. Myxoid liposarcoma: study of ten cases. Ultrastruct Pathol. 1:157–169.

Chang HR, Hajdu SI, Collin C, Brennan MF. 1989. The prognostic value of histologic subtypes in primary extremity liposarcoma. Cancer. 64:1514–1520.

Day MJ, Lucke VM, Pearson H. 1995. A review of pathological diagnoses made from 87 canine splenic biopsies. J Small Anim Pract. 36:426–433.

Dennis MM, McSporran KD, Bacon NJ, Schulman FY, Foster RA, Powers BE. 2011. Prognostic factors for cutaneous and subcutaneous soft tissue sarcomas in dogs. Vet Pathol. 48:73–84.

Goldblum JR, Folpe AL, Weiss SW. 2013. Enzinger & weiss's soft tissue tumors. 6th ed. Philadelphia (PA): Elsevier Saunders. Chapter 15, Liposarcoma; p. 484–523.

Goldschmidt MH, Shofer FS. 1992. Skin tumors in the dog and cat. Oxford: Pergamon Press. Chapter 24, Cutaneous lipoma and liposarcoma; p. 192–203.

Gross TL, Ihrke PJ, Walder EJ, Affolter VK. 2005. Skin diseases of the dog and cat: clinical and histopathologic diagnosis. 2nd ed. Oxford: Blackwell Science. Chapter 30, Lipocytic Tumors; p. 766–772.

Hendrick MJ, Mahaffey EA, Moore FM, Vos JH, Walder EJ. 1998. Histologic classification of mesenchymal tumors of skin and soft tissues of domestic animals. Washington (DC): Armed Forces Institute of Pathology. p. 19–20.

Spangler WL, Culbertson MR. 1992. Prevalence, type, and importance of splenic diseases in dogs: 1,480 cases (1985–1989). J Am Vet Med Assoc. 200:829–834.

Spangler WL, Culbertson MR, Kass PH. 1994. Primary mesenchymal (nonangiomatous/nonlymphomatous) neoplasms occurring in the canine spleen: anatomic classification, immunohistochemistry, and mitotic activity correlated with patient survival. Vet Pathol. 31:37–47.

Weinstein MJ, Carpenter JL, Schunk CJ. 1989. Nonangiogenic and nonlymphomatous sarcomas of the canine spleen: 57 cases (1975–1987). J Am Vet Med Assoc. 195:784–788.

Feline Upper Respiratory Tract Lymphoma: Site, Cyto-histology, Phenotype, FeLV Expression, and Prognosis

S.F. Santagostino, C.M. Mortellaro, P. Boracchi, G. Avallone, M. Caniatti, A. Forlani and P. Roccabianca

Vet Pathol published online 5 June 2014
DOI: 10.1177/0300985814537529

Veterinary Pathology OnlineFirst, published on June 5, 2014 as doi:10.1177/0300985814537529

Domestic Animals–Original Article

Veterinary Pathology
1-10

DOI: 10.1177/0300985814537529
vet.sagepub.com

Feline Upper Respiratory Tract Lymphoma: Site, Cyto-histology, Phenotype, FeLV Expression, and Prognosis

S.F. Santagostino[1], C.M. Mortellaro[1], P. Boracchi[2], G. Avallone[3], M. Caniatti[1], A. Forlani[1], and P. Roccabianca[1]

Abstract

Lymphoma is the most common feline upper respiratory tract (URT) tumor. Primary nasal and nasopharyngeal lymphomas have been evaluated as distinct pathological entities; however, data on their differing clinical behavior are missing. A total of 164 endoscopic- guided URT pinch biopsies were formalin fixed and routinely processed. Imprint cytological specimens were stained with May Grünwald-Giemsa. Immunohistochemistry for anti-CD20, CD3, FeLVp27, and FeLVgp70 was performed. Prognostic significance of clinicopathological variables was investigated by univariate and multivariate analysis. Lymphoma was diagnosed in 39 cats (24%). Most cats with lymphoma were domestic shorthair (32 [82%]), were male (F/M = 0.56), and had a mean age of 10.3 years (range, 1–16 years). Lymphomas were primary nasal in 26 cats (67%), nasopharyngeal in 6 (15%), and in both locations (combined lymphomas) in 7 cats (18%). Neoplastic growth pattern was diffuse in 35 cases (90%) and nodular in 4 (10%). Epitheliotropism was observed in 10 cases (26%). Tumor cells were large in 15 cases, were small and medium in 11 cases each, and 2 had mixed cell size. Submucosal lymphoplasmacytic inflammation was observed in 23 cases (59%). Cytology was diagnostic for lymphoma in 12 of 25 cases (48%). A B-cell origin prevailed (34 [87%]). Feline leukemia virus (FeLV) p27or gp70 antigen was detected in 21 lymphomas (54%). URT lymphomas were aggressive, with survival varying from 0 to 301 days (mean, 53 days). Epitheliotropism in 8 B-cell lymphomas (80%) and in 2 T-cell lymphomas (20%) correlated with prolonged survival. Age younger or older than 10 years had a negative prognostic value. Lymphoplasmacytic inflammation and FeLV infection may represent favoring factors for URT lymphoma development.

Keywords

feline, FeLV, lymphoma, nasal, nasopharyngeal, phenotype, prognosis, respiratory

Lymphomas are among the most common feline malignancies, representing more than 50% of all tumors in cats.[18] Feline lymphoma prevalence rates are approximately 1.6% of cats in the general population and 4.7% of hospitalized sick cats.[18]

The most common sites of occurrence are intestinal and mediastinal,[18] while primary nasal or nasopharyngeal lymphomas represent a rare manifestation,[18] accounting for less than 1% of all feline tumors. Nasal lymphomas seem more common in male cats,[12,14,25] presumably because of behavioral characteristics that make transmission of feline leukemia virus (FeLV) more efficient. The upper respiratory tract (URT) is considered a relatively rare site of lymphoma development; however, lymphoma represents still approximately 50% of primary URT mesenchymal tumors[1,14,16,18,25] and is the most common primary feline nasal tumor.[1,6,14,16,22] URT lymphomas originate more frequently in the solitary nasal location,[1,6,14,16,22] while 10% are found in the nasopharynx and 8% affect both anatomical compartments.[22] In previous studies, microscopic, immunophenotypical features[5,14,25] and the role of cytology in the diagnosis of feline primary URT lymphomas have been assessed.[22] However, the evaluation of the 3 distinct presentations of URT lymphoma (nasal, nasopharyngeal, or lymphoma simultaneously developing in both locations [combined lymphomas])[22] as distinct clinicopathologic and prognostic entities seems unavailable. On the contrary, in human medicine, primary nasal and nasopharyngeal

[1]DIVET, Facoltà di Medicina Veterinaria, Università degli Studi di Milano, Milano, Italy
[2]DSCC, Unità di statistica medica e biometria, Facoltà di Medicina e Chirurgia, Università degli studi di Milano, Milano, Italy
[3]Department of Veterinary Medical Sciences, University of Bologna, Italy

Supplemental material for this article is available on the *Veterinary Pathology* website at http://vet.sagepub.com/supplemental.

Corresponding Author:
S.F. Santagostino, DIVET–Dipartimento di Scienze Veterinarie e Sanità Pubblica Sezione Anatomia Patologica Veterinaria e Patologia Aviare Facolta' di Medicina Veterinaria, Via Celoria 10, 20133 Milano, Italy.
Email: sara.santagostino@unimi.it

Table 1. Panel of Primary Antibodies Used to Characterize Primary Feline Upper Respiratory Tract Lymphomas.

Antibody	Clone/Species Specificity	Dilution	Source	Supplier	Main Cell Reactivity
CD3ε	CD3-12 human[a]	1:10	Rabbit polyclonal	Serotec, Oxford, UK	T cells
CD20	Human[a]	1:400	Rabbit polyclonal	Neomarkers, Freemont, CA	B cells
FeLV gp70	C11D8 feline	1:100	Mouse monoclonal	Custom Monoclonals International, Sacramento, CA	FeLV envelope glycoprotein 85/70
FeLV p27	PF12J-10A feline	1:100	Mouse monoclonal	Custom Monoclonals International, Sacramento, CA	FeLV capsidic protein

[a]Cross-reactive with feline tissues.

lymphomas are considered 2 clinically distinct diseases since nasal lymphoma bears a more frequent T-cell phenotype with poor response to chemotherapy and higher relapse rates.[21]

The aim of this study was the evaluation of cytological, histological, phenotypical FeLV tissue antigen expression and follow-up data of 3 different URT lymphoma presentations—nasal, nasopharyngeal, and combined tumors—to find a possible significant prognostic role of the different clinical and pathological variables.

Materials and Methods

Case Selection

Pinch biopsies from all cases of nasal or nasopharyngeal feline disease were retrospectively collected from the surgical pathology archives of the Anatomical Pathology Section of the School of Veterinary Medicine of Milan between 2000 and 2012. All tissue samples were obtained by anterograde or retrograde endoscopic biopsy. The retrograde endoscopic technique was applied for nasopharyngeal tissue samples. A total of 39 (24%) of 164 cats undergoing nasal biopsies between 2000 and 2012 were diagnosed with lymphoma, representing 50% of nasal tumors diagnosed. Other tumors were carcinomas in 25 cats (15%) and mesenchymal tumors in 14 cats (9%).

For each cat with lymphoma, signalment, presenting complaints, clinical signs, diagnostic imaging, rhinoscopic appearance, multiple endoscopic pinch biopsies, histopathology, and, when available, cytology were collected.

Histological and Cytological Evaluation

All biopsy samples were fixed in 10% neutral-buffered formalin, routinely processed, and stained with hematoxylin and eosin (HE).

In cats with URT lymphomas, a number of biopsies varying from 4 to 14 (mean, 6) were collected by endoscopy. For primary nasal and for combined lymphomas, biopsies were performed from both (left and right) nasal cavities, even when a space-occupying lesion was not detected during endoscopic examination. Biopsy sampling was repeated to check for disease progression or to confirm the preceding diagnosis in selected cases. During scheduled clinical check-ups, the cat Nos. 5, 31, and 32 were reevaluated clinically and by endoscopy. Biopsies were taken after 3 and 9 months in cat No. 5 and after 1 and 3 months in cat Nos. 31 and 32.

For lymphomas, cytological samples from impression smears, fine-needle aspirates, and brushings were air dried and stained with May-Grünwald Giemsa.

To reduce inappropriate diagnostic interpretation, all the cytological and histological slides were blindly and independently submitted to pathologists with a different degree of experience, including 1 resident (S.S.F.) and 2 board-certified pathologists, with 1 more experienced in histopathology (R.P.) and 1 more experienced in cytopathology (C.M.). Only those cases that were classified in the same way by the 3 readings were included in the caseload. URT lesions were grouped in the following diagnostic categories: lymphomas, other neoplasms, inflammatory or degenerative lesions, and miscellaneous lesions. Cases of lymphomas were selected and subsequently classified on the basis of their anatomical location (nasal/nasopharyngeal/combined), growth pattern (follicular, nodular, diffuse, epitheliotropic), and cell type and grade, applying the modified World Health Organization (WHO) classification for lymphomas.[33] Mitotic index was evaluated counting the number of mitoses at a 400× magnification in 10 fields using the same microscope.

Immunohistochemical Staining

For all cases of lymphoma, cell phenotype and FeLV antigen expression were assessed. Unstained 5-µm sections from paraffin-embedded biopsy specimens were mounted onto Superfrost Plus Slides (Menzel Glasser; Gerhard Menzel, Glasbearbeitungswerk GmbH & Co, Braunschweig, Germany). For phenotypic and FeLV antigen expression evaluation, samples were stained with primary antibodies listed in Table 1. For all antibodies, antigen retrieval was achieved by heating slides in citrate buffer at pH 6.0 in a commercial pressure cooker Decloaker (Biocare Medical, Walnut Creek, CA) for 10 minutes. Endogenous peroxidase was quenched for 30 minutes with 3% hydrogen peroxide. Sections were stained using an avidin-biotin-peroxidase technique as previously described.[15] Omission of the primary monoclonal antibody or application of an isotype-matched nonspecific monoclonal antibody anti-canine CDH5R was used as a negative control. Formalin-fixed specimens from a reactive lymph node and from a

FeLV-positive cat were used as positive controls. The immunoreaction was visualized with amino-9-ethyl-carbazole chromogen (AEC; Vector, Burlingame, CA). Sections were counterstained with Mayer's hematoxylin and mounted with glycerine.

Follow-up

Follow-up was performed when possible by the oncologists at the same institution and consisted of a clinical examination every 3 months. When this was not feasible, follow-up consisted of telephone interview with the owner or the referring veterinarian to collect clinical information, type of treatment, and time and cause of death.

Statistical Analysis

Statistical analysis was performed following when possible the guidelines of the American College of Veterinary Pathologists' Oncology Committee.[37] The end point considered for each cat with lymphoma was time to death, calculated as the time elapsed from the date of diagnosis to the date of death for any cause, or to the date of last clinical information for cats that were alive at the study closing date (right-censored times).[37] Median follow-up was estimated by the reverse Kaplan-Meier method.[29] Overall survival probability curve was estimated by the Kaplan-Meier method. First, the putative prognostic role of the considered variables (age, sex, breed, anatomical site, size of lymphomatous cells, neoplastic phenotype, FeLV status, mitotic index, and epitheliotropism) was investigated, including each single variable in a Cox regression model (univariate analysis). Aiming to evaluate the adjusted prognostic role in Cox multivariable regression models, the maximum number of variables that can be included to avoid unreliable results depends on the number of observed deaths. According to the caseload included in the study, a ratio of 1:5 was considered, as previously suggested.[36] Since it was not possible to include all the above-mentioned variables, only a subset of variables were jointly analyzed in multivariable regression models (mitotic index, age, FeLV status, phenotype, and epitheliotropism). These variables were selected according to the specific clinical experience of the authors. A model containing only variables with the greatest prognostic role was then obtained by a backward selection procedure based on the Akaike information criterion (AIC).[35] Continuous variables (age and mitotic index) were analyzed according to their original measurement scale in such a way as to maintain their maximum possible prognostic information. Potential nonlinear relationships between continuous variables and logarithm of the hazard in the Cox model were evaluated by restricted cubic spline transforms.[13]

Results are reported in terms of estimated hazard ratios (HRs) with 95% confidence intervals (CIs). For categorical variables, one of the modalities was chosen as reference. Thus, for each of the remaining modalities, the HR is the ratio between the hazard of death for this modality and the hazard of death of the reference. The null hypothesis of each regression coefficient equal to zero was evaluated by the Wald test, and the prognostic contribution of the variable to the model was evaluated by likelihood ratio test. For continuous variables, model estimates in terms of HRs cannot be easily interpreted in the case of a nonlinear relationship between the variable and model response. Thus, after identifying the value of the variable corresponding to the minimum hazard of death (reference), selected hazard ratios for values of the variable greater and lower than reference were provided to describe the prognostic behavior.

Results

URT Lymphomas: Signalment and Clinical Findings

Signalment and major clinical complaints divided for the 3 different URT lymphoma presentations are summarized in Supplemental Table S1. In cats with URT lymphoma, median age was 10.3 years (range, 1–16 years) with a female/male ratio of 0.56 and a majority of domestic short-haired (DSH) cats (32/39 [82%]). Other breeds included 3 Siamese, 2 Chartreux, 1 Persian, and 1 Devon Rex. FeLV and feline immunodeficiency virus (FIV) serology were available in 7 cats (18%); all except 1 (cat No. 29) were FeLV negative, while two cats were FIV positive (cat Nos. 1, 27). Major clinical complaints for cats with lymphoma were nasal discharge (30/39 [77%]), sneezing (26/39 [67%]), stertor (18/39 [46%]), dyspnea (9/39 [23%]), epiphora (8/39 [21%]) or ocular discharge (4/39 [10%]), epistaxis (8/39 [21%]), and anorexia (7/39 [18%]).

Skull radiographs (11 [28%]) or computed tomography (CT) scans (8 [21%]) were performed prior to rhinoscopy in some cats with URT lymphoma. Based on diagnostic imaging and rhinoscopy, 26 of 39 (67%) lymphomas were primary nasal, 6 of 39 (15%) were nasopharyngeal, and 7 of 39 (18%) had both a nasal and nasopharyngeal location and were termed *combined lymphomas* (CLs).

By rhinoscopy, lymphomas were described as exophytic, pale pink to whitish, cerebroid, and friable space-occupying lesions in 28 of 39 (72%) cases. No masses were evident in 11 cats (28%), where a rough thickened mucosa was documented.

Cytological Findings in URT Lymphomas

Cytological specimens were available in 25 of 39 cases (64%) and were obtained by impression (16 [64%]), brushing (6 [24%]), or fine-needle aspiration (3 [12%]). A diagnosis of lymphoma was attained by cytology in 12 of 25 (48%) cases, while for 11 cases (44%), a false-negative diagnosis of lymphoplasmacytic rhinitis was achieved. An inconclusive cytology was recorded in 2 cases (8%). All cytological samples, with the exception of the 2 inconclusive cases, exhibited good cellularity; small lymphocytes admixed with plasma cells, neutrophils, or macrophages were often observed in association with the neoplastic population (Fig. 1). Less frequent findings included

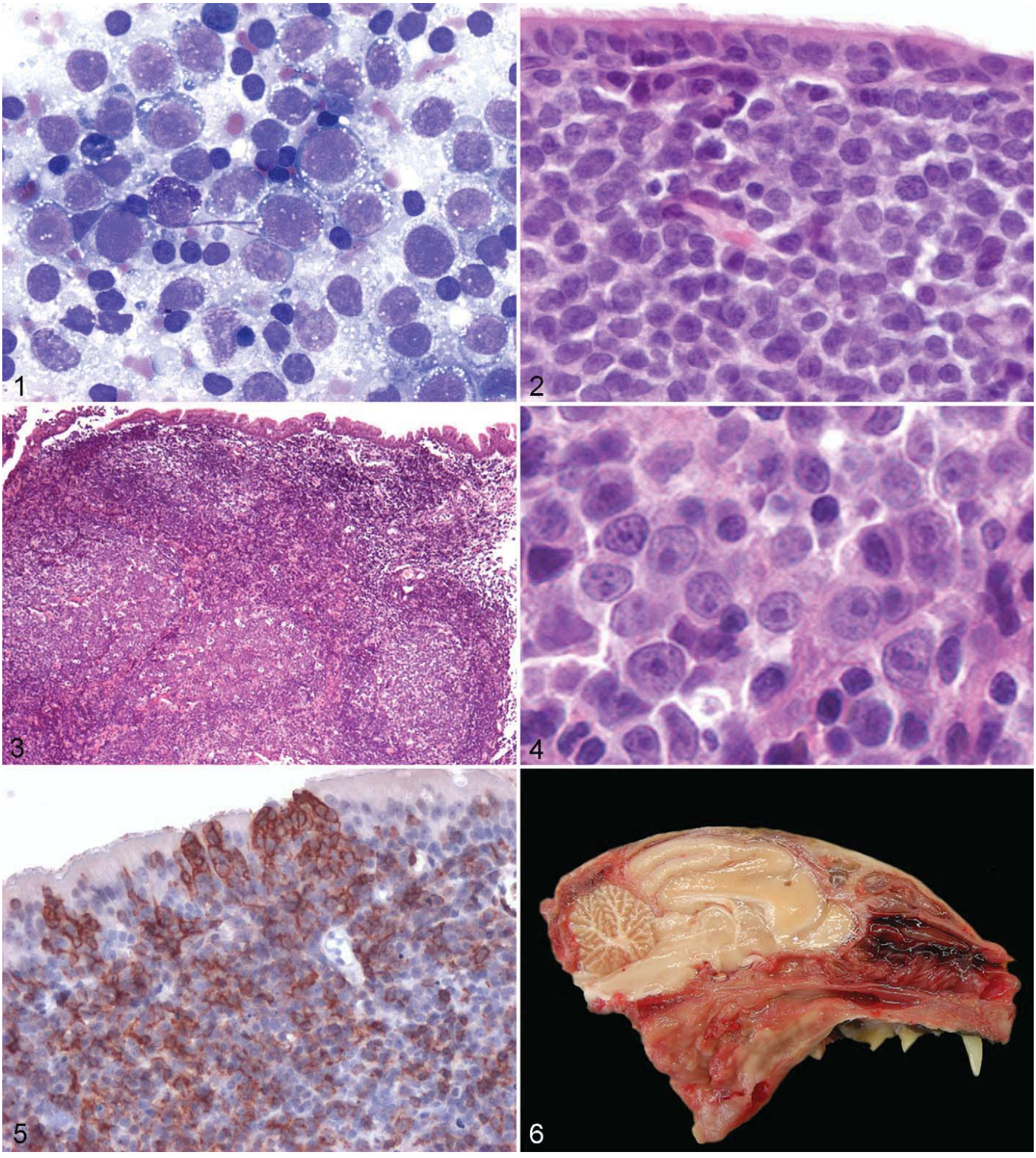

Figure 1. Nasopharynx, diffuse large B-cell lymphoma, immunoblastic morphology; cat No. 28. Nasopharyngeal brushing. Large, discrete lymphoid cells with abundant blue vacuolated cytoplasm, round nucleus, and 1 to 2 prominent nucleoli. Scattered small mature lymphocytes are visible. May Grünwald-Giemsa. **Figure 2.** Nasal cavities and nasopharynx, combined lymphoma; cat No. 34. Diffuse growth pattern of predominantly large neoplastic round cells obscuring the respiratory lamina propria. Nuclear pleomorphism is evident. Occasional plasma cells are present. Hematoxylin and eosin (HE). **Figure 3.** Nasal cavities and nasopharynx, combined lymphoma, follicular center cell lymphoma grade I; cat No. 35. Nodular growth with expansion of follicular center; loss of mantle zone and initial coalescence of follicles is evident. HE. **Figure 4.** Nasopharynx, diffuse large B-cell lymphoma, immunoblastic morphology; cat No. 28. Neoplastic cells are large with generally indistinct cell boundaries and characterized by a finely stippled chromatin pattern and a single prominent central basophilic nucleolus. Small mature

Table 2. Incidence of Cell Type Based on Tumor Location.

Location	Small Cell, No. (%)	Medium Cell, No. (%)	Large Cell, No. (%)	Mixed Cell, No. (%)	Total, No.
Nasal	8 (31)	7 (27)	11 (42)		26
Nasopharyngeal		3 (50)	2 (33)	1 (17)	6
Combined	3 (43)	1 (14)	2 (29)	1 (14)	7

hyperplastic to dysplastic respiratory epithelium, necrosis, and presence of occasional osteoclasts.

Pathology and Phenotype of URT Lymphomas

Microscopic features, lymphoma classification, and phenotype are summarized in Supplemental Table S2. The incidence of lymphoma cell type based on tumor location is summarized in Table 2.

Histological growth pattern was diffuse (Fig. 2) in 35 URT lymphomas (90%) and nodular (Fig. 3) to follicular in 4 cats (10%). Comparing the differing anatomical distributions, primary nasal lymphomas were diffuse in 25 cases (96%) and nodular in 1 cat (4%). Five cases (83%) of nasopharyngeal lymphoma had diffuse cell growth, and 1 (17%) was nodular. Combined lymphomas were observed in 7 cats (18%) and were characterized by diffuse growth in 5 cats (71%) and nodular growth in 2 cats (29%).

Comparing the cell type, 11 cases (28%) were diagnosed as small cell lymphoma, including lymphocytic (6 [55%]), prolymphocytic (4 [36%]), and plasmacytic (1 [9%]). Medium-sized cell lymphomas were diagnosed in 11 cases (28%); 8 of 11 (73%) were medium sized, not otherwise specified (NOS); 2 were plasmacytomas (18%); and 1 was a peripheral T-cell (PTCL)–like lymphoma (9%). Two follicular center cell lymphomas were observed, one grade I and one grade II. Large cell lymphoma (Fig. 4) was diagnosed in 15 cats (38%), with 13 cases having an immunoblastic morphology (87%). Of the primary nasal lymphomas, 11 were large (42%), 7 were intermediate (27%), and 8 (31%) were small cell cases. Nasopharyngeal lymphomas were large immunoblastic in 2 cats (33%), intermediate (including 1 plasmacytoma) in 3 cases (50%), and 1 case of mixed cell size (17%) diagnosed as follicular center cell lymphoma grade II. Combined lymphomas were large cell in 2 cases (29%), intermediate in 1 case (14%), and small cell in 3 cases (43%), and 1 mixed cellularity (14%) was diagnosed as a follicular center cell lymphoma grade I. Regardless of the anatomical location, in 23 cases (59%) of URT lymphomas, variable degrees (mild to severe) of submucosal plasmacytic to lymphoplasmacytic inflammation were evident.

Additional histopathological findings included multifocal mucosal ulceration with secondary neutrophilic and catarrhal inflammation, cystic dilation of mucous glands, edema, fibroplasia, and bone remodeling. Concurrent hyperemia, edema, and abundant catarrhal to purulent exudate were detected in 24 of 39 cats (61.5%).

A B-cell phenotype was identified in 34 of 39 URT lymphomas (87%). Of these, the largest number was represented by diffuse large cell lymphomas (15 [44%]), followed by small cell lymphomas (8 [24%]), intermediate cell NOS (7 [21%]), plasmacytomas (2 [6%]), and follicular lymphomas (2 [6%]). In 3 of 39 cases (8%), a T-cell phenotype was identified, comprising 2 diffuse small cell lymphomas and 1 PTCL-like lymphoma. In 2 of 39 cases (5%), 1 small cell lymphoma and 1 intermediate cell lymphoma, neoplastic cells were negative for T-cell and B-cell markers. Epitheliotropism (Fig. 5) was observed in 10 cases (26%), specifically in 8 cases of B-cell lymphomas (80%) and in 2 T-cell lymphomas (20%).

Phenotypic distribution in nasal lymphomas was characterized by a predominance of B-cell tumors (22 [85%]), with 2 cases (8%) of T-cell and 2 cases (8%) of the non B–non T-cell phenotype. All nasopharyngeal lymphomas displayed a B-cell origin. Combined lymphomas were B cell in 6 cases (86%) and T cell in 1 cat (14%).

Immunohistochemical Expression of Viral Antigens in URT Lymphomas

FeLV antigen expression in conjunction with anatomical distribution of URT lymphomas is listed in Supplemental Table S2. FeLV p27 and FeLV gp70 antigen expression either singly or in conjunction was detected by immunohistochemistry in a total of 21 of 39 cases (54%). Expression of FeLV p27 was observed only in 17 of 39 (44%), while gp70 only was observed in 12 of 39 cases (31%). Concurrent positivity for FeLV antigens was detected in 8 of 39 cats (21%). These cats were considered productively FeLV infected. Expression of either antigen in conjunction with lymphoplasmacytic inflammation was observed in 12 of 39 cats (31%).

Therapy and Follow-up

Five cats were lost to follow-up at 7, 7, 10, 43, and 54 days after diagnosis. Combination chemotherapy and/or radiation therapy were always offered but refused by owners in all but 1 cat that received radiation therapy (cat No. 5).

Figure 4. (Continued) lymphocytes are also present. HE. **Figure 5.** Nasal cavities and nasopharynx, combined lymphoma, follicular center cell lymphoma grade I; cat No. 35. Accumulation of neoplastic CD20-positive B cells (epitheliotropism) in the nasal mucosa. CD20 immunohistochemical stain, AEC chromogen, hematoxylin counterstain. **Figure 6.** Longitudinal section of head; cat No. 28. Presence of a whitish, cerebroid mass obliterating the nasopharyngeal cavity.

Table 3. Univariate Analysis.

Variable	HR	95% CI	z	P	χ^2	P
Age					**3.25**	**.1972**
Linear term	0.8264	0.6800–1.004	–1.916	.0553		
Nonlinear term	1.2323	0.9709–1.564	1.717	.0859		
Sex					**0.65**	**.4205**
Female [reference]						
Male	0.7214	0.3285–1.584	–0.813	.416		
Breed					**0.08**	**.7709**
DSH [reference]						
Other	0.8794	0.3672–2.106	–0.288	.773		
Site					**0.19**	**.909**
Nasal cavity [reference]						
Nasopharynx	1.2795	0.4258–3.844	0.439	.661		
Combined	0.9959	0.3900–2.543	–0.009	.993		
FeLV gp70					**0.62**	**.4309**
Negative [reference]						
Positive	0.7238	0.3182–1.646	–0.771	.441		
FeLV p27					**0.06**	**.8064**
Negative [reference]						
Positive	0.7238	0.3182–1.646	0.245	.806		
FeLv gp70 and FeLv p27					**0.13**	**.7153**
Negative-negative [reference]						
At least 1 positive	1.152	0.537–2.471	0.363	.717		
Cell size					**1.32**	**.5166**
Small [reference]						
Medium	1.078	0.3894–2.984	0.144	.885		
Large	1.613	0.6409–4.058	1.015	.310		
Mitotic index					**1.49**	**.2225**
One-unit increase	1.018	0.9911–1.046	1.309	.191		
Phenotype					**0.03**	**.8568**
B [reference]						
Other than B	0.8962	0.268–2.996	–0.178	.859		
Epitheliotropism					**2.9**	**.08831**
Negative [reference]						
Positive	0.4642	0.1817–1.186	–1.604	.109		

Cox model results: HR = hazard ratio, 95% C.I.= 95% confidence interval.
Z= Wald statistic and corresponding P value are referred to the test for each HR.
X^2= likelihood ratio test and corresponding P value are referred to the test for the contribution of the variable to the model.

According to the reverse Kaplan-Meier method, median follow-up was 301 days, the first quartile (25%) was 60 days, and the third quartile (75%) was 381 days. The survival probability at 30, 60, and 300 days after surgery was 0.793 (95% CI, 0.6751–0.932), 0.375 (95% CI, 0.2422–0.581), and 0.153 (95% CI, 0.0595–0.396), respectively.

Major causes of death were euthanasia (21 cats) due to the severity of respiratory obstruction caused by the disease. At the end of the study, 6 cats were still alive, with 1 cat affected by a small B-cell lymphocytic lymphoma treated with radiation therapy surviving for 1293 days (cat No. 5).

In 4 cats, lymphoma was confirmed by full necropsy (cat Nos. 1, 27, 28, 33). Multiorgan involvement was found in 3 cases (cat Nos. 1, 27, 33), with renal (cat Nos. 27, 33) and myocardial infiltration (cat No. 27) and contiguous central nervous system (CNS) involvement by ethmoidal bone lysis (cat Nos. 1, 33). In 1 case (cat No. 28), lymphoma was limited to the nasopharyngeal location (Fig. 6). In this cat, severe monolateral dysplasia of the bronchial walls was also evident.

Statistical Analysis

In univariate analysis, concerning age, a nonlinear relationship was considered because the fit of a 3-knots spline function was better than the fitting by only a linear term (likelihood ratio test for the model with spline = 3.25, $P = .1972$; likelihood ratio test for the model with only the linear term = 0.55, $P = .4578$; likelihood ratio test for the contribution of the nonlinear term = 2.6958, $P = .10$). No variables showed a significant prognostic value based on a significance level of .05 (Table 3).

When mitotic index, age, FeLV positivity, phenotype, and epitheliotropism were jointly considered in a multiple regression model (Table 4), a significant prognostic role was obtained only for epitheliotropism (likelihood ratio test

Table 4. Multivariate Analysis.

Variable	HR	95% CI	z	P	χ^2	P
Initial model						
Age					**3.6975**	**.1574**
Linear term	0.8108	0.6529–1.0069	−1.898	.0577		
Nonlinear term	1.2949	1.0002–1.6765	1.961	.0498		
Mitotic index					**0.3463**	**.5562**
One-unit increase	1.0108	0.9765–1.0463	0.611	.5412		
FeLv gp70 and FeLv p27					**0.5404**	**.4623**
Negative-negative [reference]						
At least 1 positive	0.7063	0.2807–1.7775	−0.738	.4603		
Phenotype					**0.4546**	**.5001**
B [reference]						
Other than B	1.6127	0.4239–6.1352	0.701	.4833		
Epitheliotropism					**4.5316**	**.03327**
Negative [reference]						
Positive	0.3115	0.1019–0.9523	−2.046	.0408		
Final model (backward selection)						
Age					**4.2817**	**.1176**
Linear term	0.8106	0.6709–0.9795	−2.175	.0296		
Nonlinear term	1.2863	1.0109–1.6366	2.048	.0405		
Epitheliotropism					**3.9396**	**.04716**
Negative [reference]						
Positive	0.3981	0.1505–1.0533	−1.855	.0636		

Cox model results: HR = hazard ratio, 95% C.I.= 95% confidence interval.
Z= Wald statistic and corresponding P value are referred to the test for each HR.
X^2= likelihood ratio test and corresponding P value are referred to the test for the contribution of the variable to the model.

= 4.5316, $P = .03327$), where the subjects with negative epitheliotropism showed a greater risk of death than did subjects with positive epitheliotropism (hazard ratio = 0.3115). After applying the backward selection procedure to the above-mentioned model, only age and epitheliotropism were maintained as putative prognostic factors.

Considering 10 years as the reference, a U-shaped behavior of the hazard was observed as a function of age. Thus, the estimated hazards of death of 3-, 5-, and 7-year-old cats are about 1.47, 2.22, and 3.38 times greater than the hazard of death of a cat aged 10 years, respectively, and the estimated hazards of death of 12-, 13-, and 15-year-old cats are about 1.18, 1.47, and 2.46 times greater than the hazard of death of a cat aged 10 years. The hazard of death of subjects with negative epitheliotropism is about 2.5 times greater than the hazard of death of subjects with positive epitheliotropism.

Discussion

This report describes and compares pathological findings, FeLV antigen expression, and survival of feline URT lymphomas by their division into nasal, nasopharyngeal, or combined primary anatomical locations. Nasal or nasopharyngeal tumors have been mostly evaluated separately,[5,12] and lymphomas in the 3 distinct presentations seldom have been compared.[22] Histopathology in conjunction with diagnostic imaging (radiographs and CT scans) resulted in the classification of URT lymphomas into 26 nasal, 6 nasopharyngeal, and 7 combined nasal-nasopharyngeal lymphomas. The predominance of primary nasal lymphomas paralleled the frequency reported previously.[22] No major differences in phenotype, classification, and prognosis were evident. Of particular note were that nasopharyngeal lymphomas always had a B-cell origin and that combined lymphomas did not express FeLV antigens. Also, epitheliotropism was a positive prognostic factor, while age correlated with a poor prognosis.

The 39 cats with lymphoma were drawn from a case series of 164 cats biopsied for nasal lesions. Of these, lymphomas were 24% of all lesions, accounting for 50% of tumors. This distribution resembled frequencies previously reported, with lymphoma being the most common URT tumor.[1,6,14,16,25] Our findings closely paralleled a retrospective study of nasopharyngeal disease in 53 cats reporting that 49% had lymphoma and 28% had polyps.[1]

Of 164 nasal biopsies, 163 were diagnostic. The result of the diagnostic accuracy of histopathology was not comparable with other veterinary reports since studies on the diagnostic precision of endoscopic nasal biopsy evaluation seem not to be available. However, this result seems to represent a high success rate compared with what has been reported for the diagnosis of primary nasal carcinoma in humans, in whom 5% percent of cancers are missed at endoscopic biopsy.[20] The diagnostic success rate observed herein may derive from the expertise of the surgeon providing samples of large size and an adequate number of biopsies that ranged from 4 to 14 per single case. In humans, for nasal carcinoma diagnosis, an average of 6 biopsies from both diseased and adjacent apparently healthy nasal tissue are suggested as the minimum number for the correct diagnosis.[20] Also, in this study, depth of biopsies was pivotal

since the inclusion of the deep lamina propria and turbinates allowed the evaluation of the distribution and of the infiltrative behavior of tumors. Besides, endoscopic-guided biopsy permitted the visualization of nasal and nasopharyngeal mucosa, assisting in the selection of lesional areas to sample.[20] The success rate of histology contrasted with the poor results of cytology, which was diagnostic only in 50% of lymphomas. The main problem encountered was sample contamination by inflammation, leading to misdiagnosis. Our results parallel the observation that many of the cytological sampling techniques have an unacceptably low yield of diagnostic material for nasal specimens.[2,23] In concordance with previous reports,[2,6] impression smears from biopsies and fine-needle aspiration biopsies detected lymphoma more accurately compared with brushing. Brushing is a technique performed blindly,[2,6] and thus small tumors can be missed and inflammatory findings may be misleading. Also, most lymphomas of this caseload developed in the mid to deep lamina propria, which is not sampled by brushing. Similar problems have been reported for nasopharyngeal masses,[1] since cytology is undertaken without direct visualization of the nasopharyngeal area, leading to an inaccurate diagnosis.[1] Crush cytological specimens have demonstrated a better diagnostic yield.[6] Unfortunately, contrary to imprints, crush sample biopsies need to be sacrificed, reducing the subsequent diagnostic capability of histopathology. Despite a low diagnostic potential, in this report, cytology was extremely useful for lymphoma classification thanks to a better assessment of cell morphology. The correct WHO cytological classification of lymphomas is essential for their prognostication. Thus, for lymphoma diagnosis, cytology should be performed when possible and evaluated in conjunction with histopathology.

Cats developing URT lymphomas were mostly adult to aged males, similar to previous reports,[12,25] but contrasting with findings in other caseloads.[14] The predominance of male cats has been hypothesized to derive from the male territorial behavior that makes transmission of FeLV more efficient.[18] In our caseload, FeLV antigen positivity demonstrated by immunohistochemistry was distributed almost equally among sexes, contrasting with this hypothesis. FeLV serological positivity has been correlated to the anatomical form of lymphoma, with most positive cats having mediastinal lymphoma (90%) and multicentric lymphoma (80%) and less than 10% having cutaneous lymphoma.[18] FeLV serology has been seldom evaluated in URT lymphomas. In this study, most cats were not tested for FeLV, likely owing to their old age; however, 6 of 7 cats tested were negative. FeLV p27 capsid and gp70 envelope immunohistochemical protein expression by neoplastic cells was documented in 54% of our cases, but combined URT lymphomas were always negative. A comparison with other URT lymphoma caseloads was not possible due to the lack of data regarding FeLV tissue antigen expression. The old age of cats developing URT was considered incongruent with a causal role of FeLV since it is well established that FeLV-positive cats generally develop lymphomas at a young age;[17] thus, the finding of FeLV protein expression by neoplastic cells was surprising. Significantly, old seronegative cats may still bear the virus at the genomic level and can transcribe FeLV upon reactivation or neoplastic transformation of infected cells.[7] Noteworthy, FeLV gp70 expression was observed in 12 cats. Expression of FeLV gp70 denotes viral particle assembly, confirming a productive infection.[30] Thus, FeLV might still be involved in feline URT lymphoma development.

A concurrent plasmacytic inflammation was observed in 59% of URT lymphomas. Chronic rhinitis-rhinopharyngitis is considered a consequence of prior infection with either feline herpesvirus type 1 or feline calicivirus.[34] Up to 80% of cats that recover from acute viral URT infections may become chronic carriers, which can lead to persistent clinical signs and inflammation.[10] In addition, viral infection causes injuries that predispose to secondary bacterial disease.[14] Chronic inflammation is considered a risk factor for the development of a variety of cancers, including hematopoietic malignancies in humans.[8,11,28] In humans, B-cell lymphomas developing after longstanding chronic inflammation[4,26,31] seem common, and the association between bacterial and viral infections with lymphoma development is well documented for mucosa-associated lymphoid tissue (MALT) B-cell lymphomas.[8,11,28] Notably, in our caseload, inflammation and FeLV tissue antigen positivity were concurrently documented in 31% of cats. Specifically, chronic persistent rhinitis may favor expansion of virally transfomed B-lymphoid cells, explaining the higher frequency of URT lymphomas with a B-cell phenotype observed in this and other caseloads.[5,22,25]

The histological diagnosis of lymphoma was performed using the modified WHO classification.[32,33] In other studies of feline URT lymphomas, the Revised European American Lymphoma (REAL)/ revised WHO classification[5] and the National Cancer Institute working formula classification[22] have been applied. Large cell lymphomas were mostly identified in our series (39%), with a prevalence of immunoblastic morphology, paralleling other studies.[5,22] Interestingly, small cell lymphomas were also frequent (28%). As for these cases, rare lymphoma variants such as plasmacytoid/plasmacytic[22] follicular grade II,[5] as well as anaplastic large and small cell lymphomas,[14] have rarely been described.

Epitheliotropism was unexpectedly identified in B-cell lymphomas of the 3 URT anatomical types. In cats, epitheliotropism usually has been described in cutaneous and gastrointestinal T-cell lymphomas;[3,9,24,27] however, this growth pattern has also been occasionally reported in feline URT lymphomas.[22,25] Human studies have documented epitheliotropism of B cells in tonsillar hyperplasia and in MALT lymphomas.[19] Interestingly, in our study, epitheliotropism was statistically associated with a prolonged survival time of diseased cats. Considering other histological variables, mitotic index, cell size, phenotype, and FeLV antigen expression had no significant correlation with mortality. Epitheliotropism and age, evaluated on a continuous scale, were the only prognostic factors identified; however, lack of statistical evidence of other variables having a significant prognostic impact should be considered with caution. In fact, power of statistical tests may be low, and the reduced sample size did not permit a full evaluation of the joint

prognostic role of the considered variables. For a more reliable evaluation, a case series with at least 100 deaths would be needed. Also, an increased number of combined and nasopharyngeal lymphomas are necessary to obtain a representative selection of cases providing a suitable cohort for statistical analysis of potentially significant prognostic variables.

In conclusion, URT lymphomas are aggressive tumors with a prevailing primary nasal B-cell origin. Lymphoplasmacytic inflammation is frequently associated with URT lymphomas and may represent alone, or in conjunction with FeLV infection, a possible favoring factor in lymphoma development.

Declaration of Conflicting Interests

The author(s) declared no potential conflicts of interest with respect to the research, authorship, and/or publication of this article.

Funding

The author(s) received no financial support for the research, authorship, and/or publication of this article.

References

1. Allen H, Broussardv J, Noone K. Nasopharyngeal diseases in cats: a retrospective study of 53 cases (1991–1998). *J Am Anim Hosp Assoc*. 1999;**35**:457–461.
2. Caniatti M, Roccabianca P, Ghisleni G, et al. Evaluation of brush cytology in the diagnosis of chronic intranasal disease in cats. *J Small Anim Pract*. 1998;**39**:73–77.
3. Carreras J, Goldschmidt M, Lamb M, et al. Feline epitheliotropic intestinal malignant lymphoma: 10 cases (1997–2000). *J Vet Intern Med*. 2003;**17**:326–331.
4. Copie-Bergman C, Niedobitek G, Mangham DC, et al. Epstein-Barr virus in B-cell lymphomas associated with chronic suppurative inflammation. *J Pathol*. 1997;**183**:287–292.
5. Day MJ, Henderson S, Bellshaw Z, et al. An immunohistochemical investigation of 18 cases of feline nasal lymphoma. *J Comp Pathol*. 2004;**130**:152–161.
6. De Lorenzi D, Bertoncello D, Bottero E. Squash-preparation cytology from nasopharyngeal masses in the cat: cytological results and histological correlations in 30 cases. *J Fel Med Surg*. 2008;**10**:55–60.
7. Favrot C, Wilhem S, Grest P, et al. Two cases of FeLV-associated dermatoses. *Vet Dermatol*. 2005;**16**:407–412.
8. Ferreri AJ, Ernberg I, Copie-Bergman C. Infectious agents and lymphoma development: molecular and clinical aspects. *J Intern Med*. 2009;**265**:421–438.
9. Fontaine J, Heimann M, Day MJ. Cutaneous epitheliotropic T-cell lymphoma in the cat: a review of the literature and five new cases. *Vet Dermatol*. 2011;**22**:454–461.
10. Gaskell RM, Wardley R. Feline viral respiratory disease: a review with particular reference to its epizootiology and control. *J Small Anim Pract*. 1978;**19**:1–16.
11. Grivennikov SI, Greten FR, Karin M. Immunity, inflammation, and cancer. *Cell*. 2010;**140**:883–899.
12. Haney S, Beaver L, Turrel J, et al. Survival analysis of 97 cats with nasal lymphoma: a multi-institutional retrospective study (1986–2006). *J Vet Intern Med*. 2009;**23**:287–294.
13. Harrell F, Lee K, Mark D. Multivariable prognostic models: issues in developing models, evaluating assumptions and adequacy, and measuring and reducing errors. *Stat Med*. 1996;**15**: 361–387.
14. Henderson SM, Bradley K, Day MJ, et al. Investigation of nasal disease in the cat—a retrospective study of 77 cases. *J Feline Med Surg*. 2004;**24**:245–257.
15. Hsu S, Raine L, Fanger H. Use of avidin-biotin-peroxidase complex (ABC) in immunoperoxidase techniques: a comparison between ABC and unlabeled antibody (PAP) procedures. *J Histochem Cytochem*. 1981;**29**:577–580.
16. Hunt G, Perkins M, Foster S, et al. Nasopharyngeal disorders of dogs and cats: a review and retrospective study. *Comp Cont Pract Vet*. 2002;**24**:184–200.
17. Jackson M, Wood S, Misra V, et al. Immunohistochemical identification of B and T lymphocytes in formalin-fixed, paraffin-embedded feline lymphosarcomas: relation to feline leukemia virus status, tumor site, and patient age. *Can J Vet Res*. 1996; **60**:199–204.
18. Jacobs RM, Messick JB, Valli VE. Tumors of the hemolymphatic system: lymphoid tumors. In: Meuten DJ, ed. *Tumors in Domestic Animals*. 4th ed. Ames: Iowa State Press; 2002:119–198.
19. Jaspars L, Beljaards R, Bonnet P, et al. Distinctive adhesion pathways are involved in epitheliotropic processes at different sites. *J Pathol*. 1996;**178**:385–392.
20. King A, Vlantis A, Bhatia K, et al. Primary nasopharyngeal carcinoma: diagnostic accuracy of MR imaging versus that of endoscopy and endoscopic biopsy. *Radiology*. 2011;**258**:531–537.
21. Lei K, Suen J, Hui P, et al. Primary nasal and nasopharyngeal lymphomas: a comparative study of clinical presentation and treatment outcome. *Clin Oncol (R Coll Radiol)*. 1999;**11**: 379–387.
22. Little L, Patel R, Goldschmidt M. Nasal and nasopharygeal lymphoma in cats: 50 cases (1989–2005). *Vet Pathol*. 2007;**44**: 885–892.
23. McCarthy TC. Rhinoscopy: the diagnostic approach to chronic nasal disease. In: McCarthy TC, ed. *Veterinary Endoscopy for the Small Animal Practitioner*. St Louis, MO: Elsevier Saunders; 2005:137–200.
24. Moore P, Rodriguez-Bertos A, Kass P. Feline gastrointestinal lymphoma: mucosal architecture, immunophenotype, and molecular clonality. *Vet Pathol*. 2012;**49**:658–668.
25. Mukaratirwa S, Van der Linde-Sipman J, Gruys E. Feline nasal and paranasal sinus tumors: clinicopathological study, histomorphological description and diagnostic immunohistochemistry of 123 cases. *J Feline Med Surg*. 2001;**3**:235–245.
26. Petitjean B, Jardin F, Joly B, et al. Pyothorax-associated lymphoma: a peculiar clinicopathologic entity derived from B cells at late stage of differentiation and with occasional aberrant dual B- and T-cell phenotype. *Am J Surg Pathol*. 2002;**26**:724–732.
27. Pohlman L, Higginbotham M, Welles E, et al. Immunophenotypic and histologic classification of 50 cases of feline gastrointestinal lymphoma. *Vet Pathol*. 2009;**46**:259–268.

28. Sadrzadeh H, Abtahi SM, Fathi AT. Infectious pathogens and hematologic malignancy. *Discov Med*. 2012;**14**:421–433.
29. Schemper M, Smith TL. A note on quantifying follow-up in studies of failure time. *Control Clin Trials*. 1996;**17**:343–346.
30. Suntz M, Failing K, Hecht W, et al. High prevalence of non-productive FeLV infection in necropsied cats and significant association with pathological findings. *Vet Immunol Immunopathol*. 2010;**136**:71–80.
31. Swerdlow S, Campo E, Lee Harris N, et al. *WHO Classification of Tumors of Haematopoietic and Lymphoid Tissues*. 4th ed. Lyon, France: IARC; 2008.
32. Valli VE. *Veterinary Comparative Hematopathology*. Ames, IA: Blackwell; 2007.
33. Valli VE, San Myint M, Barthel A, et al. Classification of canine malignant lymphomas according to the World Health Organization criteria. *Vet Pathol*. 2011;**48**:198–211.
34. Van Pelt D, Lappin M. Pathogenesis and treatment of feline rhinitis. *Vet Clin North Am Small Anim Pract*. 1994;**24**:807–823.
35. Venables W, Ripley B. *Modern Applied Statistics With S*. 4th ed. New York, NY: Springer; 2002.
36. Vittinghoff E, McCulloch C. Relaxing the rule of ten events per variable in logistic and Cox regression. *Am J Epidemiol*. 2007; **165**:710–718.
37. Webster J, Dennis M, Dervisis N, et al. Recommended guidelines for the conduct and evaluation of prognostic studies in veterinary oncology. *Vet Pathol*. 2011;**48**:7–18.

REVISED VERSION JAVMA 14-01-0029

Pathology in Practice

This report was submitted by Annalisa Forlani, DVM, PhD; Chiara Palmieri DVM, PhD; Sara F. Santagostino, DVM; Roberta Queliti, DVM; and Paola Roccabianca, DVM, PhD; from the Department DIVET, School of Veterinary Medicine, University of Milan, Via Celoria n° 10, 20010, Milan, Italy (Forlani, Santagostino, Roccabianca); the School of Veterinary Science, University of Queensland, Gatton, 4343, Australia (Palmieri); and Bracco Imaging S.p.a., via Ribes n° 5, 10010, Colleretto Giacosa, Turin, Italy (Queliti).

Poster presentation at the 10th Annual Congress of the Italian Association of Veterinary Pathology (Giulianova Lido, Teramo, Italy, May 2013) and the 31st Annual Congress of the European College of Veterinary Pathology and European Society of Veterinary Pathology (London, UK, September 2013).

Address correspondence to Dr. Forlani (annalisa.forlani.9@gmail.com).

Pulmonary alveolar proteinosis/phospholipidosis in an English bulldog.

History

A 7-year-old 31-kg (68.2-lb) intact male English Bulldog was referred for evaluation of severe expiratory dyspnea that was unresponsive to treatment with furosemide. The dog had a history of idiopathic juvenile epilepsy and was currently in treatment with phenobarbital (100 mg, PO, q 12 h) and bromide (400 mg, PO, q 12 h). At the referral evaluation , the emergency care provided included administration of cephalexin (30 mg/kg [13.6 mg/lb], IV, q 12 h), enrofloxacin (5 mg/kg [2.27 mg/lb], IV, q 12 h), beclomethasone dipropionate (aerosol, q 8 h), butorphanol tartrate (0.2 mg/kg [0.09 mg/lb], IM, single administration), oxygen via nasal probe (65 mL/kg [2.20 fl oz x body weight (kg)]) and fluid therapy (50 mL/kg/24 h, IV). Despite treatment, the dog developed respiratory arrest 12 hours after admission and cardiopulmonary resuscitation was unsuccessful.

Clinical and Gross Findings

Respiratory tract signs persisted in the dog from admission until death, despite treatment. Antemortem thoracic radiography revealed an alveolar to interstitial pattern. A CBC and serum biochemical analysis revealed mild leukocytosis (17.9 X 10^3 leukocytes/µL; reference interval, 6 X 10^3 to 17 X 10^3 leukocytes/mL) with neutrophilia (13.96 X 10^3 neutrophils/µL; reference interval, 3 X 10^3 to 11.5 10^3 neutrophils/mL) and monocytosis (2.5 X 10^3 monocytes/µL; reference interval, 0.15 X 10^3 to 1.35 X 10^3 monocytes/mL), numerous platelets aggregates, and high activities of aspartate aminotransferase (34 U/L; reference interval, 0 to 32 U/L), alanine aminotransferase (208 U/L; reference interval, 15 to 90 U/L), alkaline phosphatase (356 U/L; reference interval, 0 to 85 U/L), and γ-glutamyltransferase (49 U/L; reference interval 0 to 10 U/L).

At necropsy, the liver was severely, diffusely enlarged (weight: 1.85 kg [4.07 lb]), soft, and friable with an enhanced lobular pattern; these findings were associated with severe dilation of the abdominal vena cava (> 3 times its typical diameter), which was interpreted as a pathologic change secondary to hypertension. The apical, accessory, and right principal lobes of the lung contained multifocal to coalescing, up to 0.6 cm in diameter, round, firm umbilicated lesions (Figure 1). Moderate right ventricular dilation along with minimal endocardiosis of the mitral valve was also evident.

Histopathological Findings

Liver and lung tissues samples were fixed in buffered 10% formalin for 5 days, routinely processed, and stained with H&E stain. Histochemical special stains (Periodic acid-Schiff [PAS], von Kossa, and Congo red) were applied to selected pulmonary sections; lung tissue samples were also submitted for transmission electron microscopy (TEM).

In hepatic tissue sections, there was evidence of diffuse and severe congestion, severe multifocal to coalescing vacuolar degeneration, and centrilobular hemosiderosis. In lung tissue sections, most of the alveoli were filled with abundant, pale eosinophilic, homogeneous, amorphous material (Figure 2). The histochemical special staining revealed that the material was PAS stain positive, von Kossa stain negative, and Congo red stain negative. Within the lumens of the alveoli, multifocal edema associated with high numbers of alveolar macrophages, occasional multinucleated giant cells, and fewer neutrophils was present. The pulmonary interstitium was expanded by moderate, multifocal to coalescing deposition of collagen (fibrosis). Anthracosis was observed in the regions of interstitial fibrosis. Multifocal mineralization, confirmed by the von Kossa staining, was observed in the interstitium and the alveolar septae. In the interventricular septum and, to a lesser extent, in the right ventricle, myofibers were multifocally replaced by adipose tissue. Multifocal areas of fibrosis were also dissecting the myofibers of the right ventricle.

Transmission electron microscopy of the material accumulated within the alveoli revealed short lamellar 3.125 nm thick fascicles at 6.25 nm interlamellar distance (Figure 2). This morphology was consistent with abnormal surfactant.

Morphological diagnosis and Case summary:

Morphological diagnosis: severe, diffuse, pulmonary alveolar proteinosis (PAP) and histiocytosis with multifocal to coalescing mild pyogranulomatous pneumonia, multifocal interstitial fibrosis, and mineralization.

Case summary: PAP (also known as phospholipidosis) in a English Bulldog.

Comments

Pulmonary alveolar proteinosis is a rare disease in humans, dogs, rats, hamsters, guinea pigs, and goats.[1–3] Although only 3 dogs of different breeds (Cocker Spaniel, Shih Tzu, and Golden Retriever) have been reported to have PAP,[2,4,5] it should be considered one of the differential diagnoses for interstitial lung disease in dogs.

Pulmonary alveolar proteinosis is characterized by abnormal surfactant homeostasis with alveolar accumulation of PAS stain-positive proteinaceous material.[1] Mice lacking surfactant protein D develop alveolar lipoproteinosis,[6] because surfactant protein D is able to form tubular myelin-like structures from surfactant phospholipids and enhance surface activity.[7] Three types of PAP in humans have been described: autoimmune (previously named primary or idiopathic), secondary (acquired), and genetic.[8] Genetic PAP is most commonly observed in children, and the severity of the disease depends on the type of mutation.[3] Autoimmune and secondary PAP are the more frequent forms.[3] Autoimmune PAP is caused by anti-granulocyte macrophage colony stimulating factor (GM-CSF) antibodies that inhibit macrophage function and, therefore, clearance of surfactant,[3] as demonstrated in mice homozygous for the disrupted GM-CSF gene.[9] Secondary PAP is associated with exposure to toxins or drugs as well as systemic inflammatory disorders and malignancies.[3]

Pulmonary alveolar proteinosis is a subacute and subtle disease that is generally diagnosed months or years after its initiation.[1] The accumulation of abnormal material within the alveolar spaces leads to a left to right shunt, impaired diffusion, and ventilation-perfusion mismatch.[10] Clinical signs in affected dogs and humans are nonproductive cough, fever, and progressive exercise intolerance.[1,2] Hematologic findings include neutrophilia, eosinophilia, or both,[2] which most likely develop secondary to bacterial infections favored by the accumulation of abnormal material in the alveoli and impairment of the alveolar defense mechanisms.[2] Thoracic radiography commonly reveals a fine, diffuse perihilar alveolar or interstitial pattern.[2] A crazy-paving appearance of the lungs (defined as scattered or diffuse ground-glass attenuation superimposed on a network of interlobular septal thickening and intralobular lines) in high-resolution CT images is a characteristic but not diagnostic feature of this disease, given that a similar appearance of the lungs has also been reported for a variety of interstitial and airspace pulmonary disorders.[1,3] Bronchoalveolar lavage is considered an additional useful diagnostic aid.[1–3] Grossly, bronchoalveolar lavage fluid may be milky and opaque, composed of a thick sediment and a translucent supernatant.[1,2] In dogs, globules of mucus, protein, and cholesterol clefts with small numbers of inflammatory cells are also cytologically detectable.[2] Numerous lamellar bodies that are structurally similar to myelin have been observed in human bronchoalveolar lavage fluid.[3] Bronchoalveolar lavage fluid examination data were not available for the dog of the present report because a fluid sample was not collected during cardiopulmonary resuscitation. Histologic examination of lung biopsy specimens represents the gold standard test for PAP diagnosis.[1] Typically, histopathologic changes include alveoli that are filled with PAS stain-positive granular eosinophilic material in an otherwise intact alveolar architecture.[1–3] This material corresponds to the tubular myelin-like multilamellar structures observed by electron microscopy.[11] Multilamellar structures appear to be abnormal forms of tubular myelin that lack the regular

architecture found in lungs of healthy humans and other animals.[11] Small tubular myelin-like structures may be detected in healthy lungs, but never in such large amounts and bizarre arrangement as those found in lings of individuals with PAP.[11] Whole-lung lavage is commonly used as treatment for patients with clinical signs of alveolar proteinosis and severe hypoxemia.[1,3] Numerous treatments that theoretically could enhance surfactant clearance have been attempted such as administration of exogenous GM-CSF or plasmapheresis to reduce anti–GM-CSF antibody concentration.[1,3] Silverstein et al[2] described the application of lung lavage in a dog with PAP-associated clinical signs and, although follow-up information was not available, treatment results seemed encouraging (ie, absence of clinical respiratory tract signs 20 months after lung lavage).[2]

The accumulation of phospholipids in the lungs induced by cationic amphiphilic medications is generally referred as phospholipidosis, although the term alveolar proteinosis has also been used to describe this condition.[11] In cats, bromide-induced lower airway diseases, specifically endogenous lipid pneumonia with suppurative inflammation[12] and bronchitis resulting from a hypersensitivity reaction[13] has been described. Potassium bromide-associated alterations of bronchial secretions, mucociliary function, and cytokine stimulation in humans[14] have been described although the pathophysiology of this drug-induced reaction is still unclear. In dogs, adverse effects associated with bromide administration are usually mild and self-limiting; polyphagia, vomiting, polyuria, ataxia, and sedation are most frequently observed.[15,16] Respiratory lesions associated with bromide-treatment in dogs have not been reported to our knowledge. In the case described in the present report, findings of histochemical analysis and histologic and transmission electron microscopic examinations warranted a diagnosis of PAP (phospholipidosis). Potassium bromide and phenobarbital may be used in combination as a treatment for idiopathic epilepsy in dogs.[17] Despite the lack of data regarding a possible association between epilepsy treatment and alveolar proteinosis or

lipoproteinosis in dogs, the prolonged administration of both drugs from an early age may have contributed to the development of alveolar proteinosis or lipoproteinosis in the dog of the present report. The 2 drugs have mechanisms of action similar to those of active agents that have been correlated with abnormal accumulation of alveolar surfactant in humans.[11]

References

1. Khan A, Agarwal R. Pulmonary alveolar proteinosis. Respir Care 2011;56:1016–1028.
2. Silverstein D, Green C, Gregory C, et al. Pulmonary alveolar proteinosis in a dog. J Vet Intern Med 2000;14:546–551.
3. Borie R, Danel C, Debray MP, et al. Pulmonary alveolar proteinosis. Eur Respir Rev. 2011;20:98–107.
4. Cummings AC, Spaulding KA, Scott KD, et al. Imaging diagnosis—pulmonary alveolar proteinosis in a dog. Vet Radiol Ultrasound 2013;54:634–637.
5. Jefferies AR, Dunn JK, Dennis R. Pulmonary alveolar proteinosis (phospholipoproteinosis) in a dog. J Small Anim Pract 1987;28:203–214.
6. Hawgood S, Ochs M, Jung A, et al. Sequential targeted deficiency of SP-A and -D leads to progressive alveolar lipoproteinosis and emphysema. Am J Physiol Lung Cell Mol Physiol 2002;283:L1002–L1010.
7. Poulain FR, Akiyama J, Allen L, et al. Ultrastructure of phospholipid mixtures reconstituted with surfactant proteins B and D. Am J Respir Cell Mol Biol 1999;20:1049–1058.
8. Patel SM, Sekiguchi H, Renolds JP, et al. Pulmonary alveolar proteinosis. Can Respir J 2012;19:243–245.
9. Stanley E, Lieschke GJ, Grail D et al. Granulocyte/macrophage colony-stimulating factor-deficient mice show no major perturbation of hematopoiesis but develop a characteristic pulmonary pathology. Proc Natl Acad Sci US 1994;7;91(12):5592–5596.

10. Rogers RM, Levin DC, Gray BA, et al. Physiologic effects of bronchopulmonary lavage in alveolar proteinosis. Am Rev Respir Dis 1978;118:255–264.
11. Hook GE. Alveolar proteinosis and phospholipidoses of the lungs. Toxicol Pathol 1991;19:482–513.
12. Bertolani C, Hernandez J, Gomes E, et al. Bromide-associated lower airway disease: a retrospective study of seven cats. J Feline Med Surg 2012;14:591–597.
13. Boothe DM, George KL, Couch P. Disposition and clinical use of bromide in cats. J Am Vet Med Assoc 2002;221:1131–1135.
14. Diener W, Sorini M, Ruile S, et al. Panniculitis due to potassium bromide. Brain Dev 1998;20:83–87.
15. Dewey CW. Anticonvulsivant therapy in dogs and cats. Vet Clin North Am Small Anim Pract 2006;36:1107–1127.
16. Rossmeisl JH, Inzana KD. Clinical signs, risk factors, and outcomes associated with bromide toxicosis (bromism) in dogs with idiopathic epilepsy. J Am Vet Med Assoc 2009;234:1425–1431.
17. Thomas WB. Idiopathic epilepsy in dogs and cats. Vet Clin North Am Small Anim Pract 2010;40:161–179.

Figure 1—Photographs of lungs and heart from a 7-year-old intact male English Bulldog that was evaluated because of severe expiratory dyspnea that was unresponsive to treatment with furosemide. The dog died 12 hours after admission. A—Notice the diffuse severe edema and hyperemia with disseminated focal lesions (more severe in the left cranial and caudal lung lobes). The heart has a rounded outline owing to moderate right ventricular dilation. B—Closer view of the cranial left ling lobe. Notice the presence of multifocal umbilicated lesions.

Figure 2—Photomicrographs (A and B) and transmission electron micrograph (C) of sections of lung tissue from the dog in Figure 1. A—The alveoli are filled with pale blue-gray amorphous homogeneous material associated with large numbers of alveolar macrophages and occasional multinucleated giant cells. H&E stain; bar = 120 μm. B—The material within the lumens of the alveoli is variably PAS stain positive. PAS stain and hematoxylin counterstain; bar = 121 μm. C—The substance in the lumens of the alveoli is composed of short lamellar 3.125 nm thick fascicles at 6.25 nm periodic distance interlamellar consistent with accumulation of abnormal surfactant. Lead citrate and uranyl acetate stain; bar = 500 nm.

Case Series

jfms Journal of Feline Medicine and Surgery

Pericardial lymphoma in seven cats

Journal of Feline Medicine and Surgery
2014, Vol. 16(6) 507–512

DOI: 10.1177/1098612X13506199
jfms.com
SAGE

Maria Amati[1], Luigi Venco[1], Paola Roccabianca[2], Sara Francesca Santagostino[2] and Walter Bertazzolo[1]

Abstract

A presumed primary pericardial lymphoma was diagnosed in seven cats. Clinical findings at presentation included poor body condition, dehydration and dyspnoea. Thoracic diagnostic imaging was performed in six cases and revealed pleural effusion and a diffuse thickening of the pericardium. A cytological diagnosis of lymphoma was obtained in six cases; in four cases the diagnosis was confirmed at necropsy. Immunophenotyping was performed in six cases: three cases were classified as T-cell and three as B-cell lymphoma. Four cats did not receive any treatment. One cat received only prednisone and two cats received chemotherapy. Six cats lived 7–11 days, except for one cat that received a multi-drug chemotherapy protocol and was still alive at the time of writing (750 days after diagnosis). Primary pericardial lymphoma is a rare extranodal feline lymphoma that has never been described previously.

Accepted: 22 August 2013

Introduction

Lymphomas, formerly referred also as malignant lymphoma or lymphosarcoma, are a group of neoplasms that originate from lymphoreticular cells, which are primarily found in lymphoid tissues (eg, lymph nodes, spleen and bone marrow), but they are also present in all other tissues in the body. Lymphoma is one of the most commonly diagnosed neoplasms in cats.[1] Many lymphomas in cats have been associated with feline leukaemia virus (FeLV) infection. However, despite a decreasing frequency of FeLV infection in recent years, the incidence of feline lymphoma has increased, becoming especially relevant in veterinary oncology.[1,2] At present, fewer than a quarter of cats with lymphoma are associated with FeLV antigenicity.[1]

Lymphomas in cats can be grouped into lymph-nodal and extra-nodal forms, the latter being the most common. The extra-nodal forms are classified, according to anatomic location, in, for example, mediastinic, alimentary, renal, ocular, retrobulbar, nervous, nasal and cutaneous lymphoma tissue, with the gastrointestinal form being the most common.[3,4] Over time, the median age of cats diagnosed with each anatomic tumour group has remained the same: the anatomical forms traditionally associated with FeLV infection, such as the mediastinal form, tend to occur in younger, FeLV-positive cats; the alimentary form occurs most often in older, FeLV-negative cats.[2,3,5,6] In this article, we describe seven cases of feline extra-nodal lymphoma involving primarily the pericardium, a location that has not been previously described in cats.

Materials and methods

Seven cases of feline pericardial lymphoma were diagnosed at the Veterinary Hospital of the City of Pavia and at the Veterinary University of Milan between 1995 and 2012. All cases were retrospectively identified and underwent full clinical examination, except for one cat (cat 7), which was diagnosed only at necropsy. This cat came from a colony of stray cats and did not undergo extensive diagnostic investigation. Routine haematology and clinical biochemistry were performed in 5/7 cats. A serum FeLV antigenic test [Snap Test (Idexx) or Wittness Test (Symbiotics)] was performed in 6/7 cats. Three cats underwent a feline immunodeficiency virus (FIV) antibody test (Snap Test; Idexx). Thoracic radiography and ultrasonography (US) were performed in all but one cat (the cat diagnosed at necropsy). Antemortem presumptive diagnosis was based on a combination of

[1]Veterinary Hospital of the City of Pavia, Pavia, Italy
[2]Department of Veterinary Sciences and Public Health (DIVET), University of Milan, Milan, Italy

Corresponding author:
Maria Amati DVM, Veterinary Hospital of the City of Pavia, Viale Cremona, 179, Pavia 27100, Italy
Email: mariaamati@libero.it

the following: US thoracic findings (six cases), pleural effusion cytology (four cases), fine-needle cytology of the pericardium (three cases) and pericardial effusion cytology (one case). Complete necropsy and histopathology were available in four cases. Immunophenotyping was available in six cases and was performed by immunohistochemistry in three cases, by immunocytochemistry in two cases and by both methods in one case. For the purpose of phenotypic evaluation, histological cases were stained with anti-CD3-ε (clone CD3-12 Rat IgG1, human cross reactive with cat; Serotec) for T-cells and with anti-CD79a (clone HM-57 Mouse IgG1, human cross reactive with cat; Dako) for B-cells. Immunocytochemistry was performed utilizing primary antibodies anti-CD3-ε (clone CD3-12 Rat IgG1, human cross reactive with cat; Serotec), CD8α [clone Fe1.10E9, feline-specific (Leukocyte Antigen Biology Laboratory, UC Davis, CA, USA) available only for cat 1] and CD21 (Ca2.1D6 anti-canine cross reacting with cat; Leukocyte Antigen Biology Laboratory).

In three cases, FeLV antigen expression was also assessed by immunohistochemistry utilizing primary monoclonal antibodies recognizing the FeLV gp70 envelope protein (clone C11D8; Custom Monoclonal International) and FeLV p27 core protein (clone PF12J-10A; Custom Monoclonal International).

Results

Signalment and clinical presentation

All the cats described in this report were domestic shorthairs. Age at presentation ranged from 2 to 10 years, with a median age of 5 years. Two cats were neutered males and five were spayed females.

History and clinical presentation were identical for the six cases evaluated clinically, and included weight loss, poor appetite and reluctance to move (Table 1). Physical examination showed poor body condition, dyspnoea, pale mucous membranes, dehydration, weak femoral pulse, and dull heart and lung sounds on thoracic auscultation. The remainder of physical examination was unremarkable.

Haematology, biochemistry and serology

Complete blood cell counts showed lymphopenia and neutrophilia in two cases (cats 3 and 5) and mild anaemia in one case (cat 1). Blood chemistry showed an increased alanine transaminase activity in two cats (cats 1 and 5). FIV antibody test results were available for three cats (cats 3, 4 and 5); the results were negative.

Diagnostic imaging

Thoracic lateral radiographs were performed in 6/7 cases and revealed the presence of pleural effusion. In these six cases, thoracentesis yielded 70–160 ml fluid. Repeated thoracic radiographs after thoracentesis did not allow for clear identification of the heart silhouette as the section between the cranial part of the thorax and the caudal part of cardiac silhouette was radiopaque. Vessels and pulmonary parenchyma were obscured by a radiopaque mass, causing the trachea to be severely dorsally displaced – almost coming in contact with thoracic spine (Figure 1).

Ecocardiography revealed pleural effusion and an extremely thickened pericardium in six cases and no cranial mediastinal mass was in evidence. The pericardium was 1–1.8 cm thick, with a non-homogeneous echogenicity ('brain-like' aspect) (Figure 2). Abdominal US was performed in all but one case, and no lymph node enlargement or echostructure changes of intra-abdominal organs were detected. Mild pericardial effusion was observed in three cases.

Cytology

Pleural effusion analysis was performed in five cases. In 4/5 cases (cats 4, 5, 6 and 7), it was consistent with a neoplastic lymphoid effusion (Figure 3), while in cat 3 the effusion analysis was consistent with a protein-rich transudate. When performed (cats 1, 3 and 5), US-guided fine-needle aspiration cytology of the thickened pericardium showed a single population of immature lymphoid cells of medium-to-large size (>2–3 red blood cells), with scant basophilic cytoplasm, and round-to-pleomorphic nuclei with evident nucleoli.

A few millilitres of pericardial effusion were collected and analysed in two cases (cats 3 and 6): in cat 3 it was consistent with a protein-rich transudate, whereas in cat 6 it was consistent with a neoplastic lymphoid effusion.

Treatment and follow-up

Four cats (cats 1, 2, 6 and 7) did not receive any medication. Survival time of cats 1, 2 and 6 ranged from 7 to 10 days, with a median survival time of 9 days. Survival time of cat 7 was not recorded.

Two cats were administered chemotherapy: one received a modified University of Wisconsin–Madison chemoterapy protocol (UWM) (cat 3), which included cyclophosphamide, doxorubicin, vincristine and prednisone, but no L-asparaginase.[1] The other cat (cat 4) received doxorubicin as a single-agent therapy at 25 mg/m^2. One cat received only prednisone at the dosage of 2 mg/kg per day subcutaneously (cat 5).

The cat that underwent UWM protocol is still alive at the time of writing and has been in complete remission for 750 days, with complete remission being intended as the resolution of all clinically detectable diseases confirmed by thoracic radiology and US. The cat that was administered only doxorubicin survived 10 days and did not respond to the treatment.

The cat that received prednisone had a survival time of 11 days, with no response to treatment.

Table 1 Signalment, and main clinical and pathological findings in seven cats with pericardial lymphoma

Cat	Signalment	Age (y)	FeLV status	Thoracic US	Cytology	Histology	Immunophenotype	Treatment	Follow-up*
1	DSH Mn	7	Negative	Yes	Yes (pericardium) Large-cell lymphoma	Yes Large-cell lymphoma	IHC and ICC CD3+ CD8+ CD79a- T-cell	None	Died 7 days
2	DSH Fs	3	Positive	Yes	NP	Yes Intermediate-cell lymphoma	IHC CD79a+ CD3- B-cell FeLV p27+ FeLVgp70+	None	Died 10 days
3	DSH Fs	4	Positive	Yes	Yes (pleural effusion and pericardic effusion and pericardium) Medium-size cell lymphoma	NP	NP	Modified UWM	Alive (750 days on complete remission)
4	DSH Fs	5	Positive	Yes	Yes (pleural effusion) Large-cell lymphoma	NP	ICC CD3+ CD79a- CD20- T-cell	Doxorubicin	Died 10 days
5	DSH Mn	2	Positive	Yes	Yes (pleural effusion and pericardium) Large-cell lymphoma	NP	ICC CD3+ CD79a- CD20- T-cell	Prednisone	Died 11 days
6	DSH Fs	5	Positive	Yes	Yes (pleural and pericardial effusion) Small–cell lymphoma	Yes Small-cell lymphocytic lymphoma	IHC CD79a+ CD3- B-cell FeLV p27+ FeLV gp70-	None	Died 9 days
7	DSH Fs	10	Positive (performed only on IHC)	No	Yes (pleural effusion) Intermediate-cell lymphoma	Yes Lymphoblastic intermediate-cell lymphoma	IHC CD79a+ CD3- B-cell FeLV p27+ FeLV gp70+	None	Unknown

FeLV = feline leukaemia virus; US = ultrasonography; DSH = domestic shorthair; Mn = male neutered; Fs = female spayed; IHC = immunohistochemistry; NP = not performed; ICC = immunocytochemistry; UWM = University of Wisconsin–Madison chemotherapy protocol
*The survival time is defined as the time from diagnosis to death

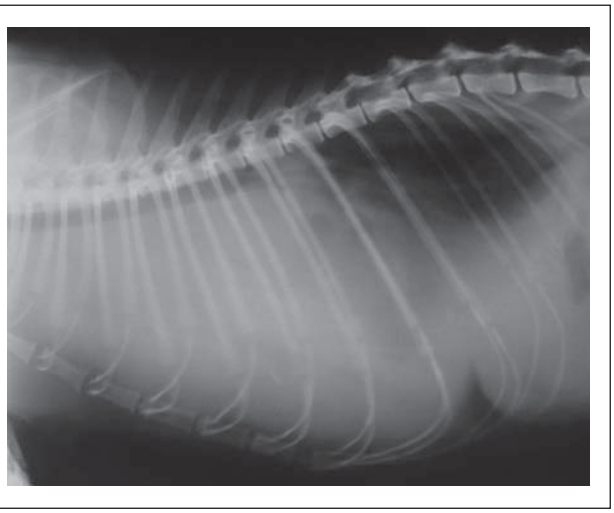

Figure 1 Right lateral thoracic radiograph of a cat with pericardial lymphoma, showing pleural fluid accumulation and a dorsal displacement of the trachea

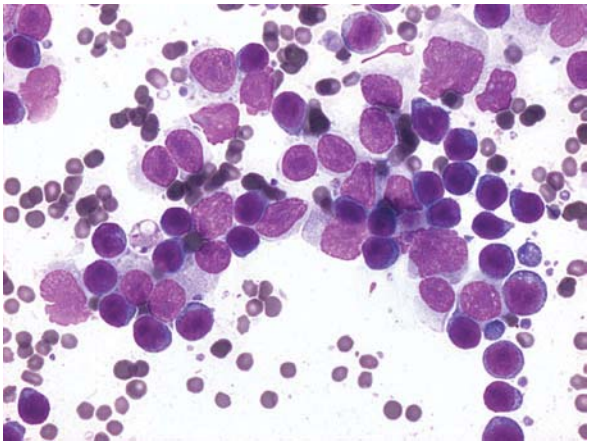

Figure 3 Cytology from a pleural effusion in a cat with pericardial lymphoma. Middle-size (2–3 red blood cells [RBC] in size) to large immature (>3 RBC) lymphoid cells are present (May–Grünwald–Giemsa stain, x 1000)

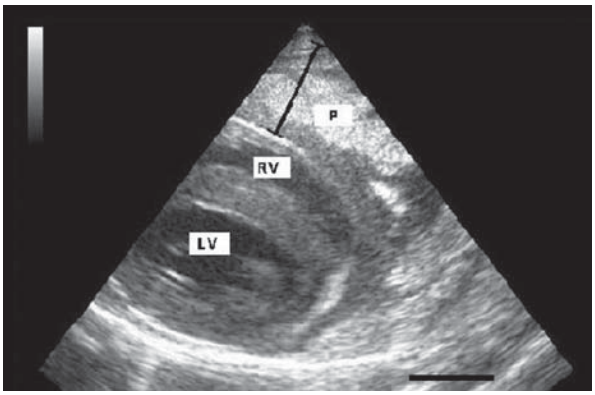

Figure 2 Echocardiographic appearance of a cat with pericardial lymphoma. Marked pericardial thickening is evident. The black bar in the bottom right corresponds to 1 cm. P = pericardium; RV = right ventricle; LV = left ventricle

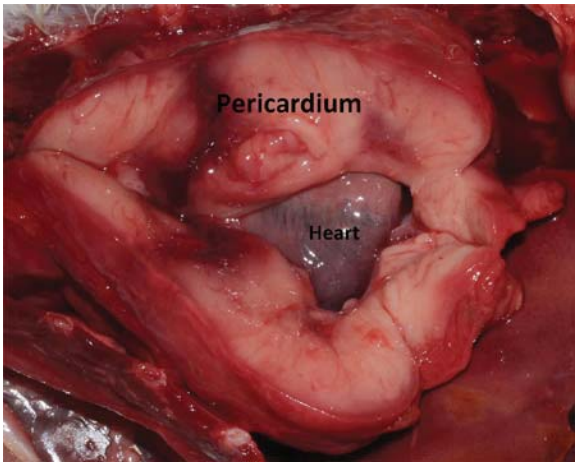

Figure 4 Gross aspect of pericardial lymphoma in a cat at necropsy. Marked diffuse pericardial thickening is evident

Gross findings, histology and immunophenotyping

Necropsy was performed in four cases. In these cats, the pericardium appeared markedly and diffusely thickened by a solid tissue proliferation (Figure 4). Other thoracic and abdominal organs appeared macroscopically not involved by the tumour. Pleural effusion was present in all cases, although the volume of fluid was not recorded. Pericardial effusion was mild in all cases.

A combination of histology and immunohistochemistry was available in four cases (cats 1, 2, 6 and 7). In all cases examined, severe diffuse expansion of the pericardium (up to 2 cm) by a population of uniform, round cells was detected (Figure 5a). Of these cases, three were classified as small or medium B-cell lymphoma (cats 2, 6 and 7) (Figure 5b) and one was a large T-cell lymphoma (cat 1). Case 1 tested also positive for CD8 on immunocytochemistry. In two cases, histology was not available, but immunophenotype was obtained by immunocytochemistry (cats 4 and 5) from pleural effusion; both were diagnosed as large T-cell lymphoma.

In cats 2,6 and 7, myocardium from the different cardiac sectors was examined microscopically and found not to be infiltrated by neoplastic cells. In cat 2, intravascular neoplastic emboli of lymphoid cells were observed in the myocardium, but never in the interstitium.

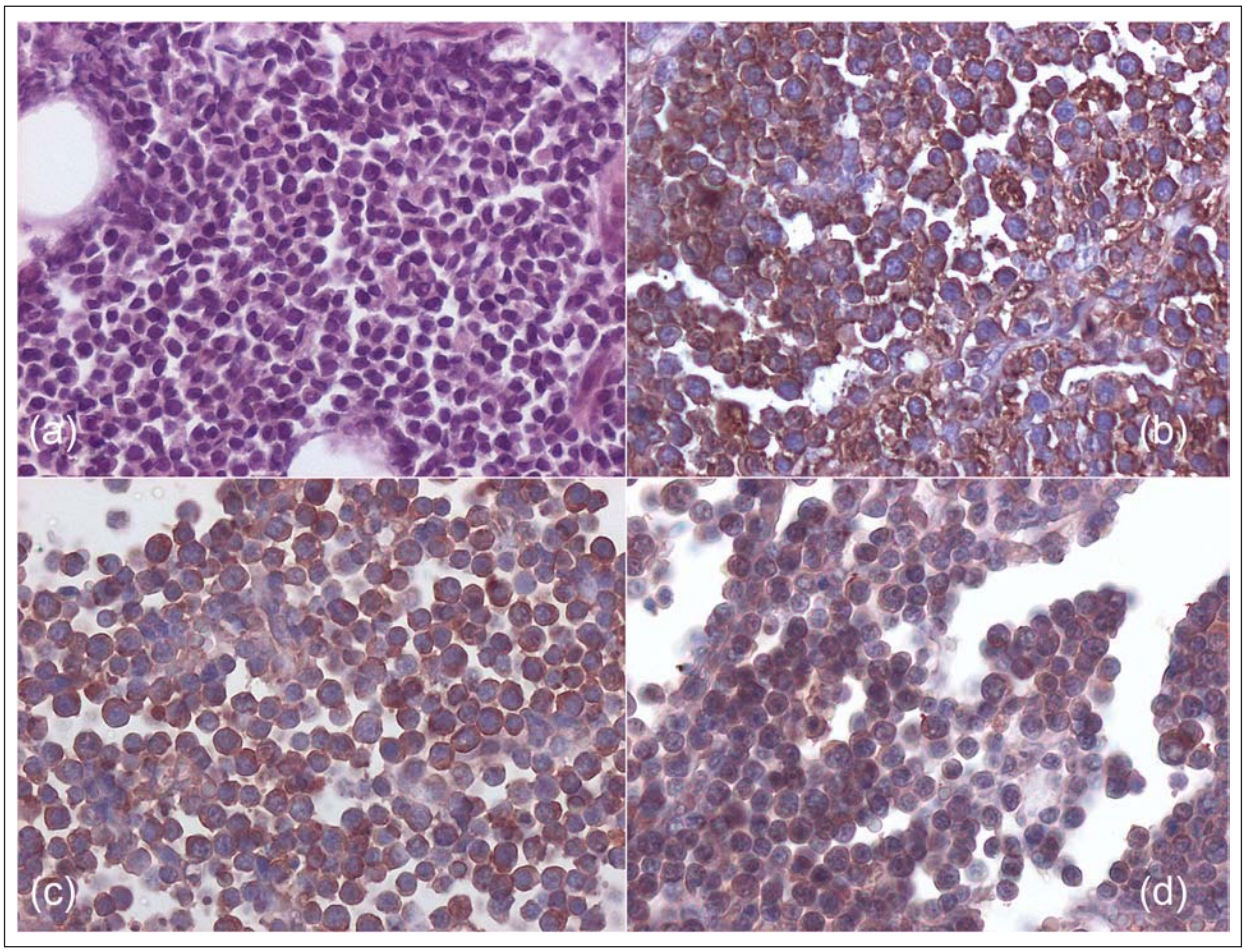

Figure 5 (a) Histology from medium-size B-cell pericardial lymphoma of cat 2, showing a monomorphic population of round cells (haematoxylin and eosin, x 200). (b) Immunohistochemistry from cat 2, showing a diffuse strong cytoplasmic positivity for CD79a (B-cell phenotype) (avidin–biotin peroxidase method, x 400). (c,d) Immunohistochemistry from cat 2 showing positive reactivity for feline leukaemia virus antigen p27 (c) and gp70 (d) (avidin–biotin peroxidase method, x 400)

FeLV status

Only cat 1 was FeLV-negative; all the others were FeLV-positive: three on serology (cats 3, 4 and 5), one on immunohistochemistry (cat 7), and two on both serology and immunohistochemistry (cats 2 and 6) (Figure 5c, d).

Discussion

In this article we have described a small series of presumptive primary pericardial lymphoma in cats. The pericardium was presumed to be the primary site of origin as it was the only organ grossly affected by the tumour. To our knowledge, this study represents the first description of primary lymphoma of the pericardium in cats, even if this case series is based on a retrospective case retrieval, and complete clinical, laboratory and pathological findings were not available for all seven cats. Pericardial lymphoma should therefore be considered a rare extranodal feline lymphoma

Pericardium can be involved in primary or metastatic tumours. In terminally ill human patients, lymphoma, leukaemia, breast or lung tumours can secondarily affect pericardium with microscopic metastasis or small effusion without clinical relevance.[7] In the group of cats described herein, the pericardium appeared markedly and uniformly thickened by the tumour's growth. This thickening was clearly visible by thoracic US. US findings were always strongly suggestive of pericardial malignancy, and all tested cats showed similar US pericardial abnormalities. Thoracic US examination and findings should therefore be considered the first strong sign of pericardial lymphoma in cats.

The median age of affected cats in this study (5 years) is similar to the median age of FeLV-positive cats affected by other forms of lymphoma.[8] FeLV status was positive in all but one case. The FeLV-negative cat was tested only by serum antigenic test, but immunohistochemistry and polymerase chain reaction were not performed on

affected tissues, so we cannot exclude the presence of the retrovirus. Dehydration and weight loss were present in all cases, and might have been caused by severe dyspnoea. Lymphopenia and neutrophilia were present in 2/7 cases and might be considered stress-induced.

Pleural effusion could be caused by impaired cardiac diastolic function due to pericardial thickening, to reduced preload from compressed intra-thoracic vessels or to a combination of both mechanisms. Direct exfoliation of neoplastic cells and fluid transudation from the tumour could also have contributed to fluid accumulation.

Cytology from effusion or pericardium was indicative of lymphoma in six cases. Cytology is a simple, but powerful, diagnostic technique, and the cytological diagnosis of lymphoma is quite straightforward in the presence of a single population of immature lymphoid cells.

Staging of lymphoma was not performed in these cats owing to the owners' financial constraints and to the severity of the cats' condition, which did not allow for extensive imaging and biopsy procedures. However, in the four cases that underwent necropsy, gross involvement of other thoracic or abdominal organs was not documented. Microscopic myocardial emboli were found on histopathology only in one case (cat 2). We cannot exclude involvement of other tissues in the remaining three cases; therefore, the diagnosis of primary pericardial lymphoma in these three cats should be considered presumptive.

Immunophenotype was B-cell in three cases and T-cell in three cases. Although the number of cats in our study is very small, this prevalence is different to the higher prevalence of the T-cell phenotype reported in cats with mediastinal lymphoma.[1]

The survival time of the cat that was administered prednisone did not differ significantly from that of the cats that were not treated. The cat that received only doxorubicin did not respond to the treatment and survived comparably to the ones that were administered prednisone or no treatment. The lack of response to doxorubicin is consistent with the literature, showing it to be a poor induction agent when used alone.[9,10] The cat that underwent the modified UWM protocol went into complete remission 2 days after the first administration of treatment and remained in complete remission until the time of writing (750 days). This is consistent with studies showing that response to therapy is the strongest reported prognostic factor for cats treated for lymphoma.[5,11]

Conclusions

The presence of pleural effusion, an enlarged globoid cardiac silhouette with dorsally displaced trachea in association with clinical signs and the animal's age can be indicative of cardiac or pericardial disease. Echocardiography can be used to confirm that the displacement of the trachea is caused by thickening of the pericardium. Cytology of the pericardium or of the thoracic effusion can be useful in reaching the diagnosis of lymphoma.

Funding This research received no specific grant from any funding agency in the public, commercial, or not-for-profit sectors.

Conflict of interest The authors do not have any potential conflicts of interest to declare.

References

1 Vail DM. **Feline lymphoma and leukemia**. In: Withrow SJ and Vail D (eds). Withrow & MacEwen's small animal clinical oncology. 4th ed. St Louis, MO: Saunders-Elsevier, 2007, pp 733–756.
2 Lowerens M, London CA, Pedersen NC and Lyons LA. **Feline lymphoma in the post-feline leukaemia virus era**. *J Vet Intern Med* 2005; 19: 329–335.
3 Court EA, Watson ADJ and Peaston AE. **Retrospective study of 60 cases of feline lymphosarcoma**. *Aust Vet J* 1997; 75: 424–427.
4 Marconato L, Rossi F, Bettini G, Comazzi S, Bonfanti U and Buchholz J. **Linfoma**. In: Marconato L and Amadori D (eds). Oncologia medica veterinaria e comparata. 1st ed. Milan: Poletto editore, 2012, pp 759–817.
5 Vail DM, Moore AS, Oglilvie GK and Volk LM. **Feline lymphoma (145 cases): proliferation indices, CD3 immunoreactivity and their association with prognosis in 90 cats receiving therapy**. *J Vet Intern Med* 1998; 12: 349–354.
6 Gabor LJ, Canfiled PG and Malik R. **Immunophenotypic and histological characterization of 109 cases of feline lymphosarcoma**. *Aust Vet J* 1999; 77: 436–441.
7 Lestuzzi C. **Neoplastic pericardial disease: old and current strategies for diagnosis and management**. *World J Cardiol* 2010; 26: 270–279.
8 Mooney SC, Hayes AA, Matus RE, Geary A and Shurgot BA. **Treatment and prognostic factors in lymphoma in cats: 103 cases (1977–1981)**. *J Am Vet Med Assoc* 1989; 194: 696–699.
9 Peaston AE and Maddison JE. **Efficacy of doxorubicin as an induction agent for cats with lymphosarcoma**. *Aust Vet J* 1999; 77: 442–444.
10 Kristal O, Lana SE, Ogilvie GK, Cotter SM and Moore AS. **Single agent chemotherapy with doxorubicin for feline lymphoma**. *J Vet Intern Med* 2001; 15: 125–130.
11 Teske E, van Straten G, van Noort R and Rutteman GR. **Chemotherapy with cyclophosphamide, vincristine, and prednisolone (COP) in cats with malignant lymphoma: new results with an old protocol**. *J Vet Intern Med* 2002; 16: 179–186.

Proceedings of the 12th Annual Scientific Meeting

of the

Veterinary Endoscopy Society

April 12-14 , 2015

Santa Barbara, California, USA

How To Get Profitable Biopsies From Nasopharyngeal Space-Occupying Lesions In Cats: 13 Cases (2012-2015). Santagostino SF, Carotenuto A, Roccabianca P, Bonacini S, Caniatti M, Borghi L, Mortellaro CM. University of Milano, Italy

Objective: To describe a novel endoscopic bioptic technique to obtain multiple diagnostic samples from nasopharyngeal lesions in cats.

Designs: Prospective study between 2012-2015

Materials and Methods: Cats with nasopharyngeal space occupying lesions were entered in the study. Anterograde and retrograde endoscopic examinations were performed with a 2.7 mm 0° arthroscope and a 4.9 mm video-bronchoscope, respectively. Biopsies were collected from each lesion for histopathological evaluation. Nasopharyngeal specimens of 0.2-0.6 cm were attained with anterograde insertion of bioptic opposing-cups forceps or other small devices into the nostrils under retrograde endoscopic view.

Results: Biopsies from 13 cases of nasopharyngeal space-occupying lesions were collected. Most cats were domestic shorthair (n=7), male (F/M=0.5) with a mean age of 11.2 years (range 5-16.5). After premedication with dexmedetomidine and methadone, general anaesthesia was induced with propofol and maintained with isofluorane in 100% oxygen. Several biopsies varying from 1 to 24 (mean of 6.4) were collected. Cytology was also obtained in 5/13 cats. Diagnostic distribution of respiratory lesions was non-neoplastic (3), lymphoma (7), malignant epithelial neoplasia (2), sarcoma (1). For each case, a mean of 4.3 biopsies was often necessary to achieve a correct diagnosis. A lymphoplasmacytic inflammation was present in 5 out of 10 neoplasms.

Conclusion: The recognition of primary nasopharyngeal disease is not considered straightforward, and diagnosis of neoplasia is often delayed for the simultaneous presence and prevalence of inflammation. A high index of clinical suspicion along with imaging techniques and adequate sampling protocols with multiple biopsies (minimum 4-5) are required for a definitive diagnosis.

Proceedings, 10th Annual Meeting

May2-4, 2013
Hilton Key Largo

Key Largo, FL, USA

Nasopharyngeal lymphomas vs. lymphoplasmacitic nasopharyngitis in cats: the endoscopist-pathologist alliance to meet the challenge.

Carlo Maria Mortellaro*, Sara Santagostino†, Mario Caniatti†, Paola Roccabianca†.
DIVET- Dipartimento di Scienze Veterinarie e Sanità Pubblica-
(Dept. of Clinical Sciences and Public Health)
Università degli Studi di Milano
Via Celoria ,10 MILANO

Nasal and nasopharyngeal lymphomas are the most common feline upper respiratory tract tumors. However, nasopharyngeal lymphoma has been seldom considered a separate clinico-pathological entity. Nasopharyngeal lymphoma mimics severe inflammation and thus poses a challenge in its diagnosis. A high index of clinical suspicion along with multiple deep adequately sized and appropriately processed biopsies submitted for histology and immunohistochemistry are usually needed to achieve the correct diagnosis. Attempts to sample the tumors using endoscopic instruments are often unsuccessful because of the limited working space that can lead to the collection of non-diagnostic biopsies. In fact, an adequate amount of non-traumatized tissue sample is required for a definitive diagnosis since the frequent coexistence of the neoplasia with necrosis and inflammation.
Commonly, nasopharyngeal lymphomas present as extensive multilobulated masses, that may, in severe cases, fill the caudal nasopharynx. In early cases, these lesions mimic clinically lymphofollicular inflammatory processes. Both lesions may be easily visualized by retrograde nasopharyngoscopy using flexible pediatric videobronchoscope. Combining retrograde nasopharyngoscopy with concurrent anterograde insertion of a large bioptic opposing-cups forceps trough the nares, allows to obtain larger and less damaged tissue samples for histopathology, under continuing endoscopic guidance.
Patients often initially misdiagnosed as affected by chronic inflammation on clinical grounds had their diagnosis revised after histopathological examination of multiple samples excised with this technique. Microscopical examination often revealed the concomitance of lymphoma with chronic lymphoplasmacytic inflammation. This "anterograde-retrograde" technique proved ideal to sample primary nasopharyngeal lesions to confirm the diagnosis of inflammation versus lymphoma.

* Division of Small Animal Surgery
† Division of Pathology

Title: **The Economics and Feasibility of Incorporating Rigid Endoscopy in General Practice**

Authors: Brian Evans, DVM; J. Brad Case, DVM, MS, DACVS
Affiliations: Coastal Animal Hospital (Evans), Encinitas, CA 92024.

Objectives: To describe the economic and clinical characteristics of implementing rigid endoscopy in a new, single doctor general veterinary practice.
Design: Descriptive study
Animals included: Dogs and cats examined and treated at Coastal Animal Hospital in Encinitas, CA.
Methods: Invoices and medical records were evaluated for equipment and procedural

THE 31ST MEETING OF THE
EUROPEAN SOCIETY & COLLEGE
OF VETERINARY PATHOLOGISTS
LONDON 2013

31st Meeting of the European Society of Veterinary Pathology

and the

European College of Veterinary Pathologists

4th – 7th September 2013

Programme

The Institute of Education
University of London
London, UK

ESVP

ecvp
European College of Veterinary Pathologists

RVC Royal Veterinary College University of London

CORRELATION BETWEEN CYTOLOGY AND HISTOPATHOLOGY IN THE DIAGNOSIS OF SPLENIC NEOPLASMS IN DOGS

Summary

Spleen can be affected by a variety of diseases and cytology represents a useful diagnostic technique. However, few studies have addressed the accuracy of cytology in the evaluation of splenic lesions and specifically of neoplasms. The aim of the study is to evaluate the cyto-histological correlation in the diagnosis of canine splenic tumors. Splenic cytological and corresponding histopathological samples obtained between 1998 and 2013 were retrospectively evaluated. Concordance between cytology and histology was determined. Accuracy, sensibility, specificity, positive and negative predictive value of cytology for the diagnosis of splenic neoplasias was determined considering histopathology as the gold standard. Sixty-seven cases were collected. Thirty-one cytological samples were classified as nonneoplastic (12 true negatives, 19 false negatives compared with histopathology). Cytological diagnosis of neoplasia was obtained in 36 cases (33 true positives and 3 false positive). Cytological diagnosis was in agreement with the histopathological diagnosis in 67.2% (45/67) of cases. Cytology had a sensitivity of 89.3%, a specificity of 80%, a positive predictive value of 91.2%, and a negative predictive value of 38.7% in the diagnosis of splenic neoplasms. The majority of cases were non neoplastic (31/67). The most common tumors were sarcomas (20/67) followed by lymphoma (7/67). Although cytopathology and histopathology should be considered complementary techniques in the diagnosis of splenic lesions, cytology demonstrated to be a useful and sensitive tool for the diagnosis of splenic neoplasias.

Keywords: Cytology, Dog, Histology, Spleen

ASSOCIAZIONE ITALIANA
DI PATOLOGIA VETERINARIA

AIPVet

ASSOCIAZIONE ITALIANA DI PATOLOGIA VETERINARIA

ATTI IX CONGRESSO NAZIONALE

ISSN 1825 - 2265

Perugia

25-26 Maggio 2012

Premio Ennio Sanna 2012

IL LINFOMA NASALE DEL GATTO: VALUTAZIONE CITOLOGICA, ISTOLOGICA E IMMUNOISTOCHIMICA.

Santagostino S.F., Mortellaro C.M., Avallone G., Caniatti M., Forlani A., Roccabianca P.

Premi Rosario Preziosi 2012

VALUTAZIONE BIOCHIMICA ED ELETTROFORETICA DELLE HDL NEL VITELLO: DIFFERENZA CON I VALORI DELL'ADULTO E CORRELAZIONE CON PROTEINE INFIAMMATORIE.

Giordano A., Rossi G., Moretti P., Venturini M., Paltrinieri S.

LA HEAT SHOCK PROTEIN 90 (HSP90) E' ASSOCIATA ALL'EVOLUZIONE IPERPLASTICA E NEOPLASTICA DELLA PROSTATA DEL CANE.

Palmieri C., Mancini M., Benazzi C., Della Salda L.

Premio comunicazione presentata dal più giovane patologo

TUMORE MAMMARIO CANINO: ESPRESSIONE DEI RECETTORI DI ESTROGENO E PROGESTERONE IN DIVERSI SOTTOTIPI TUMORALI.

Mainenti M., Rasotto R., Zappulli V.

La successione delle presentazioni in questo volume degli Atti riflette, sia per le comunicazioni orali che per i poster, l'ordine di elencazione nel programma definitivo.

FELINE NASAL LYMPHOMA: CYTOLOGICAL, HISTOLOGICAL AND IMMUNOHISTOCHEMICAL ANALYSIS

Santagostino Sara Francesca1, Mortellaro Carlo Maria2, Avallone Giancarlo1, Caniatti Mario1, Forlani Annalisa1, Roccabianca Paola1

1Dipartimento di Patologia Animale Igiene e Sanità Pubblica Veterinaria, Facoltà di Medicina Veterinaria, Università degli Studi di Milano, Italia. 2Dipartimento di Scienze Cliniche Veterinarie, Facoltà di Medicina Veterinaria, Università degli Studi di Milano, Italia

Lymphomas are the most common primary nasal tumors in cats. Few reports on feline nasal diseases and nasal lymphomas are currently available. Nasal endoscopic biopsies of 156 cats were analyzed; all samples were formalin-fixed and routinely processed. Lymphomas (35), epithelial neoplasias (23), sarcomas (17) and non neoplastic process (79) were diagnosed. Lymphomas were primary nasal in 26 cats, nasal and nasopharyngeal in 6 and only nasopharyngeal in 3. In 26/35 cases cytology was also available. Lymphomas were classified according to the WHO criteria. Immunohistochemistry for CD20, CD3, FeLVp27, FeLVgp70 and Calicivirus was performed. Most cats were DSH (n=28), with a mean age of 10,5 years (range 1-19) and a male prevalence (F/M=0,54). Lymphomas were diffuse (31) or nodular (4). Epitheliotropism was observed in 6 cases. Cytotypes of lymphomas were 13 small cell lymphomas, 12 large cell types, 6 medium sized, 1 centrocitic-centroblastic grade I and 3 plasmacytomas. Cytology and histology were in agreement in 50% of cases. B cell phenotype was observed in 30 cases and a FeLV positivity was detected in 21 cases. Necropsy was performed in 4 cats; in one cat lymphoma was limited to the nasopharynx while internal organ invasion was evidenced in the other 3. Despite a variable cytotype and phenotype, most lymphomas demonstrated an aggressive clinical course and poor prognosis.

Keywords: lymphoma, cat, nasal cavities, phenotype, FeLV.

HEMOPHILIC POLYARTHROPATHY IN A DOG: CLINICO-PATHOLOGIC FINDINGS

Author

S.F. Santagostino[], J.B. Engiles[], B.J. Turek[], M.D. Sánchez[]

1 Department of Pathobiology, School of Veterinary Medicine, University of Pennsylvania, Philadelphia, PA []
Department of Pathobiology - New Bolton Center, School of Veterinary Medicine, University of Pennsylvania, Philadelphia, PA

Presentation ,
Section Diagnostic Pathology
Poster Number Poster D-19

A 2-month-old intact male great Dane presented for ambulatory difficulties with severe swelling and pain of the right and left stifle joints and right tarsus. Radiographs revealed soft tissue swelling, widening of articular spaces, osteopenia, and enlargement of the distal epiphyses. Complete blood count and coagulation tests indicated regenerative anemia, thrombocytopenia, prolonged PTT and severe reduction of factor VIII levels. Autopsy revealed widespread subcutaneous, intramuscular and periarticular ecchymoses with edema and hemarthrosis. Synovial fluid had reduced viscosity with thickening and hyperemia of the synovial membranes. There was erosion of the articular cartilage with exposure of subchondral bone and osteophytes on the right humeral condyles, the right olecranon fossa, and the distal femoral condyles. Histology revealed the presence of abundant intraarticular granulation tissue with pannus formation, hemorrhage, and a diffuse lymphoplasmacytic and proliferative synovitis with edema and periarticular osteophytes. These lesions were compatible with a subacute hemophilic arthropathy which describes degenerative joint lesions following

recurrent hemarthrosis secondary to factor VIII deficiency. In addition, growth plates contained irregular cartilaginous blebs and islands of disorganized matrix with dysplastic chondrocytes, multiple linear fissures and aberrant blood vessels. Hemophilic arthropathy is a rarely described manifestation of factor VIII deficiency in dogs. Although the pathogenesis is not fully elucidated, the excessive iron deposition from repeat intraarticular bleeding may trigger inflammation with damage to the synovium and articular cartilage, synovitis and pannus formation. The findings of hemarthrosis, joint swelling and recurrent shifting lameness in juvenile dogs may represent important clinical indicators of hemophilia.

ENDOSCOPIC-GUIDED PALLIATIVE DEBULKING OF NASOPHARYNGEAL NEOPLASMS IN CATS:
2 CASES.

A.M. Carotenuto* , S.F. Santagostino° , P. Roccabianca° ECVP, L. Borghi* , C.M. Mortellaro* . Dept. of Veterinary Sciences and Public Health, *Division of Small Animal Surgery °Division of Pathology University of Milan, Milan, Italy

Dyspnea, nasal discharge and stertor are the most common clinical signs documented in cats with nasopharyngeal space-occupying lesions. The aim of this report is to describe minimally invasive endoscopic-guided palliative surgery in 2 selected cases of nasopharyngeal tumors in cats whose owners refused recommended chemotherapy or radiotherapy. A 6-year-old exotic shorthair (case 1) and a 14-year-old domestic shorthair (case 2) cats were included. In both cases, anterograde and retrograde endoscopic examinations were performed with a 2.7 mm 30° arthroscope and a 4.9 mm video-bronchoscope, respectively. Retrograde rhinoscopy evidenced the presence of a friable and bleeding purple mass arising from nasopharynx and extending to the right ventral nasal meatus (case 1) and multiple pale pink lesions originating from and confined to nasopharynx (case 2). In case 1, histology revealed malignant neoplastic endothelial cells in 3/17 bioptic fragments, consistent with a cavernous hemangiosarcoma. Neoplastic cells were moderately pleomorphic and form variably sized blood-filled cavities, clefts and channels. Dense sheets of round, medium sized, neoplastic lymphoid cells with abundant eosinophilic cytoplasm were detected in 18/20 bioptic samples in case 2, consistent with a diagnosis of intermediate cell lymphoma. Resection of the lesions was achieved through endoscopic-assisted surgical debulking using bioptic forceps via nares. Bleeding was controlled by cold saline 0.9% flushing. Recovery was uneventful and patients were discharged 8 hours after the procedure. A 3 month full remission of symptoms was obtained. Endoscopic-guided nasopharyngeal debulking represents an alternative palliative approach for temporary attenuation of life-threatening clinical signs in cats without other therapeutic options.

XANTHOGRANULOMATOUS COELOMITIS WITH INTRALESIONAL ACID-FAST POSITIVE BACTERIA IN A PIGEON

Author

A. Walsh, S. Santagostino, A. Durham, Department of Pathobiology , University of Pennsylvania, School of Veterinary Medicine, Philadelphia, PA

Presentation ,
Section Diagnostic Pathology
Poster Number Poster D-66

An 8-year-old female racing homer pigeon with coelomic swelling diagnosed as a xanthogranuloma with intralesional acid-fast bacteria is described. A complete blood count and serum biochemistry initially indicated marked leukocytosis characterized by heterophilia, moderate lipemia and elevated creatinine kinase (CK). The leukocytosis persisted throughout continued treatment; however, the lipemia and CK levels returned to normal values. Ultrasonographic imaging of the coelom revealed a large expansile mass that obscured the kidneys and oviduct, and an enlarged hyperechoic liver. Mycobacterium sp. and Chlamydia sp. polymerase chain reaction testing on fecal swabs were negative. A biopsy of the coelomic mass, thought to be intrahepatic, revealed granulomatous inflammation with intrahistiocytic acid-fast bacilli. At necropsy, a large soft, yellow-tan oval mass expanded the coelom and adhered to the visceral surface of the liver, coelomic walls and entrapped the gastrointestinal tract. The hepatic parenchyma was replaced by multifocal 0.1 - 1.0 cm diameter firm, white-tan nodules. Microscopically, the coelomic mass consisted of foamy macrophages, scattered lymphocytes, multinucleated cells and numerous cholesterol clefts with intrahistiocytic acid-fast bacilli. Additionally, the ovary was effaced by an ovarian carcinoma with multifocal hepatic metastases. This ovarian tumor was not noted clinically and was likely obscured during ultrasonographic imaging by the xanthogranuloma. Xanthomas are commonly associated with hyperlipidemia and

develop as discrete dermal plaques or dermal tumors. Rarely, xanthomatous formation occurs secondarily to inflammation or trauma. Few reports in avian species document xanthomatous formation secondary to inflammation, and to our knowledge this is the first case within the coelom with associated intralesional acid-fast bacilli.

FELINE PULMONARY ADENOSQUAMOUS CARCINOMA: COMPARISON OF CYTOLOGIC AND HISTOLOGIC FINDINGS

Author K.O.Loria, S.F.Santagostino, M.Sánchez, M.P.Sirivelu

Department of Pathobiology, School of Veterinary Medicine, University of Pennsylvania, Philadelphia, PA

Presentation Sunday, November 9, 2014, 2:50 p.m.-3:00 p.m.
Section Diagnostic Pathology
Poster Number Poster D-23

A 6.5-year-old male castrated domestic shorthair cat presented for acute anorexia with a two-month history of lethargy and weight loss. Thoracic radiographs and CT revealed a left cranial thoracic mass. Fine needle aspirate (FNA) of the mass revealed marked neutrophilic and macrophagic inflammation with few clusters of epithelial cells displaying mild atypia, suggesting a possible carcinoma. Due to progressive decline of the patient’s status and poor prognosis, humane euthanasia was elected. Upon necropsy, the left cranial lung lobe was effaced by a firm, tan mass. Numerous additional masses with similar macroscopic appearance were also present throughout the thoracic cavity. Histologic examination revealed a poorly demarcated, infiltrative, epithelial neoplasm replacing the normal pulmonary parenchyma. The epithelial cells had two different morphologies: neoplastic squamous epithelial cells arranged in nests and anastomosing cords surrounded by desmoplasia and cuboidal to columnar cells arranged in acinar structures (adenomatous differentiation), warranting a diagnosis of adenosquamous carcinoma. Furthermore, multifocal areas of coagulative necrosis with marked suppurative and histiocytic inflammation were also present. Cytologic imprints of

the mass indicated a pleomorphic epithelial population without clear distinction of two cell types. Cytochemical staining with Periodic acid Schiff (PAS) and Papanicolaou (Pap) revealed distinct secretory and squamous components in both histologic and cytologic samples. Interestingly, carcinomatosis lesions were diffusely Pap positive and PAS negative, indicating a squamous component contradictory to morphologic appearance of secretory epithelium. Further, analysis of the initial FNA sample with PAS and Pap stains helped highlight the epithelial population, which was otherwise obscured by the inflammation. This case demonstrates the usefulness of cytochemical staining in diagnosis of carcinoma in equivocal FNA cytology samples and fluid cytologic samples with concurrent inflammation.

ESTP Poster Abstracts

TP52: Metal exposure and toxicology in selected fish species from the Mediterranean sea: risk assessment for human consumption

Santagostino SF[1], Forlani A.[1], Roccabianca P.[1], Fedrizzi G.[2], Malandra R.[3], Ranghieri V.[4], Zaffra N.[5], Ghisleni G.[1]

[1]DIVET – Department of Veterinary Sciences and Public Health, Milano; [2]Istituto Zooprofilattico Sperimentale Lombardia Emilia Romagna, Bologna, [3]National Health Service, ASL Veterinary Service, Milano, [4]Veterinary Food Safety Consultants, Fish Market of Milano, [5]Market Manager, Sogemi Spa, General Markets of Milano, Italy

Introduction: Myriads of toxic substances are released into our environment daily, either deliberately manufactured or accidentally produced. Aquatic systems throughout the world are increasingly under a wide array of anthropogenic stressors. However, some of aquatic environments can sustain fish populations, indicating that they are able to tolerate toxic levels of metals.

Aim: The concentration levels of different chemical compounds in pelagic and benthopelagic fish species from the Mediterranean sea were examined by testing specific tissues involved in the bioaccumulation pathway with GC/MS.

Materials and Methods: Fish samples were collected monthly from April 2013 to September 2013. No abnormalities were evidenced on macroscopical examination. The presence of twenty-seven heavy metals and minerals (Hg, Na, Mg, Al, K, Ca, V, Cr, Mn, Fe, Co, Ni, Cu, Zn, As, Se, Sr, Mo, Ag, Cd, Sn, Sb, Ba, Tl, Pb, Th, U) was investigated in livers and muscles collected from *Pagellus bogaraveo*, *Dentex dentex*, and *Thunnus thynnus* from the Mediterranean sea.

The mean concentration of each element was calculated. A comparison to the provisional tolerable daily or weekly intake or to the tolerable upper intake established by the Joint FAO/WHO Expert Committee on Food Additives and the EFSA was assessed. The maximum safe consumption (MSC) for adult intakes was achieved for each element with an established safety limit.

Results: Hg, Fe, Co, Ni, Zn, As, Se, Sr, Mo, Cd, Sn, Ba were variably present at higher level within muscular samples of the 3 different fish species. The MSC calculated for mercury lead to a limited recommended weekly intake for all the tested fish species.

Conclusions: This study provides preliminary information on metal concentration in the edible part of three commercial fish species. Based on MSC, mercury concentration in muscle of *Pagellus bogaraveo*, *Dentex dentex*, *Thunnus thynnus* exhibits a risk for human consumption.

NK-CELL LARGE GRANULAR LYMPHOCYTE LEUKEMIC LYMPHOMA IN A DOG

Gabriele Ghisleni1, Maria Gabriella Ferrari2, Sara Francesca Santagostino1, Annalisa Forlani.1

1 DIVET, School of Veterinary Medicine University of Milan, Italy

2 Ambulatorio Veterinario, Liscate, Milano, Italy.

Abstract

Large granular lymphocytes (LGL) are defined as lymphoid subset that constitute 1-10% of the circulating pool of lymphocytes in dogs and are characterized either by CD3 positivity (in>90% of the cases) or negativity for both T- and B- cell markers (in <10% of cases, natural killer origin). A 11-year-old, male, mongrel dog was submitted to the referring veterinarian following a 2-month history of progressive generalized weakness, vomiting, weight loss and anorexia. Physical examination revealed severe jaundice and hepatomegaly. Results of complete blood count (CBC) were within reference intervals (RI). Serum biochemical analysis revealed increases in ALT (175U/L; RI, 20-150 U/L), AST (295 U/L; RI, <80U/L) and total bilirubin (6,3 mg/dL; RI, 0,1-0,6 mg/dL). Ultrasound fine needle aspiration of the liver was also performed. Cytological examination of hepatic and blood smears revealed the presence of a large number of lymphoid cells characterized by an abundant amount of pale bluish cytoplasm containing numerous distinct magenta granules variably in sized and shape (LGL), with densely stained reniform nuclei and without apparent nucleoli. On immunocytochemistry, neoplastic cells were negative for both T- and B- cell markers. A final cytological diagnosis of LGL leukemic lymphoma of NK origin was made. Due to the poor clinical condition of the animal the owner did not allow any chemotherapeutic approach and the dog died spontaneously few days later. Large granular lymphocytes leukemias of NK-type are surface CD3-negative disorders with variable clinical behavior in dogs, are reported in humans.

NEOPLASTIC DISEASE IN THE DOMESTIC FERRET: CLASSIFICATION AND EPIDEMIOLOGICAL SURVEY OF 856 CASES

Summary

Ferrets are considered one of the most common non-conventional companion animals. Neoplastic diseases have been reported with increasing frequency over the last decades. The aim of this study is to classify and analyze the prevalence of neoplasms in Italian ferrets. All the definitive diagnosis of bioptic and necroscopic specimens received between 2000 and 2010 at the pathology service of the University of Milan were reviewed. Data concerning signalment and histology were collected from the electronic archives. The total number of samples permitted to calculate the prevalence of neoplasms. A total of 908 samples were received and processed. Of these, 688 cases included at least one tumor (75.77%). Ferrets with multiple neoplasms were commonly detected. Thus, a total of 856 tumors were collected. Our population was characterized by a median age of 5 years (range 5 months-10 years) with F/M ratio=0.99. Endocrine (63.8%), integumentary (14.7%) and hemolymphatic (8.9%) systems were most commonly affected. A high frequency of adrenal gland (25.8%), pancreatic islet cell (24.9%), and mast cell tumors (5.8%) was evidenced. Cutaneous squamous cell carcinomas (SCC) occurred together with sebaceous gland tumors. In 2.6% of cases, abdominal spindle cell tumors with primary undefined origin were observed. The tumor prevalence recorded in this study paralleled previous findings. The unusual association between SCC and sebaceous gland neoplasms and the origin of intraabdominal spindle cell neoplasms should be further investigated.

Keywords: Ferret, neoplasia, epidemiology

SUDDEN DEATH CAUSED BY MASSIVE PULMONARY ALVEOLAR LIPOPROTEINOSIS IN A ENGLISH BULL DOG

Summary

Pulmonary alveolar proteinosis (PAP) is a rare disease characterized by alveolar accumulation of phospholipids and proteins (lipoproteinosis), that may be induced by many cationic amphophilic drugs. We describe a case of a 7-year-old, male, English Bulldog with a history of juvenile idiopathic epilepsy treated with phenobarbital and bromide and developing sudden severe dyspnea with respiratory arrest 12 hours post-admission. Necropsy revealed severe hepatomegaly, mild endocardiosis and a diffuse pulmonary edema with disseminated 1-8 mm firm, umbilicated lesions in apical, accessory and right cranial lobes. Microscopically, alveoli (60-80%) were filled by a pale eosinophilic, amorphous to granular PAS-positive, von Kossa- and Congo red-negative material associated with macrophages and neutrophils. Interstitial fibrosis and mineralization were moderate. Myocardial septal and right ventricle fatty infiltration was present. TEM revealed short lamellar electron-dense haphazardly arranged 3.125 nm fascicles at 6.25 nm periodic distance compatible with accumulation of abnormal surfactant. These findings were suggestive of an alveolar lipoproteinosis/phospholipidosis. The chronic administration of bromide may be involved in the pathogenesis of this lesion.

Keywords: bromide, alveolar proteinosis, histology, electron microscopy, dog